



**Air-Conditioning, Heating and
Refrigeration Technology Institute**

Final Report

AHRTI Report No. 9008

HOT SURFACE IGNITION OF A2L REFRIGERANTS

Final Report

Date Published – November, 2017

Michael Cundy, Ph.D., P.E., C.F.E.I.

Exponent[®]

23445 North 19th Avenue
Phoenix, Arizona 85027

Prepared for

**AIR-CONDITIONING, HEATING AND REFRIGERATION TECHNOLOGY
INSTITUTE, INC**

2111 Wilson Boulevard, Suite 500, Arlington, Virginia 22201-3001

©2017 AHRTI

ASHRAE has the right to publish, reproduce, duplicate and use such report provided that the AHRTI copyright notice is included on all copies of the report distributed by AHRTI.

DISCLAIMER

This report was prepared as an account of work sponsored by the Air-Conditioning, Heating and Refrigeration Technology Institute, Inc. (AHRTI). Neither AHRTI, its research program financial supporters, or any agency thereof, nor any of their employees, contractors, subcontractors or employees thereof - makes any warranty, expressed or implied; assumes any legal liability or responsibility for the accuracy, completeness, any third party's use of, or the results of such use of any information, apparatus, product, or process disclosed in this report; or represents that its use would not infringe privately owned rights. Reference herein to any specific commercial product, process, or service by trade name, trademark, manufacturer, or otherwise, does not necessarily constitute nor imply its endorsement, recommendation, or favoring by AHRTI, its sponsors, or any agency thereof or their contractors or subcontractors. The views and opinions of authors expressed herein do not necessarily state or reflect those of AHRTI, its program sponsors, or any agency thereof.

Funding for this project was provided by (listed alphabetically):

- Air-Conditioning, Heating and Refrigeration Institute (AHRI)
- American Society of Heating, Refrigerating, and Air-Conditioning Engineers (ASHRAE)

Executive Summary

Exponent was retained by the Air-Conditioning, Heating, and Refrigeration Technology Institute (AHRTI) to carry out work related to hot surface ignition of A2L refrigerants. The scope of the study was to develop a test methodology and use the method to conduct hot surface ignition temperature (HSIT) testing for three A2L refrigerants under specific conditions prescribed by the AHRTI subcommittee. The test methodology was developed to assist in the evaluation of the propensity of A2L refrigerants (R32, R1234ze, and R452B) to ignite on hot surfaces. After multiple conversations with AHRTI, Exponent designed and constructed a test apparatus to discharge a 5 g charge of refrigerant or refrigerant/oil mixture out of a tube and onto a hot, flat plate. Five replicate tests were performed for each test condition. None of the pure refrigerants tested ignited at hot plate temperatures up to 850°C (1562°F), and none of the refrigerants mixtures with 3% oil by mass ignited with the hot plate temperatures up to 800°C (1472°F). However, it must be emphasized that the propensity for hot surface ignition is significantly dependent upon several factors including surface temperature, surface geometry and roughness, contact time with surface, ambient environment, and mixture uniformity. Therefore, it may be possible to achieve hot surface ignition at lower temperatures under different conditions with the same refrigerants tested.

The results presented in this report are valid for the specific test conditions used here which simulated releasing a refrigerant onto a flat hot surface heated by an electric heating element inside warm ductwork. Because the HSIT is dependent on many factors, consideration of additional testing with different hot surface geometries that may be found in actual heating systems (e.g. heating coils in HVAC) is recommended. The characteristics of the leak are also expected to influence the HSIT and this report did not consider testing or attempt to quantify the sensitivity of HSIT to different spray characteristics such as those encountered by cracked lines, pinholes, braze failures (with different spray velocities and dispersion characteristics) and temperatures. For these reasons, the test results may not adequately address the needs of other users of this report, or quantify the HSIT for specific HVAC equipment configurations. For

purposes of developing standards related to HSIT, due consideration to equipment geometry and leak characteristics is recommended.

Contents

| | <u>Page</u> |
|-----------------|-------------|
| List of Figures | 4 |
| Introduction | 5 |
| Test Setup | 10 |
| Test Results | 18 |
| Summary | 24 |

List of Figures

| | <u>Page</u> |
|-----------|--|
| Figure 1 | ASTM E 659 test apparatus used for determining the AIT. 6 |
| Figure 2 | Fuel vapor pressure vs. surface temperature plot illustrating the forced ignition region and the hot surface ignition region, along with the AIT and flammability limits. 7 |
| Figure 3 | Schematic of the test setup. 10 |
| Figure 4 | Test apparatus. 11 |
| Figure 5 | Photograph showing the interior of the test setup. 12 |
| Figure 6 | Photographs showing the fan assembly as viewed through the front viewing panel (left) and as viewed through the side hatch (right). 12 |
| Figure 7 | Screenshot of a video showing the heated hot plate with 0.15 m (6.0") square box channel integrated into the test chamber. 13 |
| Figure 8 | Photograph of the hot plate at approximately room temperature showing locations of the embedded thermocouples. Note that this photograph shows cartridge heaters that were used in test ID1 and ID2. The red dots indicate the insertion depth of the thermocouples. Since the plate is 0.20 m x 0.20 m (8" x 8") and a 0.15 m x 0.15 m (6" x 6") box channel was placed on top of it, the lower left thermocouple is beneath an exposed surface. 14 |
| Figure 9 | Refrigerant charge assembly. 16 |
| Figure 10 | Test to verify that applying a vacuum to the cylinder did not pull POE oil out of the cylinder. 17 |
| Figure 11 | Test ID15 data. 20 |
| Figure 12 | Screenshots of ejection in 3/120s increments for test ID15 with pure R-1234ze refrigerant and with a target hot plate temperature of 850°C (1562°F). 21 |
| Figure 13 | Test ID36 data. 22 |
| Figure 14 | Screenshots of ejection in 3/120s increments for test ID36 with R452B refrigerant mixed with 3% POE oil by mass, and with a hot plate temperature of 800°C (1472°F). 23 |

Introduction

The AHRTI issued a request for proposals (RFP) to investigate the hot surface ignition temperature (HSIT) of three A2L refrigerants. Current heating, ventilation, and air-conditioning & refrigeration (HVAC&R) equipment standards relating to hot surface temperatures are primarily based on the auto-ignition temperature (AIT), minus 100°C ($\Delta 180^{\circ}\text{F}$). In general, A2L refrigerants have a lower AIT than non-flammable refrigerants which may limit their use in some HVAC&R products if the same criteria are used. However, limiting the maximum temperature of some components in HVAC&R systems to the AIT minus 100°C ($\Delta 180^{\circ}\text{F}$) may be overly conservative as the minimum ignition energies (MIE) of the A2L refrigerants can be considerably higher than known common residential ignition sources. In addition, the burning velocities of A2L refrigerants are lower than class A2 and A3 refrigerants.

In the US, the AIT is typically determined using the ASTM E 659¹ test method and apparatus, as shown in Figure 1, although other methods are also used (EN 14522,² IEC 60079-20-1³). The ASTM E 659 test setup involves a 500 ml borosilicate round-bottom, short-necked boiling flask, whereby the chemical to be characterized is added to the flask in a specific quantity (100 μl for liquids, and 100 mg for gases and solids) and the temperature is uniformly raised until ignition is achieved. At each temperature set point the test apparatus is observed for 10 minutes, allowing the gases and vapors to mix with the air before the sample at that concentration is considered nonflammable or flammable. Different concentrations of the chemical of interest are then tested.

¹ ASTM E 659-78, *Standard Test Method for Autoignition Temperature of Liquid Chemicals*, ASTM, West Conshohocken, PA 1994.

² EN 14522, *Determination of the autoignition temperature of gases and vapours*, 2005.

³ IEC 60079-20-1, *Material characteristics for gas and vapour classification – Test methods and data*, 2012.

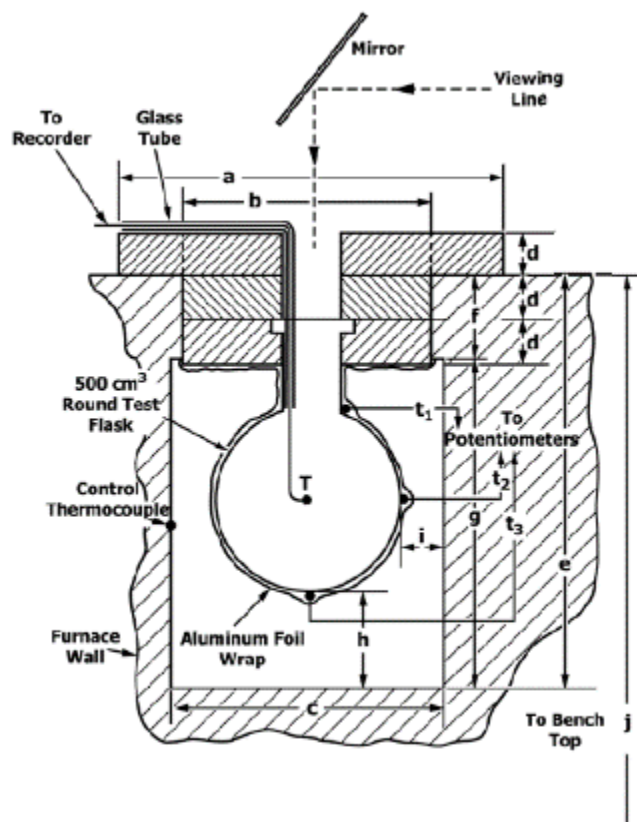


Figure 1 ASTM E 659 test apparatus used for determining the AIT.

However, the environment in the ASTM E 659 test apparatus where the lowest ignition temperature occurred for a particular chemical is not typically encountered in products and systems in use for various reasons. For example, there may be non-ideal and/or non-uniform concentrations. The effect of mole fraction (or vapor pressure) and temperature is qualitatively illustrated in Figure 2.^{4,5,6,7} The lowest temperature at which hot surface ignition may occur is at a specific, spatially uniform fuel vapor pressure. If the mole fraction is higher or lower, a higher surface temperature is required. The fuel mole fractions where hot surface ignition may occur do not reach all the way to the flammability limits primarily because of heat losses to the

⁴D. Drysdale, *An Introduction to Fire Dynamics*, 2nd edition, Chichester: John Wiley & Sons, 2002.

⁵A.M. Kanury, *Ignition of Liquid Fuels*, *SFPE Handbook of Fire Protection Engineering*, 3rd edition, Quincy, MA: National Fire Protection Association, 2002, Section 2, Chapter 8, pg. 2-189-2-190

⁶M.G. Zabetakis, *Flammability Characteristics of Combustible Gases and Vapors*, Bulletin 627, U.S. Department of the Interior, Bureau of Mines, Washington D.C., 1965.

⁷Colwell, J., and Reza, A., *Hot Surface Ignition of Automotive and Aviation Fluids*, *Fire Technology*, 41, p 105-123, 2005.

surfaces or due to convection. The region between the hot surface ignition region and the flammability limits is the forced ignition region, where a higher external energy source is required to raise the temperature of reactants high enough to initiate sustained combustion.

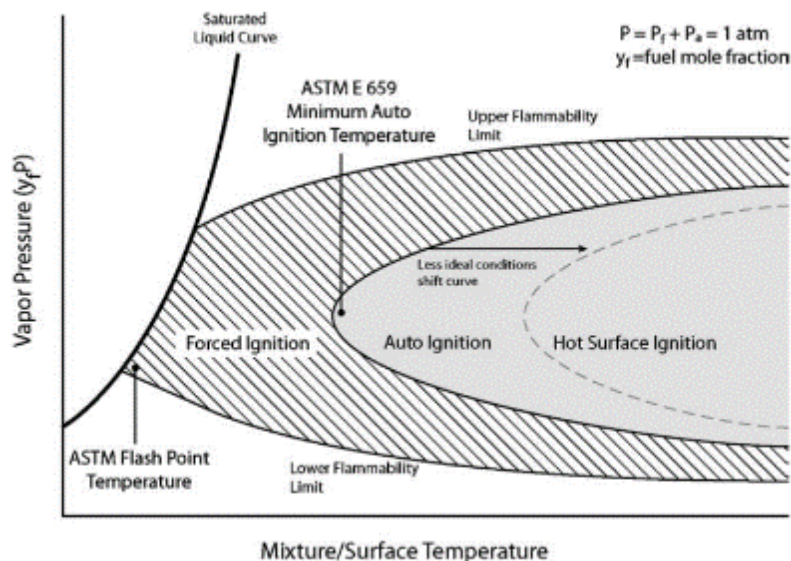


Figure 2 Fuel vapor pressure vs. surface temperature plot illustrating the forced ignition region and the hot surface ignition region, along with the AIT and flammability limits.⁸

The potential for hot surface ignition to occur in real-world systems and products is also dependent, among other factors, upon the surface shapes, roughness,⁹ and characteristics, as well as the uniformity of the surface temperatures, both of which are linked to the ambient environment by heat transfer and fluid flow. Surfaces may be concave, convex, flat, or have various contours and shapes. In an ideal case, such as in the ASTM E 659 test apparatus, the surface is a round-bottom, short-necked boiling flask, where the hot surface will heat the adjacent mixture evenly (see the AIT in Figure 2). In the case of a flat surface or a surface with contours such as an electric coil heater, the ambient temperatures will have gradients, and there will be fluid flow associated with natural and potentially forced convection.

⁸ Colwell, J., and Reza, A., *Hot Surface Ignition of Automotive and Aviation Fluids*, Fire Technology, 41, p 105-123, 2005.

⁹ Bennett, J. M., Ignition of Combustible Fluids by Heated Surfaces, *Process Safety Progress* **20**, 29-36 (2001).

HSIT is also dependent upon the local environment. The local environment is coupled to the hot surface and the surroundings by heat transfer and fluid flow, including both natural and convective heat and mass transfer mechanisms and radiation. The refrigerant temperature, as it leaves the hot surface area after making contact, is influenced by the charge storage temperature and pressure, release mechanism (or test apparatus characteristics), time in close proximity to the hot surface, hot surface temperature, and the local environment with which the heated refrigerant mixes, all of which will affect the propensity for ignition.

A literature review of published hot surface ignition studies of some liquids can be found in an article by Colwell and Reza.¹⁰ In summary, many of the studies reviewed tested a large number of test configurations including different surface geometries, air flows, and chemical application methods (sprays, streams, and different flow rates), and as a result, a range of HSITs were recorded for the tested chemicals. Colwell and Reza utilized a flat plate with no cross flow to facilitate reproducibility of tests involving liquid fuels. In this work, they dropped single droplets of fluid onto a flat, hot plate.

Another literature review by Babrauskas discusses hot surface ignition competency for gases, vapors, liquid sprays, aerosols, and other forms of ignitable liquids dispersed in the atmosphere.¹¹ This review shows that the quantity of turbine oil dropped onto a hot surface can change the HSIT (450°C at 2 drops to 315°C at 30-60 mL).¹² Babrauskas also noted an inverse relationship between HSIT and the flash point of the fuel, discussing how gasoline is difficult to ignite on a hot surface. Babrauskas suggested that detailed modeling could be performed to better understand the mixing process and temperature fields to understand this behavior. Babrauskas' article notes that for most, but not all of the hydrocarbon/air mixtures studied, ignitions were more easily achieved at the LFL. For the fuels studied, flow velocity was found to have only a small effect on ignitions unless the velocity is large, in which case ignitions were more difficult. Studies have also observed that larger surfaces facilitate ignition of

¹⁰ Colwell and Reza, *Hot Surface Ignition of Automotive and Aviation Fluids*, Fire Technology, 41, pg. 105-123, 2005.

¹¹ Babrauskas, V., *Ignition of gases, vapors, and liquids by hot surfaces*, Proceedings of the 3rd International Symposium on Fire Investigation Science and Technology, 2008.

¹² Knowles, R. E., Discussion, Institute of Marine Engineers Trans. (London) **77**, 137-138 (1965).

hydrocarbon/air, diethyl ether/air, hydrogen/air, and town gas/air mixtures.¹³ This is likely true for non-uniform mixture concentrations, as is the case in the current study.

Hot surface ignition testing of R-32 and R-410A refrigerants have been performed using a flat, hot plate by Boussouf at the University of Maryland, who selected the flat plate geometry based on testing of liquid automotive fuels.¹⁴ The test developed in this work also utilized a flat plate for consistency and to also facilitate reproducibility.

In this report, the development of the test setup and test procedure is described. The results of the tests are then presented with screenshots of video and data from selected tests. A table with details on all tests is shown in Appendix A, and plots of the recorded data are shown in Appendix B.

¹³ Babrauskas, V., *Ignition Handbook*, Fire Science and Technology, p87-88, 2003

¹⁴ Boussouf, A., *Hot Surface Ignition of R-32 and R-410A Refrigerant Mixtures with Lubricating Oil*, Master of Science Thesis, University of Maryland, College Park, 2014.

Test Setup

A schematic of the test setup can be found in Figure 3. The AHRTI subcommittee requested a test setup which could simulate a HVAC ductwork to study HSIT. Therefore, the test setup was designed such that the dimensions around the hot surface were similar to those that may be encountered in a typical HVAC ductwork. The AHRTI subcommittee also requested that the test setup be capable of generating an air flow with a uniform velocity of up to 50 fpm in a region upstream of the hot plate in order to study the effect of ventilation on ignition propensity. In order to achieve this specification, a recirculation chamber was developed. The recirculation chamber is 0.750 m tall, 0.750 m deep, and 1.50 m long (29.5" x 29.5" x 59.0") as viewed from the side. A divider panel, which defines the circulation path, is 0.500 m (19.7") above the floor and runs from the front to the back of the chamber (see the lateral panel in Figure 3).

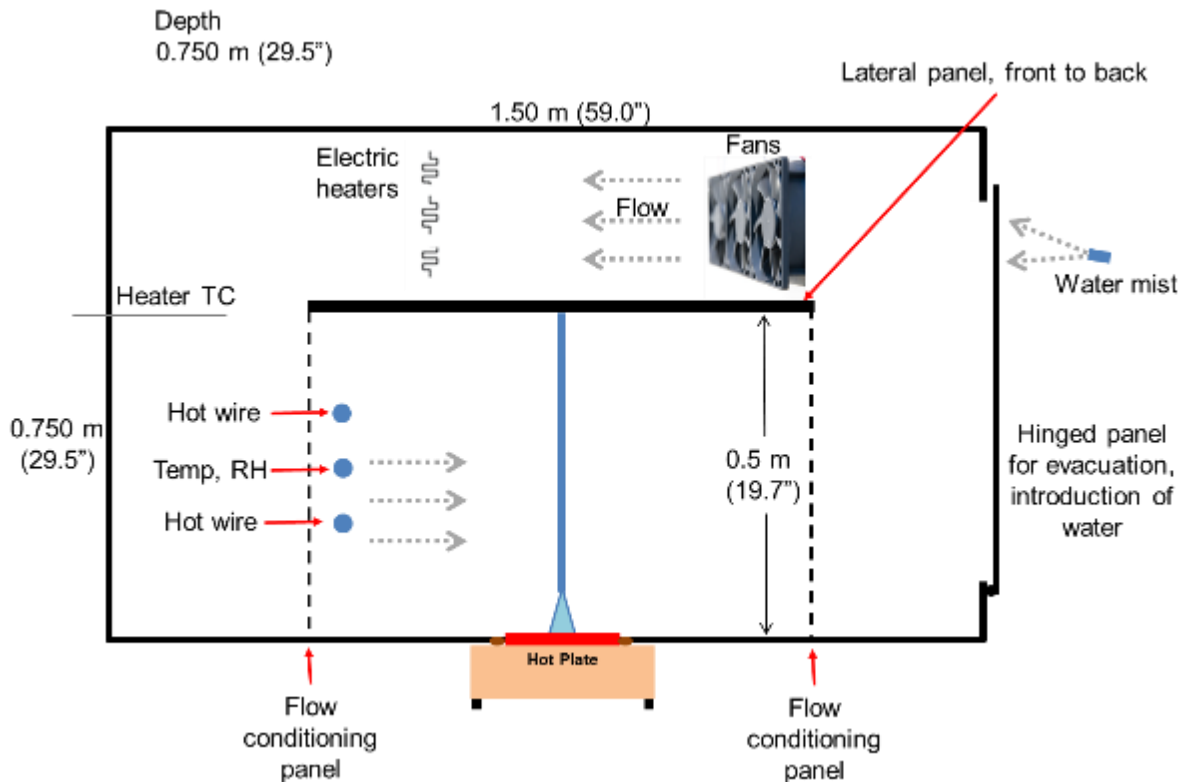


Figure 3 Schematic of the test setup.

A photograph of the test setup is shown in Figure 4. Fresh air is introduced into the chamber through a quick-release plexiglass front panel and a hinged panel on the right side of the

chamber. After introducing fresh air and purging gases from the previous test, the plexiglass panel is then reinstalled. For tests with higher absolute humidity, a water mist was sprayed using a metered spray nozzle towards the fans above the divider table through the hinged panel on the right side, and the panel was then closed (see Figure 3 and Figure 6).

Insulation panels were adhered to the outside of the chamber to facilitate reaching higher ambient temperatures within the chamber.

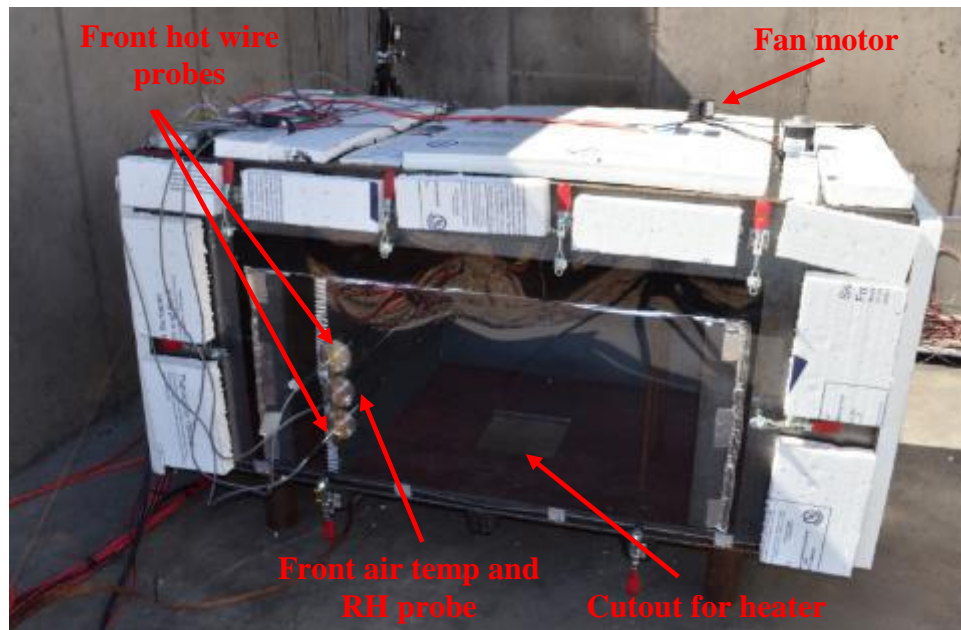


Figure 4 Test apparatus.

A photograph of the interior of the test setup is shown in Figure 5. Four nickel chromium electric heaters were installed above the divider table and to the left side of the chamber. Air was pushed across these heaters using three 0.2 m (8") diameter fan blades. Since testing conditions required a target air temperature of 93°C (200°F), the fan motor was installed outside of the test chamber, and a miter gear and chain and sprocket system was developed to drive the fan blades (see Figure 6). Combined air and relative humidity sensors (Dwyer 657-1) were installed at the mid-height level of the flow path, upstream of the hot plate, and were approximately 0.2 m (9") from the side walls of the chamber.

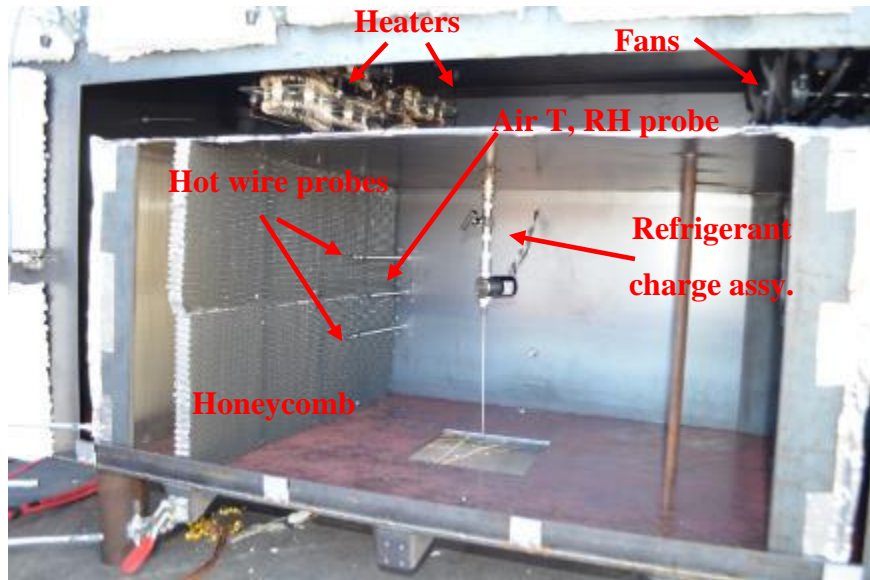


Figure 5 Photograph showing the interior of the test setup.



Figure 6 Photographs showing the fan assembly as viewed through the front viewing panel (left) and as viewed through the side hatch (right).

To achieve uniform airflow in the section that houses the hot plate, a perforated panel was used with 1.59 mm (0.0625") holes allowing for 23% open space on the leading edge of the divider table followed by 6.4 mm (0.25") honeycomb channels 2.54 cm (1.00") long, and a 30% open space perforated panel (1.59 mm, 0.0625" hole size) on the trailing edge of the divider table. Air flow rates were measured with calibrated Dwyer 641RM-12 hot wire anemometers at 4 locations in the air flow path. Two of the hot wire anemometers can be seen in Figure 5, and the other two are installed symmetrically on the plexiglass panel (see Figure 4). Each anemometer

was approximately 25 cm (10") from the nearest side wall (1/3 width) and approximately 17 cm (6.5") from the nearest lateral surface (1/3 height).

An 0.22 m x 0.22 m (8.5" x 8.5") hole was cut into the bottom of the recirculation chamber to allow for the insertion of a hot plate. A hot plate was developed for the testing. A custom Kanthal A-1 heating element was fabricated and installed below a 0.20 m x 0.20 m x 1.9 cm (8.0" x 8.0" x 3/4") copper block, and the supplied voltage was adjusted with a variable transformer. A (0.15 m) 6.0" square box channel with rounded edges, with a 1.3 cm (0.50") depth, was placed on top of the hot plate, and ceramic fiber board was placed on the outside to reduce the required heat load on the heating element and to reduce the heat load on the chamber. A screenshot of a video showing the hot plate with the box channel integrated into the bottom of the chamber can be seen in Figure 7. Two K-type thermocouples (Omega TJ36-CAIN-18U-6-CC-XCIB) were embedded in the copper block (see Figure 8; note that this photograph shows the hot plate with cartridge heaters used in test ID1 and ID2). The thermocouples had an outside diameter of 0.318 cm (1/8") and were inserted into a hole such that the top edge of the thermocouples were approximately 0.159 cm (1/16") from the surface of the copper block. This approach was selected so that oil did not accumulate on fiberglass thermocouple wire insulation and ignite, which then introduces a more competent ignition source (open flame). The location of the thermocouple bead below the surface is indicated by the red dots in Figure 8.

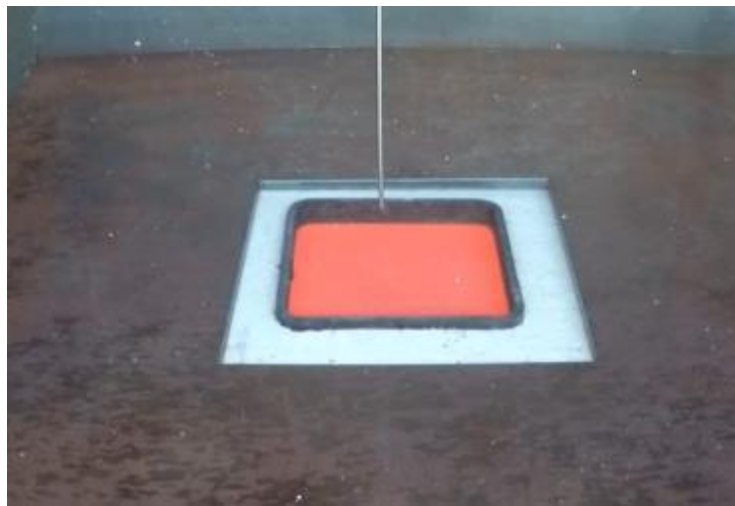


Figure 7 Screenshot of a video showing the heated hot plate with 0.15 m (6.0") square box channel integrated into the test chamber.

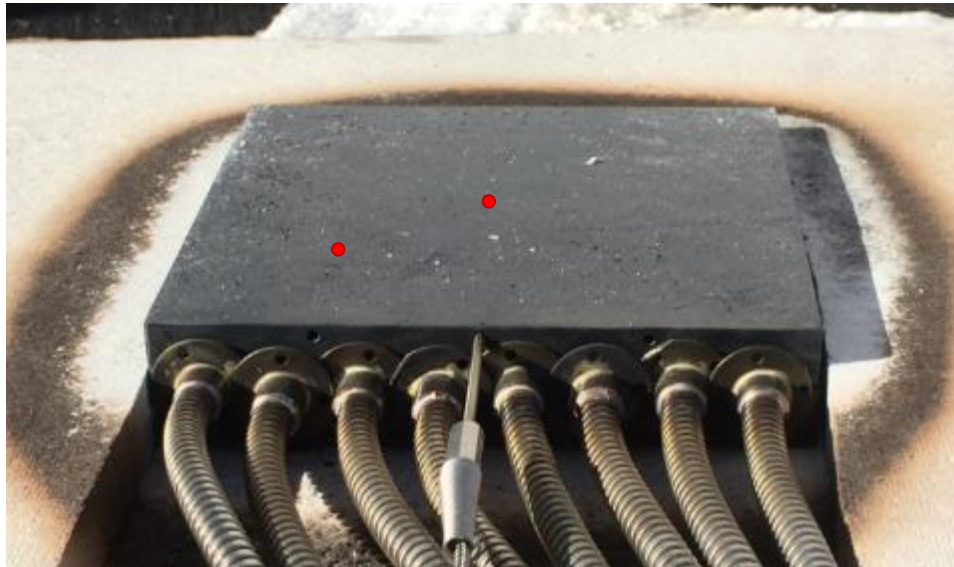


Figure 8 Photograph of the hot plate at approximately room temperature showing locations of the embedded thermocouples. Note that this photograph shows cartridge heaters that were used in test ID1 and ID2. The red dots indicate the insertion depth of the thermocouples. Since the plate is 0.20 m x 0.20 m (8" x 8") and a 0.15 m x 0.15 m (6" x 6") box channel was placed on top of it, the lower left thermocouple is beneath an exposed surface.

Hot plate temperature (2 channels), air temperature (2 channels), air relative humidity (2 channels), refrigerant ejection trigger, air velocity (4 channels), and chamber pressure were measured. Data was collected with a calibrated Graphtec GL-series data acquisition systems, running at 5 Hz. Video was recorded at 120 fps.

The AHRTI subcommittee requested that 5 g refrigerant charges be ejected onto the hot plate with a 1/8" outside diameter stainless steel tube. One of the refrigerant charge assemblies can be seen in Figure 9. The charge assembly was installed onto a refrigerant cylinder, and the contents of the charge assembly and fittings were evacuated with a vacuum pump. The valve where the vacuum pump line connected to the system was then closed, and the refrigerant cylinder valve was opened allowing refrigerant to fill the charge assembly. The valve on the charge assembly was then closed, and the assembly was removed via a quick-disconnect fitting and placed on the scale which had been previously tared with the charge assembly on-board. The charge assemblies typically had between 7-10 g of refrigerant in them at this point. The

precision needle valve was then opened slightly, allowing refrigerant to escape, and the weight was observed to slowly decrease. When the scale reached c.a. 5 g, the valve was closed and a photograph was taken to record the weight of the charge. The assembly was then installed into the recirculation chamber using a quick disconnect fitting. Note that the refrigerant cylinders were rotated in a small concrete mixer at 30 rpm for approximately one hour prior to testing in order to mix the refrigerant. The repeatability of the weight of the empty charge assemblies was evaluated by removing the assembly from the scale and placing it down in a different orientation several times, both before and during testing. All measurements were within 0.2 g of one another (standard deviation of 0.08 g on four measurements prior to testing). Following charging of discharge assembly, the assembly was installed into the chamber, and the front panel was reinstalled. A photograph showing the charge assembly installed in the test fixture can be seen in Figure 5. The nozzle exit was approximately 3.8 ± 0.8 cm (1.5 ± 0.3 "") above the hot plate. The discharge assembly solenoid was plugged in, air heaters were turned on, water mist was sprayed into the test setup, and the refrigerant was discharged onto the hot plate.



Figure 9 Refrigerant charge assembly. Note that the weight of the assembly has been tared, and the scale display is showing the charge of refrigerant in the chamber.

Testing was also done with mixtures of refrigerant and oil that were prepared by Exponent. A refrigerant recovery cylinder was acquired for each of the refrigerants. 90 g of polyol ester (POE) oil (RL32-3MAF) was added to each of the recovery cylinders, and the air and any gases inside the cylinders were evacuated using a vacuum pump. When the vacuum pump line was disconnected, a paper towel was pushed into the fitting and pulled out to verify that the application of a vacuum did not pull out oil (see Figure 10). After evacuation of the gaseous contents in each recovery cylinder, 3 kg of refrigerant was added to the cylinder. Each of these cylinders was mixed for at least one hour prior to testing, creating a mixture with 3% oil by mass.



Figure 10 Test to verify that applying a vacuum to the cylinder did not pull POE oil out of the cylinder.

Test Results

Table 1 shows a summary of the tests with test conditions. A more comprehensive table with a list of all tests can be seen in Appendix A, and the data associated with all of the tests can be found in Appendix B. No ignitions were observed in testing with either the pure refrigerant charges or the refrigerant charges with 3% POE oil by mass. All tests were run with a target ambient air temperature of 200°F and with a target humidity ratio of 0.023 kg/kg (approximately 6% RH @ 200°F). For tests at 850°C (1562°F), the center plate temperatures at the time of ejection ranged from 842°C to 860°C (1548°F to 1580°F), with the average for each of the three refrigerants over 850°C (1562°F). For all tests at 700°C (1292°F), the center plate temperatures ranged from 701°C to 716°C (1294°F to 1321°F), and for all tests at 800°C (1472°F), the center plate temperatures ranged from 800°C to 824°C (1472°F to 1515°F).

Table 1 Summary of the test conditions and results.

| Refrigerant | Oil | Target Plate Temp. (°C/°F) | Target Chamber Air Temp. (°C/°F) | Humidity Ratio (kg/kg or lb/lb) | Ignition |
|-------------|------|-------------------------------|-------------------------------------|------------------------------------|----------|
| R32 | None | 850/1562 | 93/200 | 0.023 | 0/5 |
| R-452B | None | 850/1562 | 93/200 | 0.023 | 0/5 |
| R-1234ze | None | 850/1562 | 93/200 | 0.023 | 0/5 |
| R32 | 3% | 700/1292 | 93/200 | 0.023 | 0/5 |
| R-452B | 3% | 700/1292 | 93/200 | 0.023 | 0/5 |
| R-1234ze | 3% | 700/1292 | 93/200 | 0.023 | 0/5 |
| R32 | 3% | 800/1472 | 93/200 | 0.023 | 0/5 |
| R-452B | 3% | 800/1472 | 93/200 | 0.023 | 0/5 |
| R-1234ze | 3% | 800/1472 | 93/200 | 0.023 | 0/5 |

The wind tunnel capability was not utilized in the present work, even though a wind tunnel capability with uniform flow was added to the test specifications. This is because the subcommittee assumed that the refrigerants will not be ignited at a certain hot surface temperature with forced airflow across the plate if the refrigerant is not ignited under such a temperature with no forced airflow crossing the plate. Because of the limited resources, tests associated with higher plate temperature with forced airflow crossing the plate were not conducted. It should be noted that natural convective currents did occur even though there was

no forced airflow across the hot plate for these tests. It may be of interest to increase the surface temperature to ensure ignitions and determine if adding forced airflow decreases ignition potential.

In this section, two tests are described in detail; one without oil and one with oil. In test ID15, R-1234ze was tested with no oil added at a hot plate temperature of 850°C (1562°F). The data associated with test ID15 is shown in Figure 11. Data collection began when the fans were running, which were used to assist in achieving a uniform air temperature and humidity upstream of the hot plate. The fans were then turned off, and the ejection was triggered when the measured flows stabilized at approximately 2.5 – 5.0 cm/s (5.0-10 fpm). After ejection, the hot plate center thermocouple temperature drops by approximately 7°C ($\Delta 13^\circ\text{F}$) as a result of cooling by the refrigerant jet. The embedded thermocouple would tend to measure smaller temperature drops because of its distance to the surface, but the high thermal conductivity of the copper would counteract this effect. Analysis of the video footage of several tests indicates that the refrigerant ejection typically takes place over approximately 0.07 s, which corresponds to an average flow rate of approximately 71 g/s (0.16 lb/s). Screenshots of the video at 3/120s intervals, starting with the first frame the ejection is visible can be seen in Figure 12. The flow appears multiphase as it leaves the ejection tube.

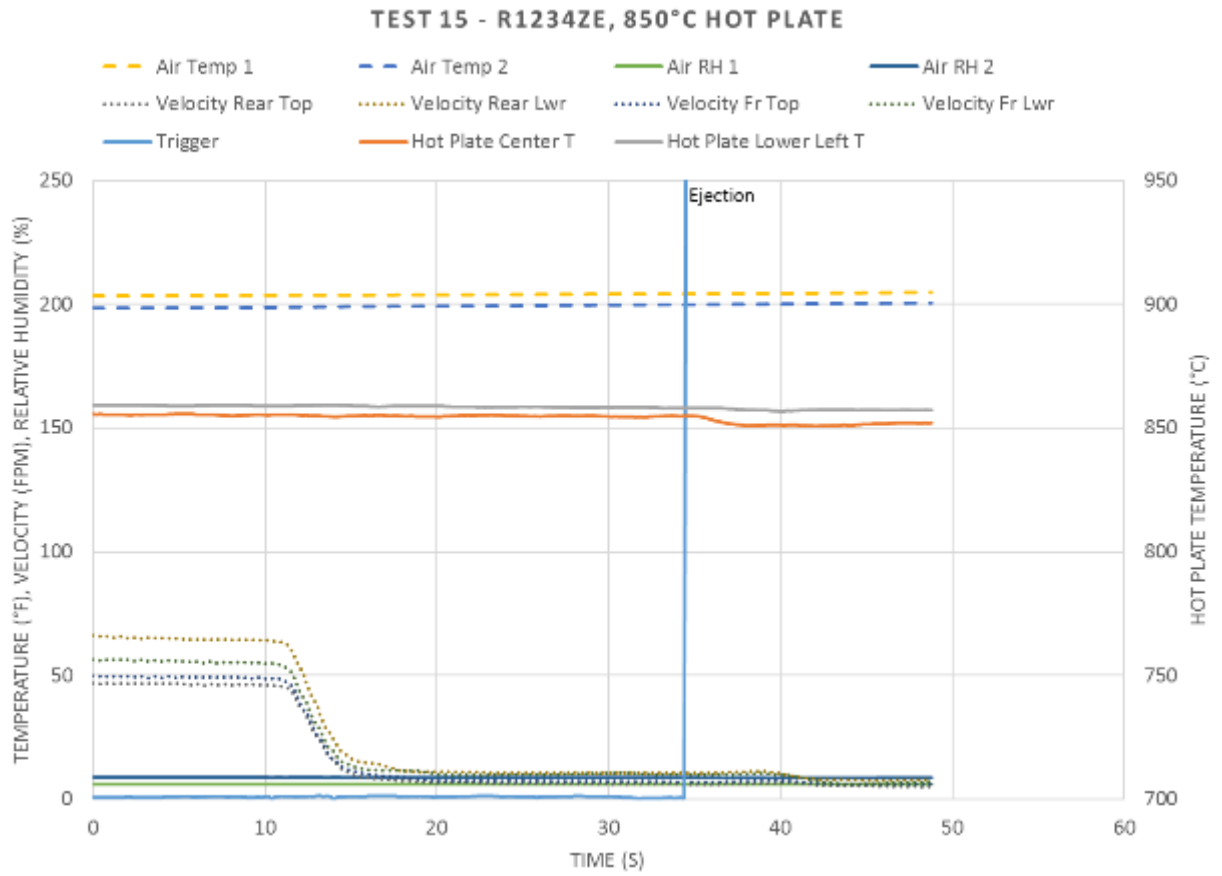


Figure 11 Test ID15 data.

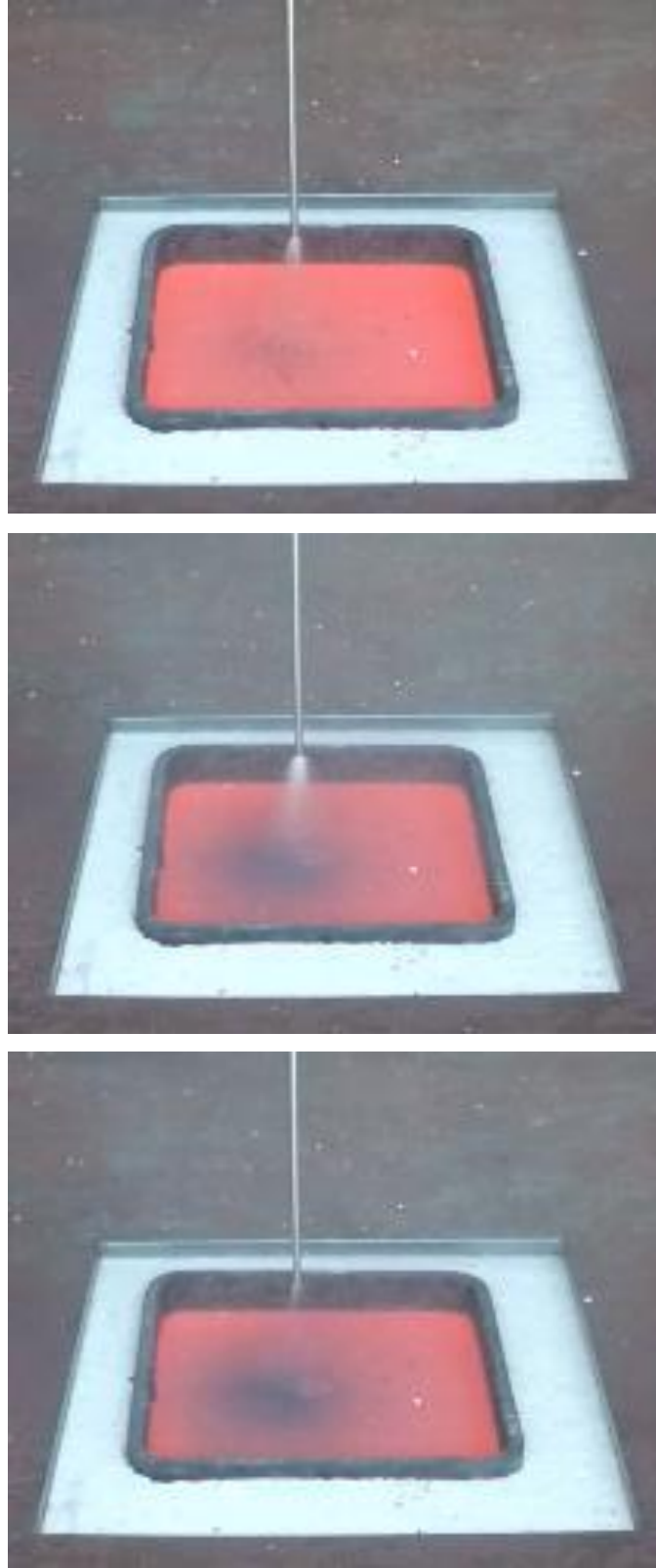


Figure 12 Screenshots of ejection in 3/120s increments for test ID15 with pure R-1234ze refrigerant and with a target hot plate temperature of 850°C (1562°F).

Test ID36 was a test with R452B mixed with 3% POE oil by mass and with a target hot plate temperature of 800°C (1472°F). The data for this test can be seen in Figure 13. The refrigerant and oil test data is substantially similar to the pure refrigerant test data, except that the central surface temperature does not decrease as much in these tests, if it decreases at all. This is evident in all of the tests with refrigerant and oil mixtures. Screenshots of the video at 3/120s intervals, starting with the first frame the ejection is visible can be seen in Figure 14. The flow appears multiphase as it leaves the ejection tube. The haze associated with atomized oil is clearly visible in these tests.

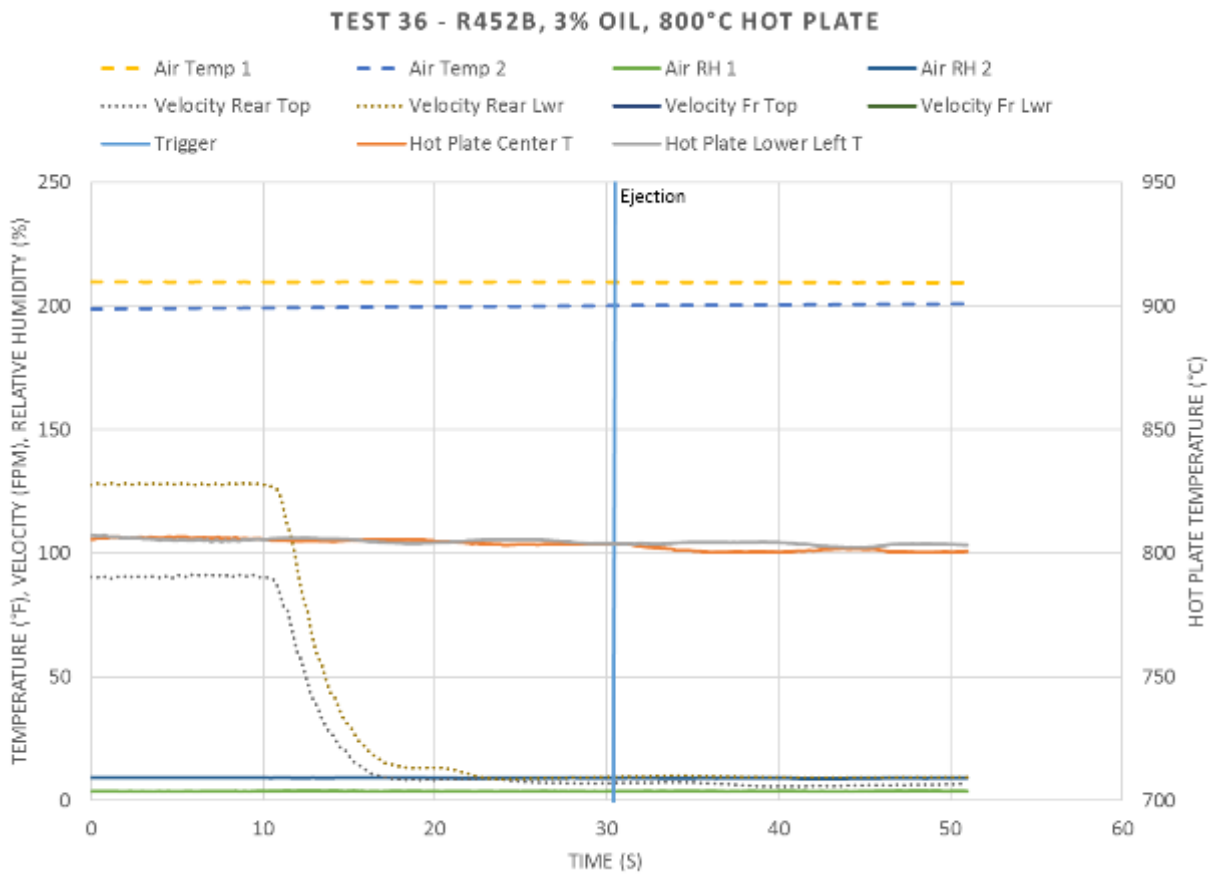


Figure 13 Test ID36 data.



Figure 14 Screenshots of ejection in 3/120s increments for test ID36 with R452B refrigerant mixed with 3% POE oil by mass, and with a hot plate temperature of 800°C (1472°F).

Summary

Hot surface ignition did not occur with pure R32, R1234ze, and R452B refrigerants on a flat, hot plate for hot plate temperatures up to 850°C (1562°F), ambient air temperatures of 93°C (200°F), humidity ratios of 0.023 kg/kg (0.023 lb/lb), and with the specific refrigerant ejection characteristics and natural convection flow characteristics in the chamber. Each refrigerant was tested 5 times in each test condition. Additionally, hot surface ignition did not occur with R32, R1234ze, and R452B refrigerants mixed with 3% POE oil by mass on a flat, hot plate for hot plate temperatures up to 800°C (1472°F), ambient air temperatures of 93°C (200°F), humidity ratios of 0.023 kg/kg (0.023 lb/lb), and with the specific refrigerant ejection characteristics and natural convection flow characteristics in the chamber.

In addition to the basic laboratory tests performed in this study, consideration of testing with actual equipment for further validation purposes is recommended. The hot surface ignition of refrigerants is a complex phenomenon which depends on surface geometry and temperature; ambient air temperature gradients and flow patterns; ambient air humidity; and the refrigerant delivery mechanism, including flow rate, flow duration, phase, temperature and pressure, and mixing with ambient air.

Potential future work in this area may include detailed modeling of the system in the current work to better understand the magnitude of natural convection currents associated with the flat, hot plate, the refrigerant release and mixing with the air, and any effects of a cross flow on the mixing process. The modeling may also provide a better understanding of the mixing process at all phases of the ejection process so that the size, location, mixture composition, and evolution of regions between the UFL and LFL can be identified. Modeling of the temperature field can be used to compare the temperatures with the AIT and assess the likelihood of ignition, and modeling of the velocity field can be used to estimate if forced and natural convective currents are high enough relative to the burning velocity of the refrigerant to inhibit ignition.

Future work may also consider a detailed survey of designs of HVAC&R units that may utilize A2L refrigerants, noting locations where a leak could be problematic, fluid characteristics in that location in the system (e.g. temperature, pressure, oil accumulation), and proximity to hot

surfaces in the system. That review could guide the design of testing in a test apparatus such as the one described in this work, or in in-situ testing, so that one may create a realistic refrigerant/oil/air mixture in the vicinity of a heater or hot surface that is the same or similar to one found in a production unit. Different variables could then be probed based on the result of that survey. It may be difficult to determine the surface temperatures of heaters or hot surfaces in production units accurately. One possibility is to develop a representative coil heater where the resistivity of the wire/coil is correlated to a temperature. Titanium wire may be a good candidate given its high change in resistivity.

Appendix A. List of Tests

| Test ID | Refrigerant | Charge (g/oz) | Oil | Target Velocity (cm/s / fpm) | Target Plate Temperature (°C/°F) | Ignition |
|---------|-------------|---------------|------|------------------------------|----------------------------------|----------------|
| 1 | R32 | 5.02/0.177 | None | <1 / <2 | 850/1562 ¹ | N |
| 2 | R32 | 4.92/0.174 | None | 25/50 | 850/1562 ¹ | N |
| 3 | R32 | 5.35/0.189 | None | <1 / <2 | 850/1562 | N ² |
| 4 | R32 | 5.21/0.184 | None | <1 / <2 | 850/1562 | N |
| 5 | R32 | 5.16/0.182 | None | <1 / <2 | 850/1562 | N |
| 6 | R32 | 5.19/0.183 | None | <1 / <2 | 790/1454 | N |
| 7 | R32 | 5.05/0.178 | None | <1 / <2 | 850/1562 | N |
| 8 | R32 | 4.65/0.164 | None | <1 / <2 | 850/1562 | N |
| 9 | R-452B | 5.32/0.188 | None | <1 / <2 | 850/1562 | N |
| 10 | R-452B | 5.11/0.180 | None | <1 / <2 | 850/1562 | N |
| 11 | R-452B | 5.3/0.187 | None | <1 / <2 | 850/1562 | N |
| 12 | R-452B | 5.21/0.184 | None | <1 / <2 | 850/1562 | N |
| 13 | R-452B | 5.33/0.188 | None | <1 / <2 | 850/1562 | N |
| 14 | R-1234ze | 5.3/0.187 | None | <1 / <2 | 850/1562 | N |
| 15 | R-1234ze | 5.28/0.186 | None | <1 / <2 | 850/1562 | N |
| 16 | R-1234ze | 5.31/0.187 | None | <1 / <2 | 850/1562 | N |
| 17 | R-1234ze | 5.05/0.178 | None | <1 / <2 | 850/1562 | N |
| 18 | R-1234ze | 5.31/0.187 | None | <1 / <2 | 850/1562 | N |
| 19 | R-1234ze | 5.11/0.180 | 3% | <1 / <2 | 700/1292 | N |
| 20 | R-1234ze | 5.04/0.178 | 3% | <1 / <2 | 700/1292 | N |
| 21 | R-1234ze | 4.81/0.170 | 3% | <1 / <2 | 700/1292 | N |
| 22 | R-1234ze | 5.09/0.180 | 3% | <1 / <2 | 700/1292 | N |
| 23 | R-1234ze | 5.26/0.186 | 3% | <1 / <2 | 700/1292 | N |
| 24 | R32 | 5.14/0.181 | 3% | <1 / <2 | 700/1292 | N |
| 25 | R32 | 5.11/0.180 | 3% | <1 / <2 | 700/1292 | N |
| 26 | R32 | 5.23/0.184 | 3% | <1 / <2 | 700/1292 | N |
| 27 | R32 | 4.81/0.170 | 3% | <1 / <2 | 700/1292 | N |
| 28 | R32 | 4.81/0.170 | 3% | <1 / <2 | 700/1292 | N |
| 29 | R-452B | 5.18/0.183 | 3% | <1 / <2 | 700/1292 | N |
| 30 | R-452B | 5.17/0.182 | 3% | <1 / <2 | 700/1292 | N |
| 31 | R-452B | 5.14/0.181 | 3% | <1 / <2 | 700/1292 | N ³ |
| 32 | R-452B | 4.89/0.172 | 3% | <1 / <2 | 700/1292 | N |
| 33 | R-452B | 4.62/0.163 | 3% | <1 / <2 | 700/1292 | N |
| 34 | DR55 | 4.64/0.164 | 3% | <1 / <2 | 800/1472 | N |
| 35 | DR55 | 5.34/0.188 | 3% | <1 / <2 | 800/1472 | N |
| 36 | DR55 | 5.45/0.192 | 3% | <1 / <2 | 800/1472 | N |
| 37 | DR55 | 5.54/0.195 | 3% | <1 / <2 | 800/1472 | N |
| 38 | DR55 | 5.22/0.184 | 3% | <1 / <2 | 800/1472 | N |
| 39 | R32 | 5.38/0.190 | 3% | <1 / <2 | 800/1472 | N |
| 40 | R32 | 5.07/0.179 | 3% | <1 / <2 | 800/1472 | N |
| 41 | R32 | 4.45/0.157 | 3% | <1 / <2 | 800/1472 | N |
| 42 | R32 | 5.39/0.190 | 3% | <1 / <2 | 800/1472 | N |
| 43 | R32 | 5.43/0.192 | 3% | <1 / <2 | 800/1472 | N |
| 44 | R-1234ze | 5.17/0.182 | 3% | <1 / <2 | 800/1472 | N |
| 45 | R-1234ze | 5.28/0.186 | 3% | <1 / <2 | 800/1472 | N |
| 46 | R-1234ze | 5.52/0.195 | 3% | <1 / <2 | 800/1472 | N |
| 47 | R-1234ze | 4.45/0.157 | 3% | <1 / <2 | 800/1472 | N |
| 48 | R-1234ze | 5.53/0.195 | 3% | <1 / <2 | 800/1472 | N |

¹ Hot plate was 8" x 8"

² Hot plate had 4" diameter planchet. Ignition in enclosed area between insulation, hot plate, and planchet. See Figure A1.

³ Ignition near enclosed area between hot plate and chamber interface.

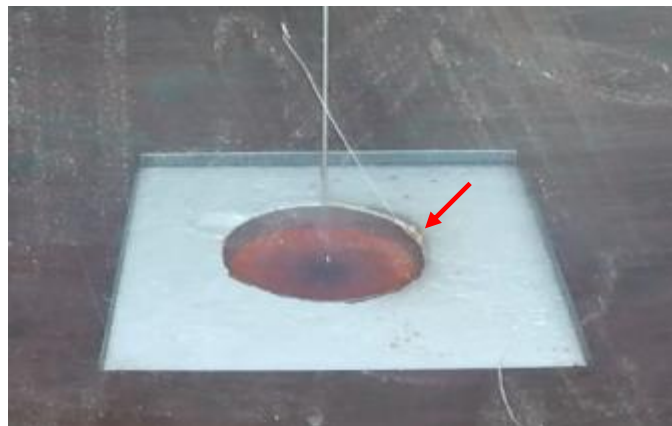
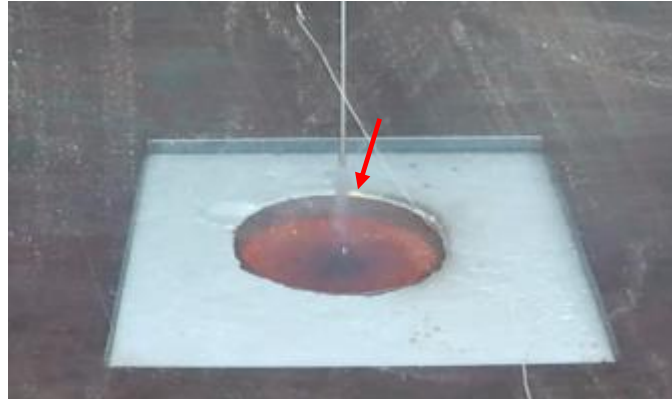
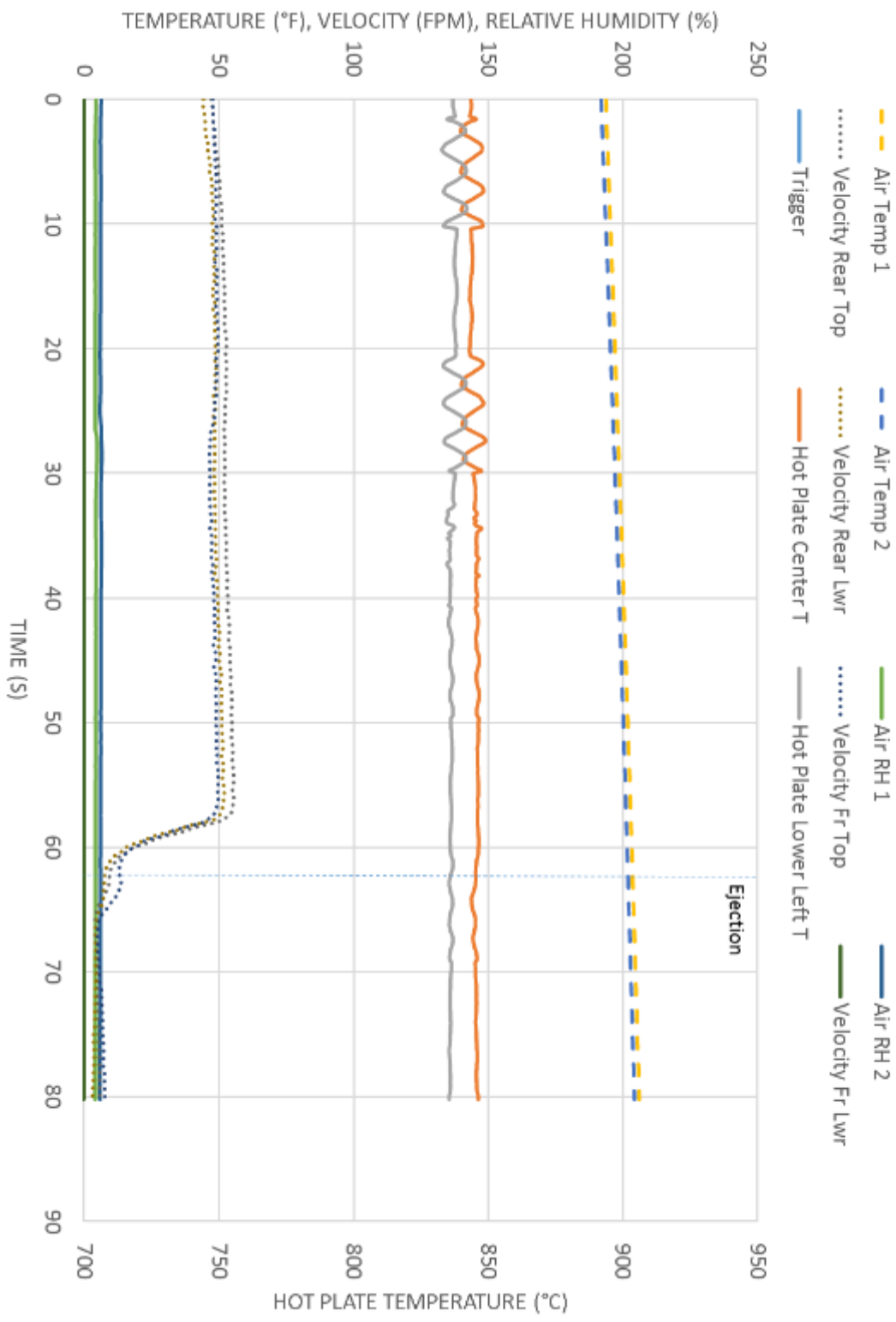


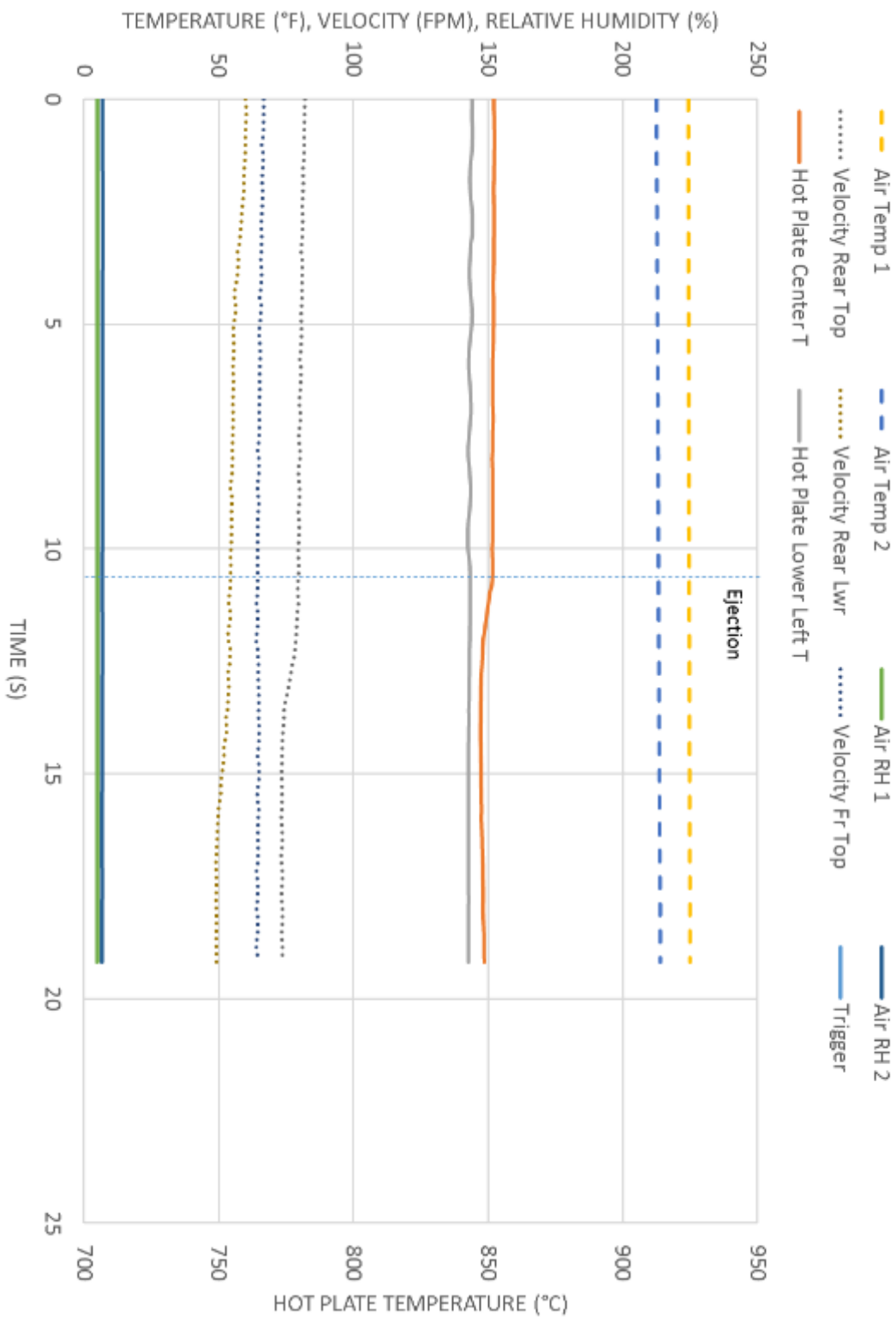
Figure A1 Screenshots from test ID3 showing a momentary ignition in the region between the hot plate, insulation, and planchet.

Appendix B. Test Data

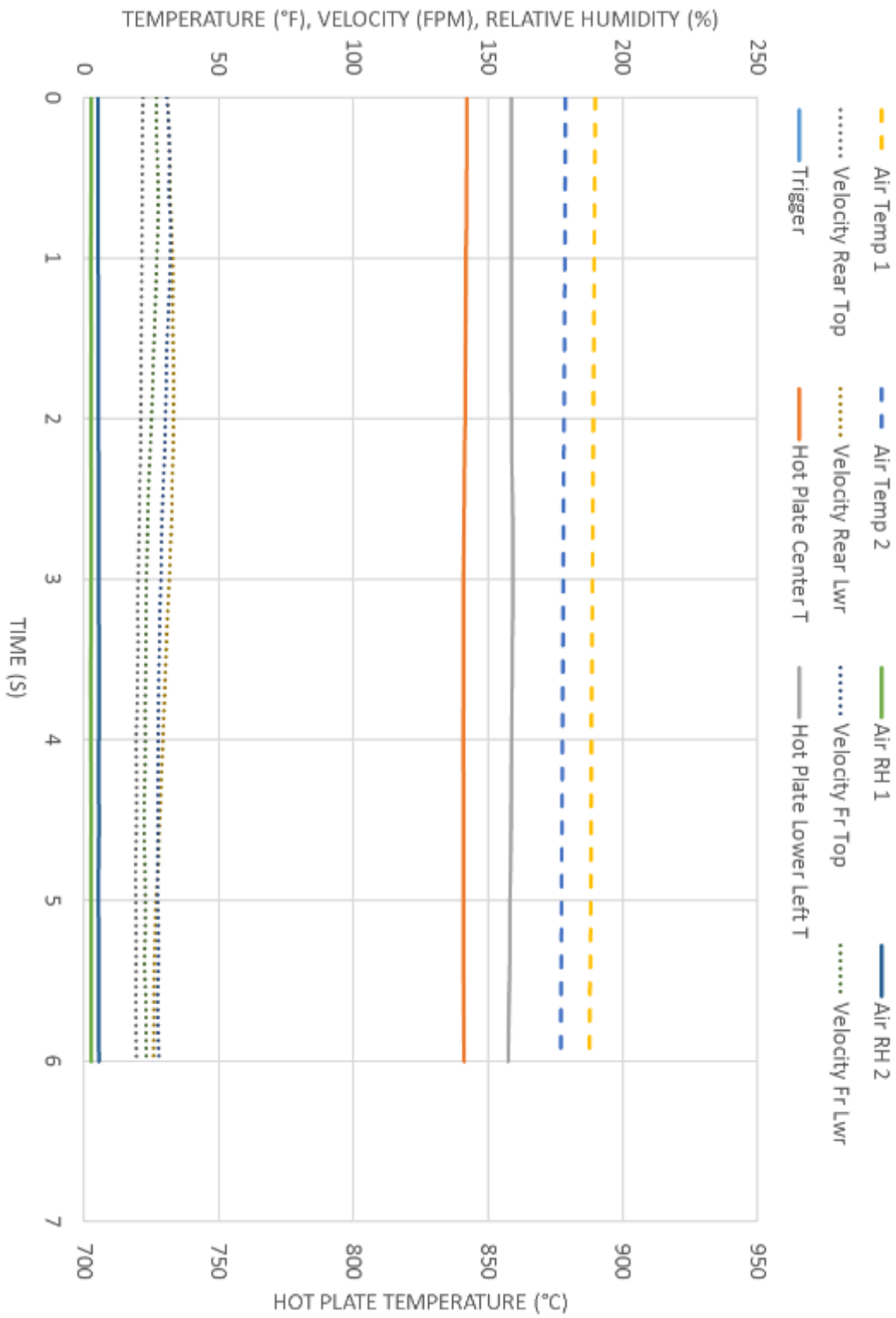
TEST 1 - R32, 850°C HOT PLATE



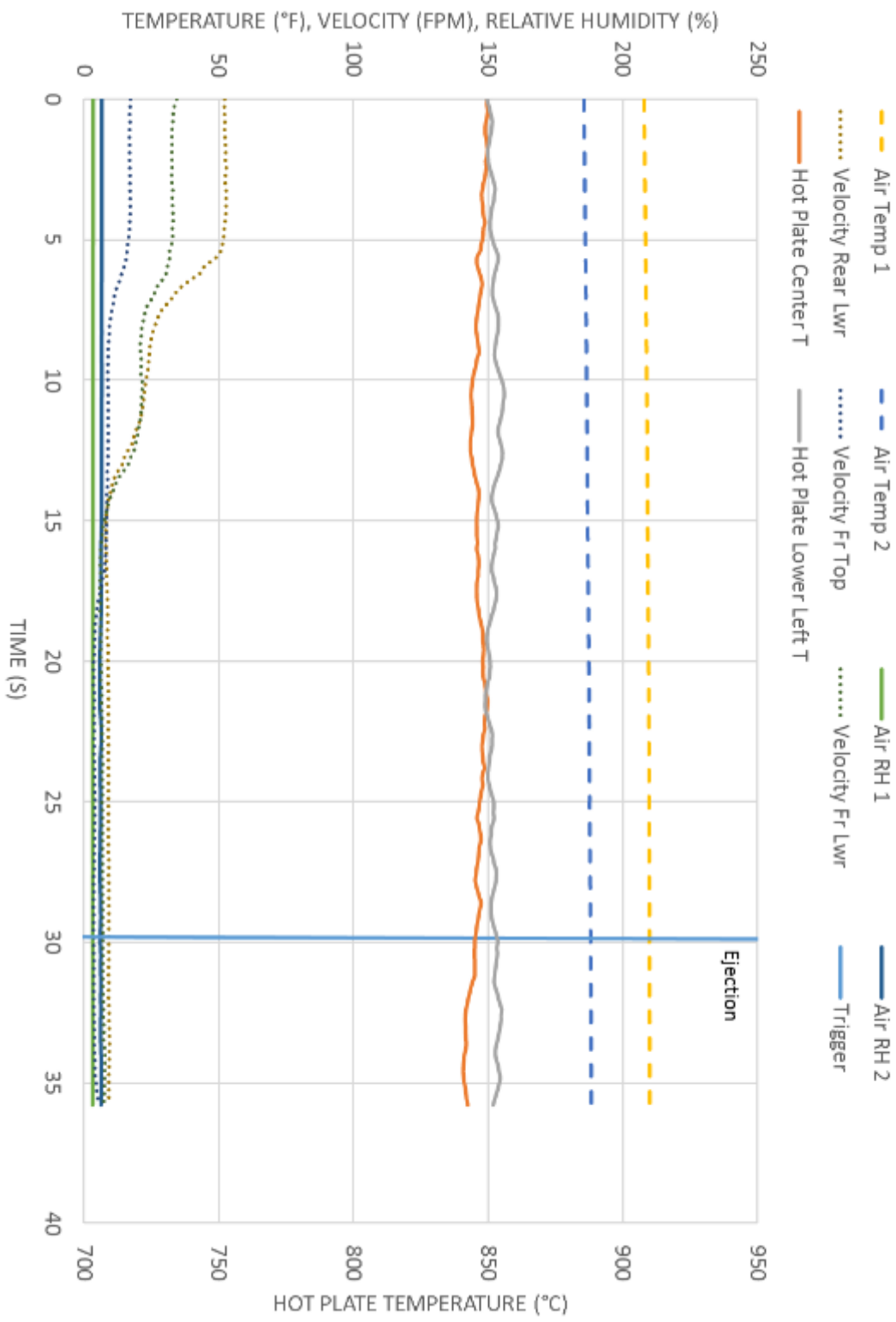
TEST 2 - R32, 850°C HOT PLATE



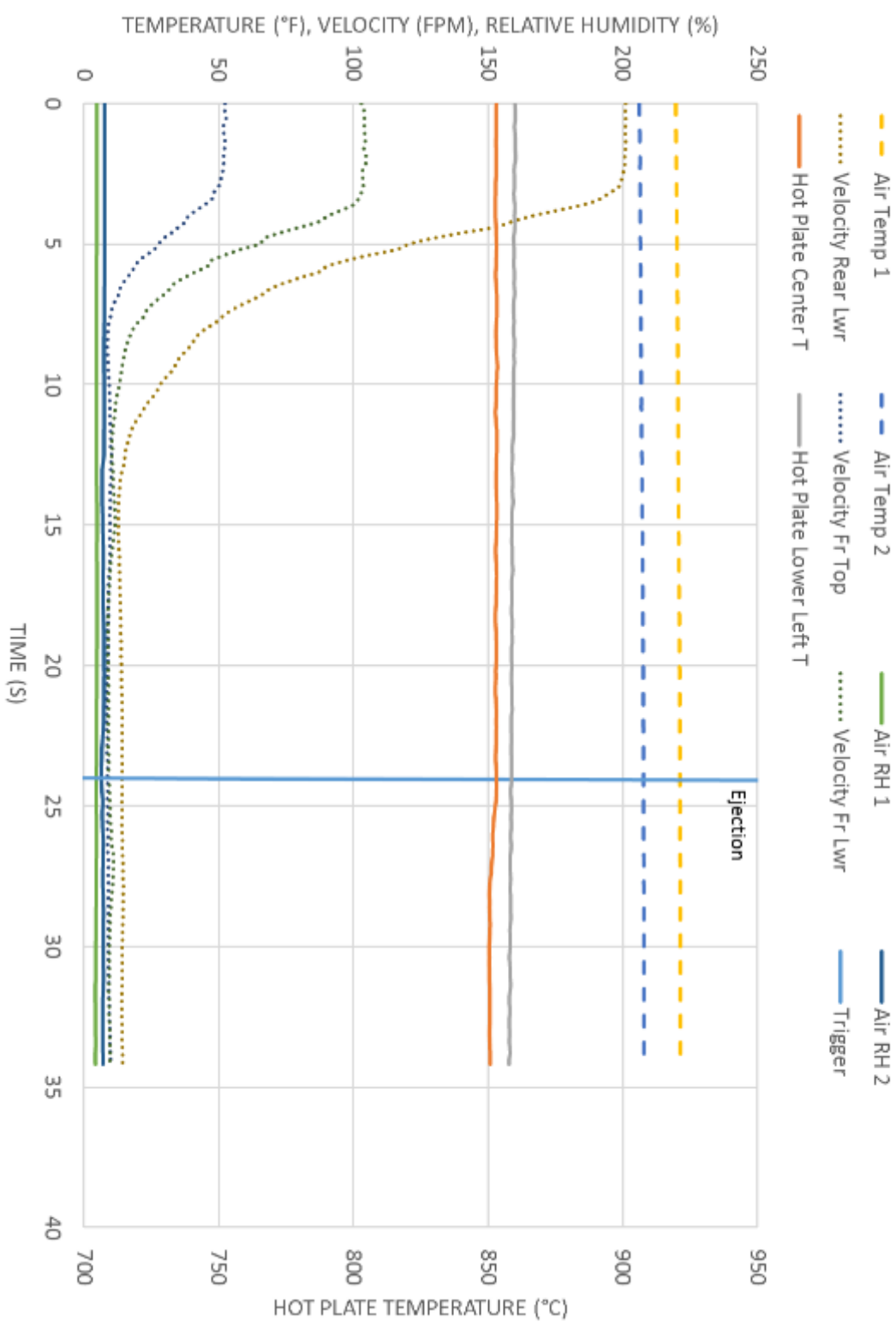
TEST 3 - R32, 850°C HOT PLATE, DATA COLLECTED AFTER EJECTION



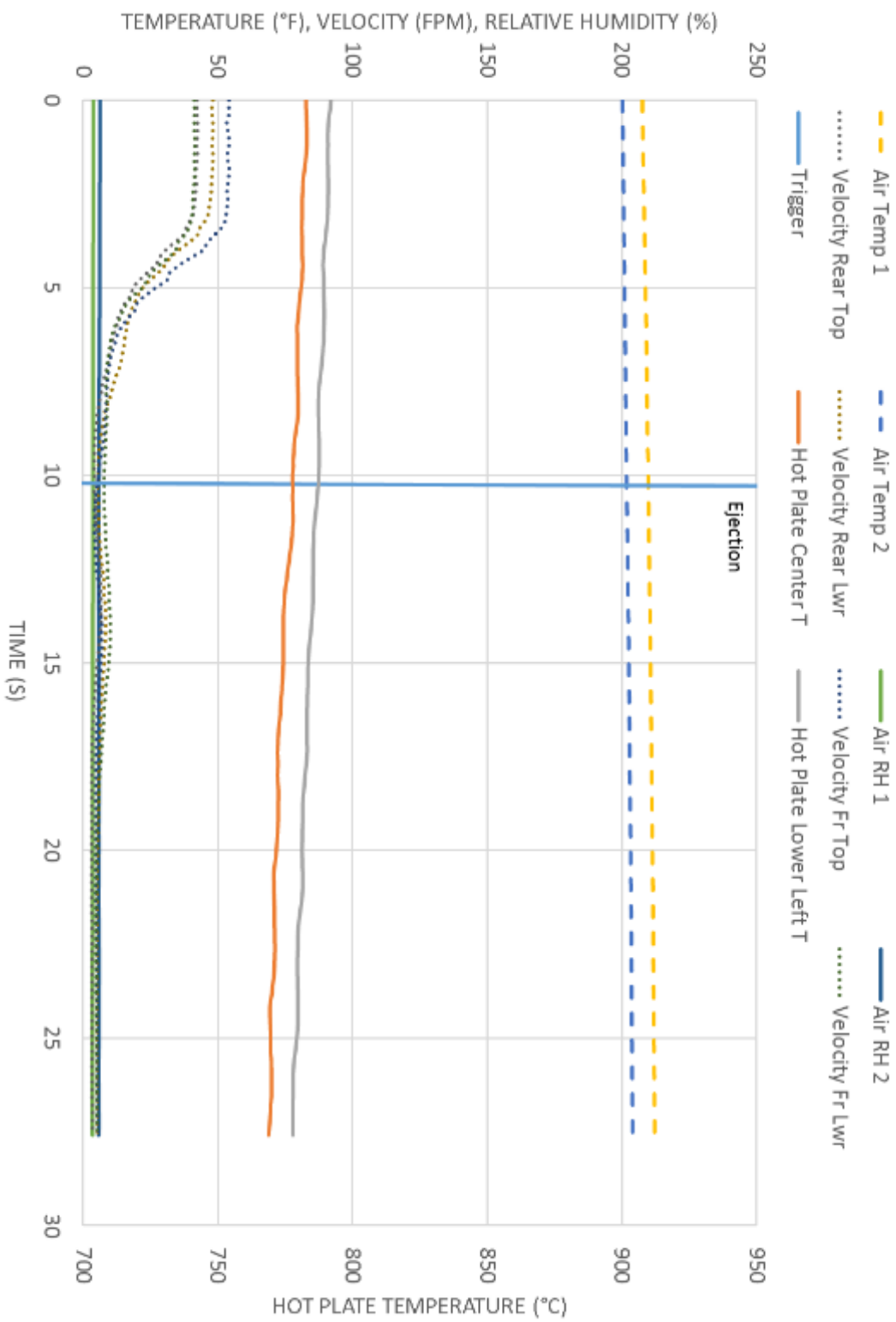
TEST 4 - R32, 850°C HOT PLATE



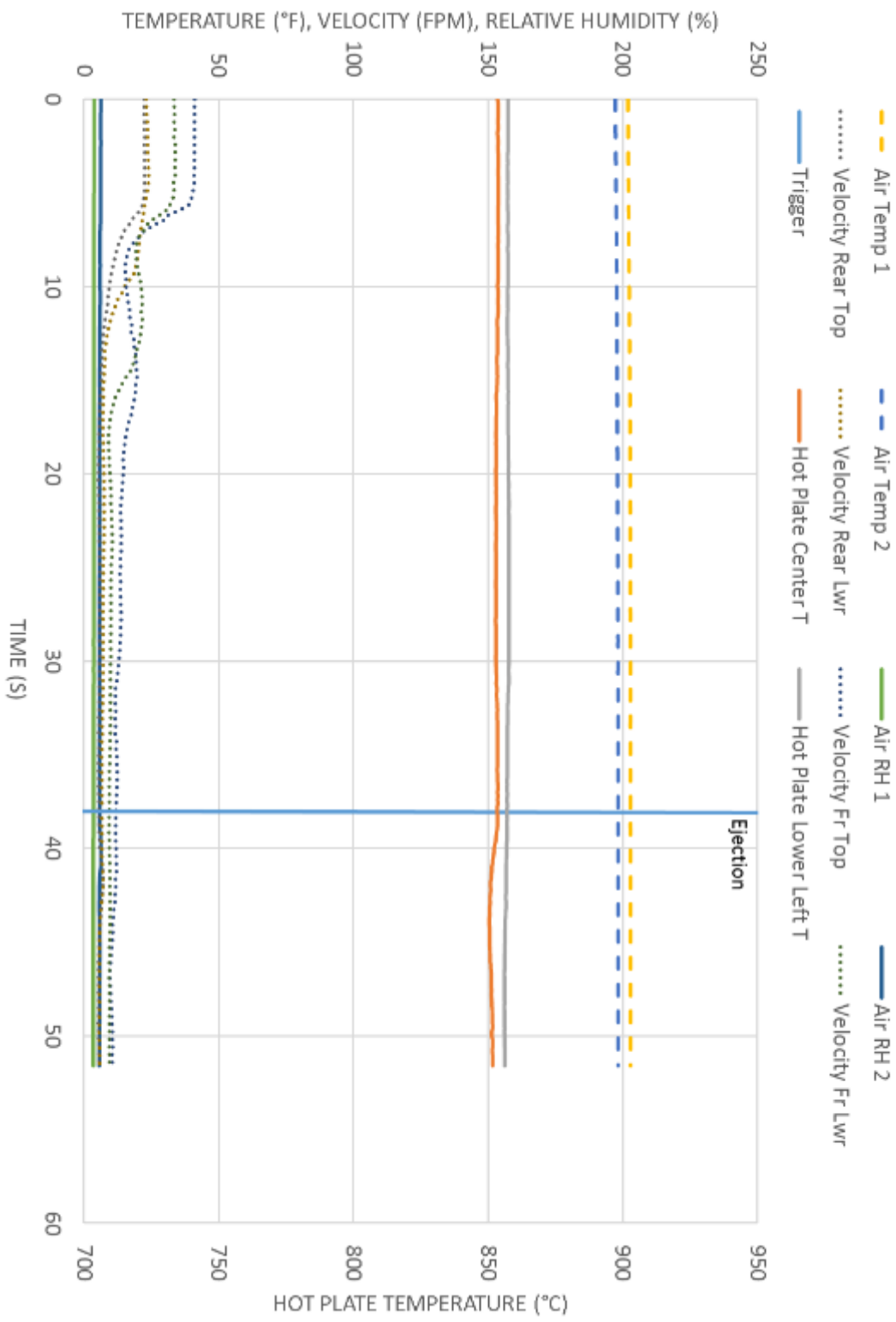
TEST 5 - R32, 850°C HOT PLATE



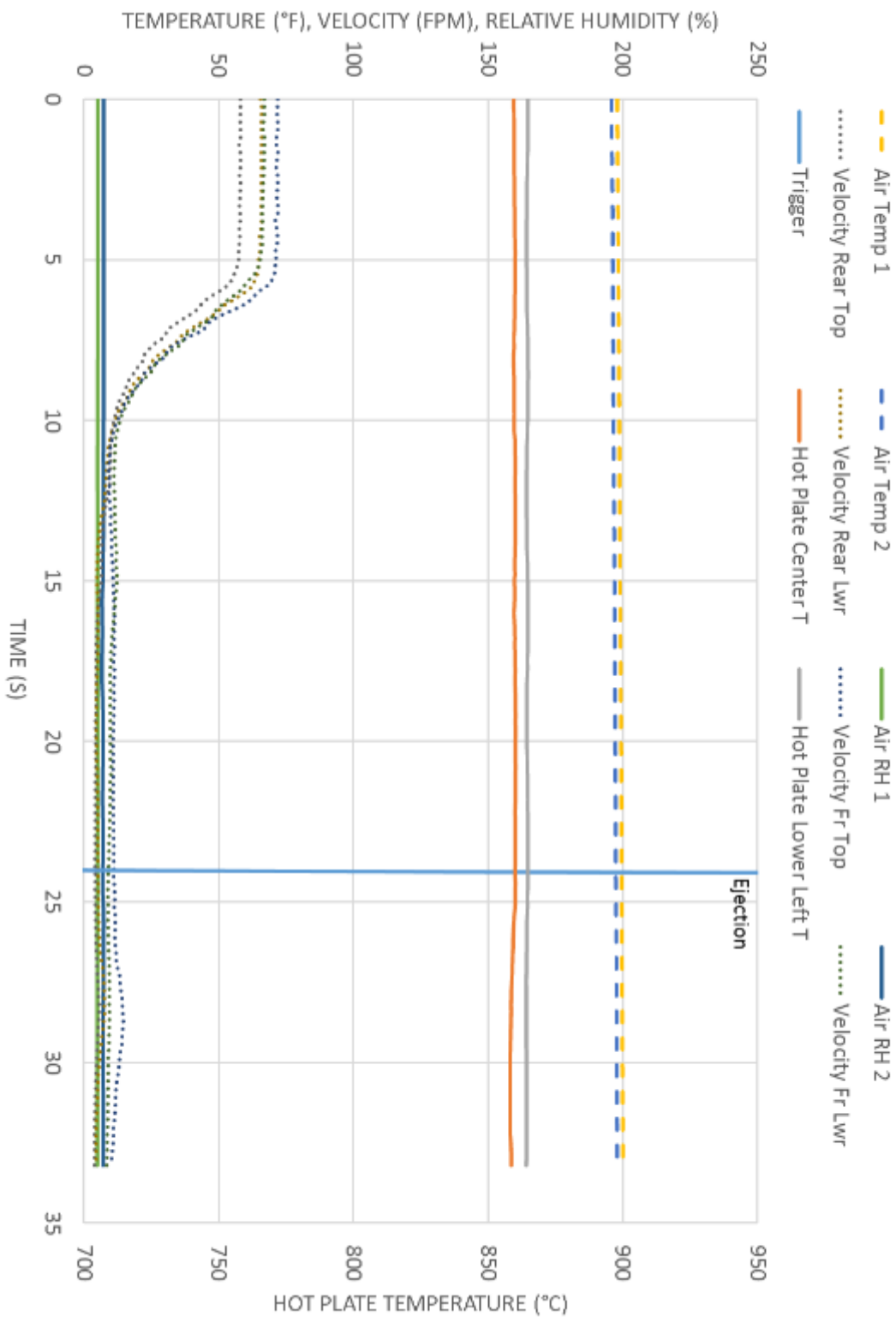
TEST 6 - R32, 790°C HOT PLATE



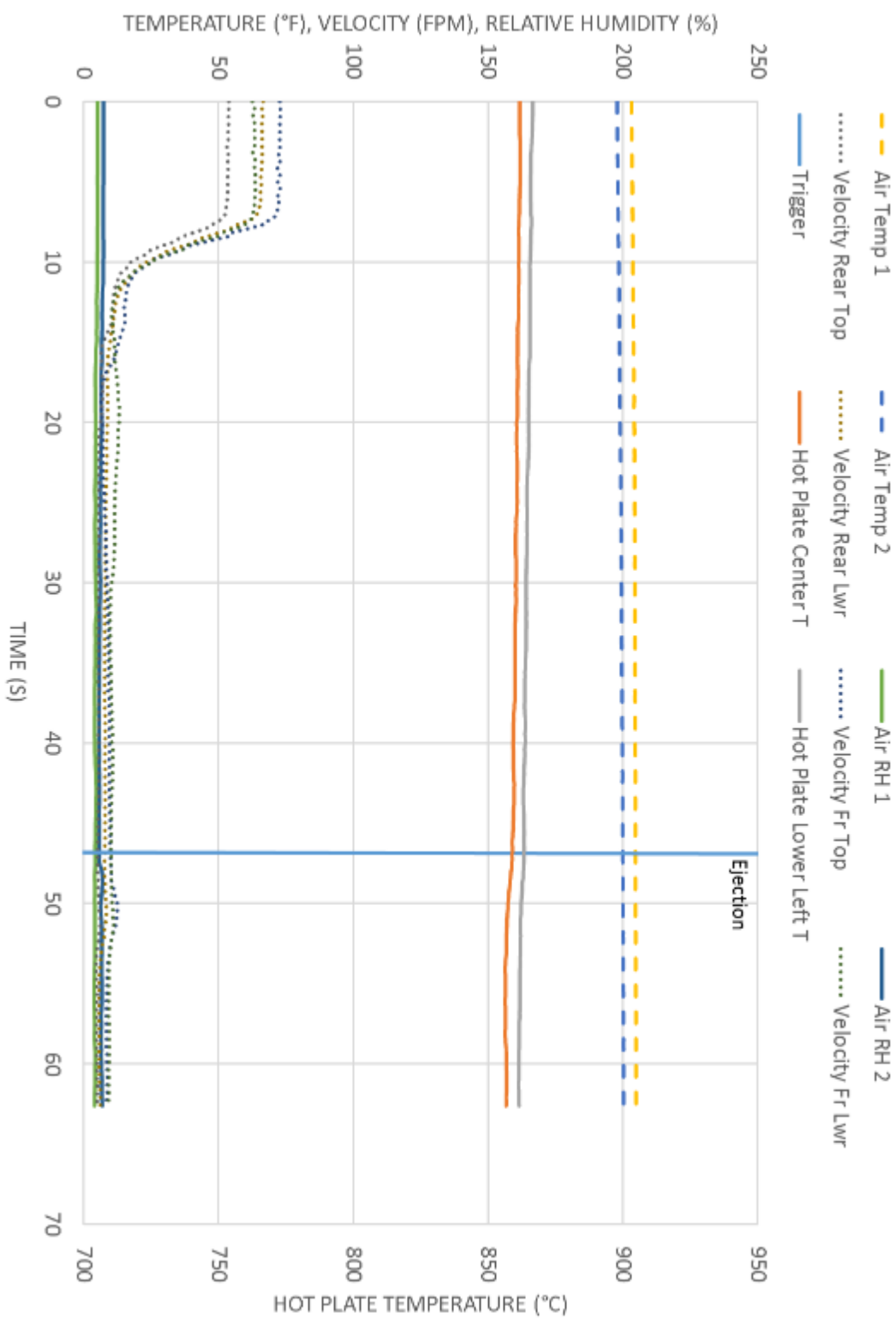
TEST 7 - R32, 850°C HOT PLATE



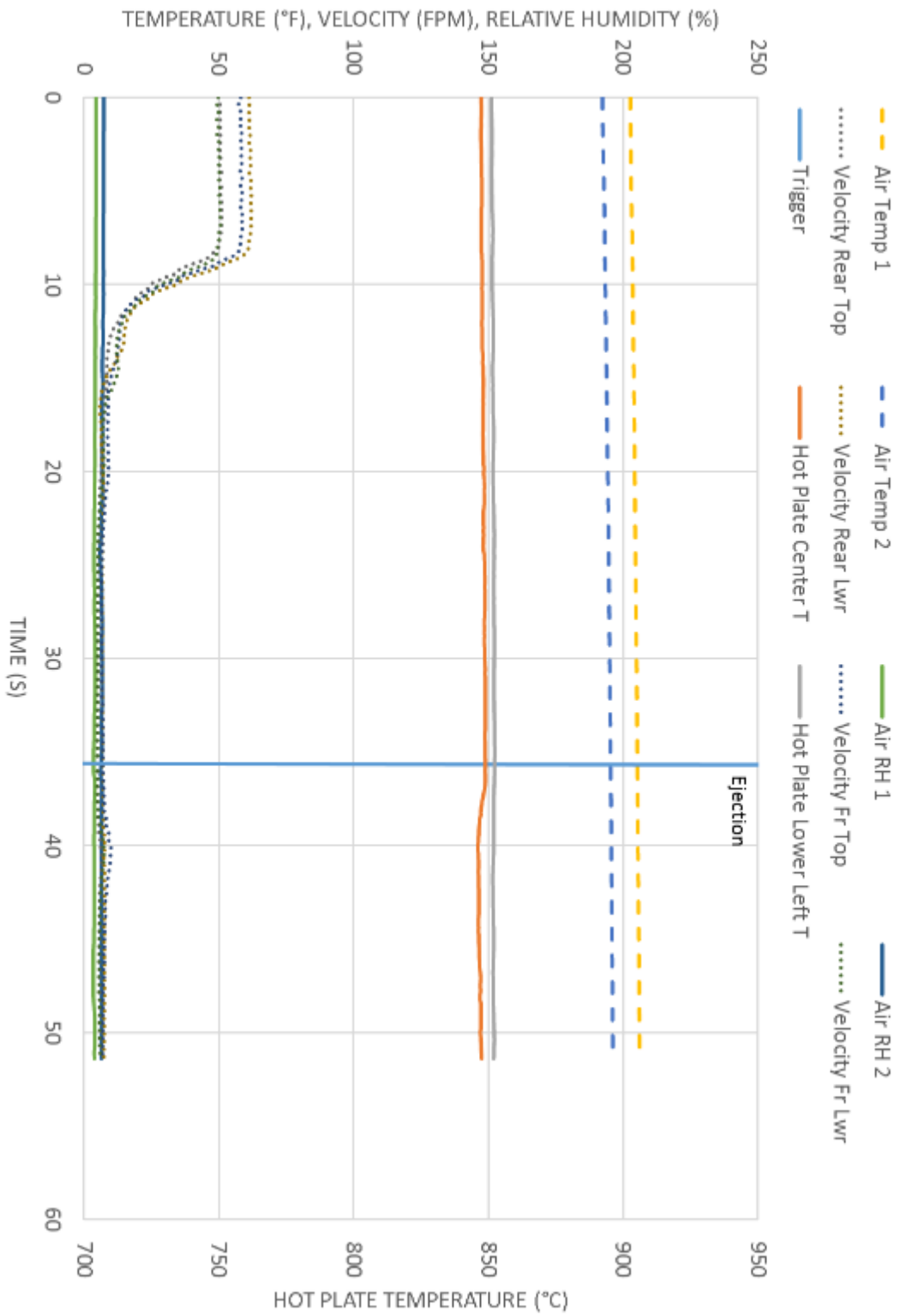
TEST 8 - R32, 850°C HOT PLATE



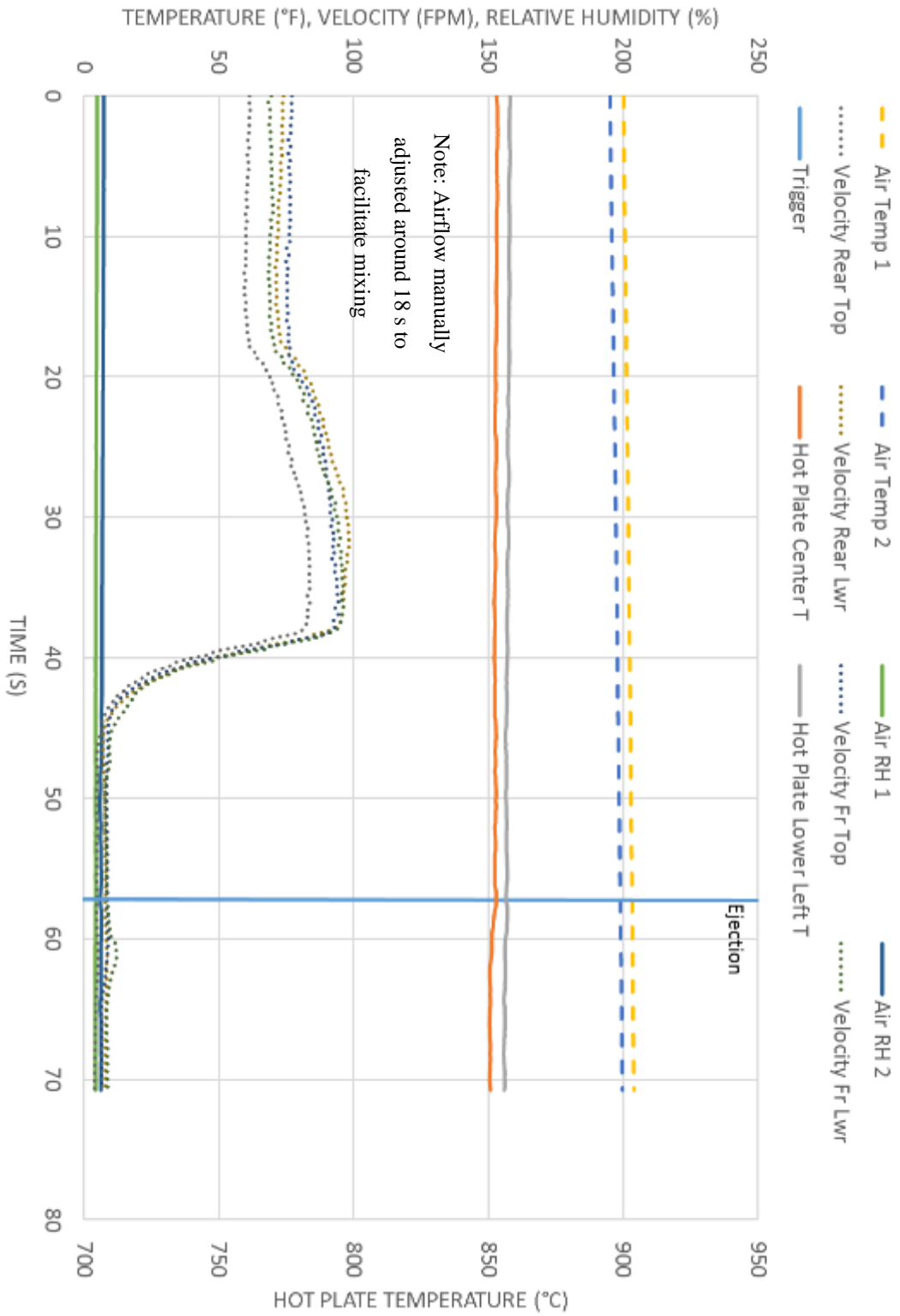
TEST 9 - R452B, 850°C HOT PLATE



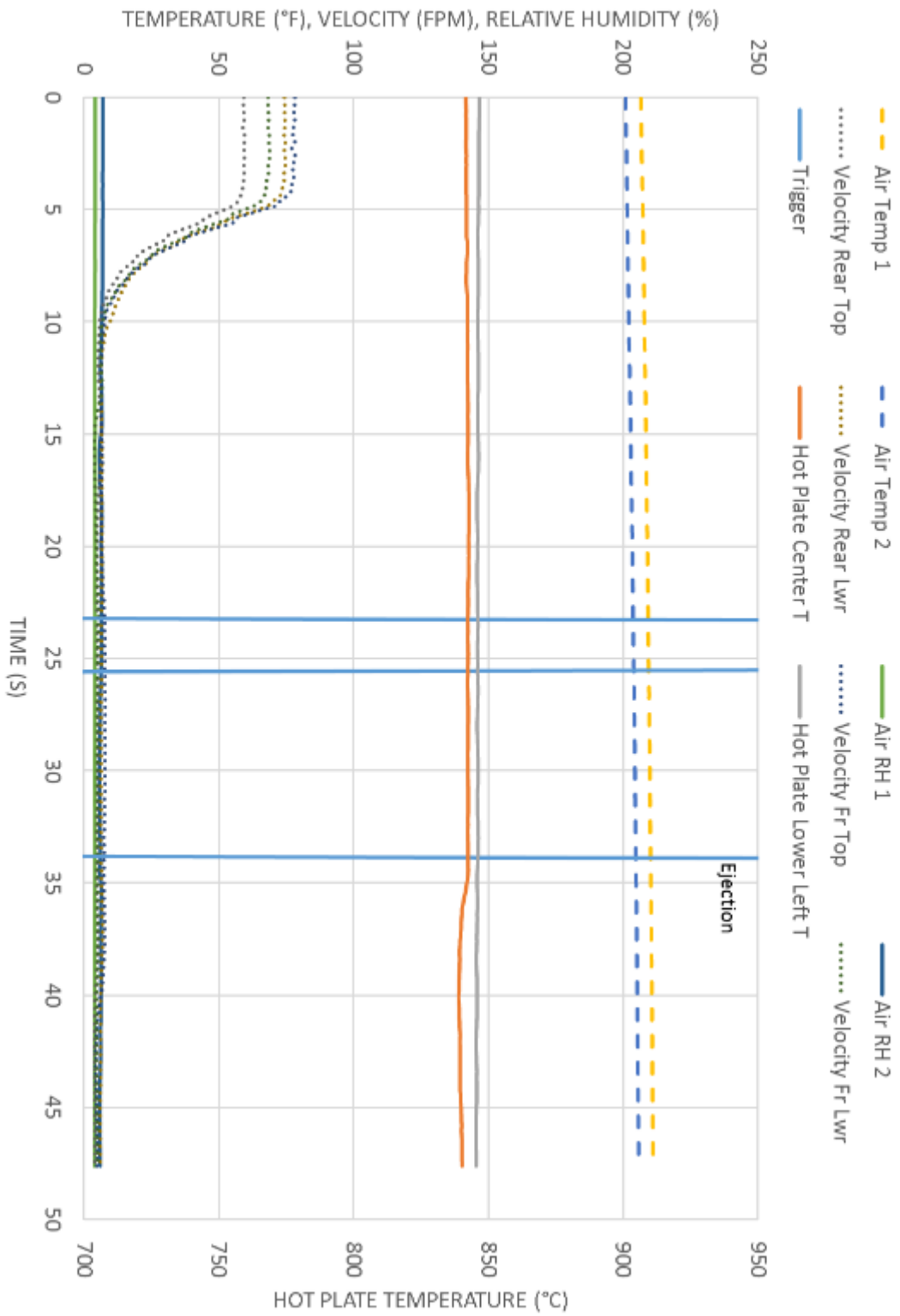
TEST 10 - R452B, 850°C HOT PLATE



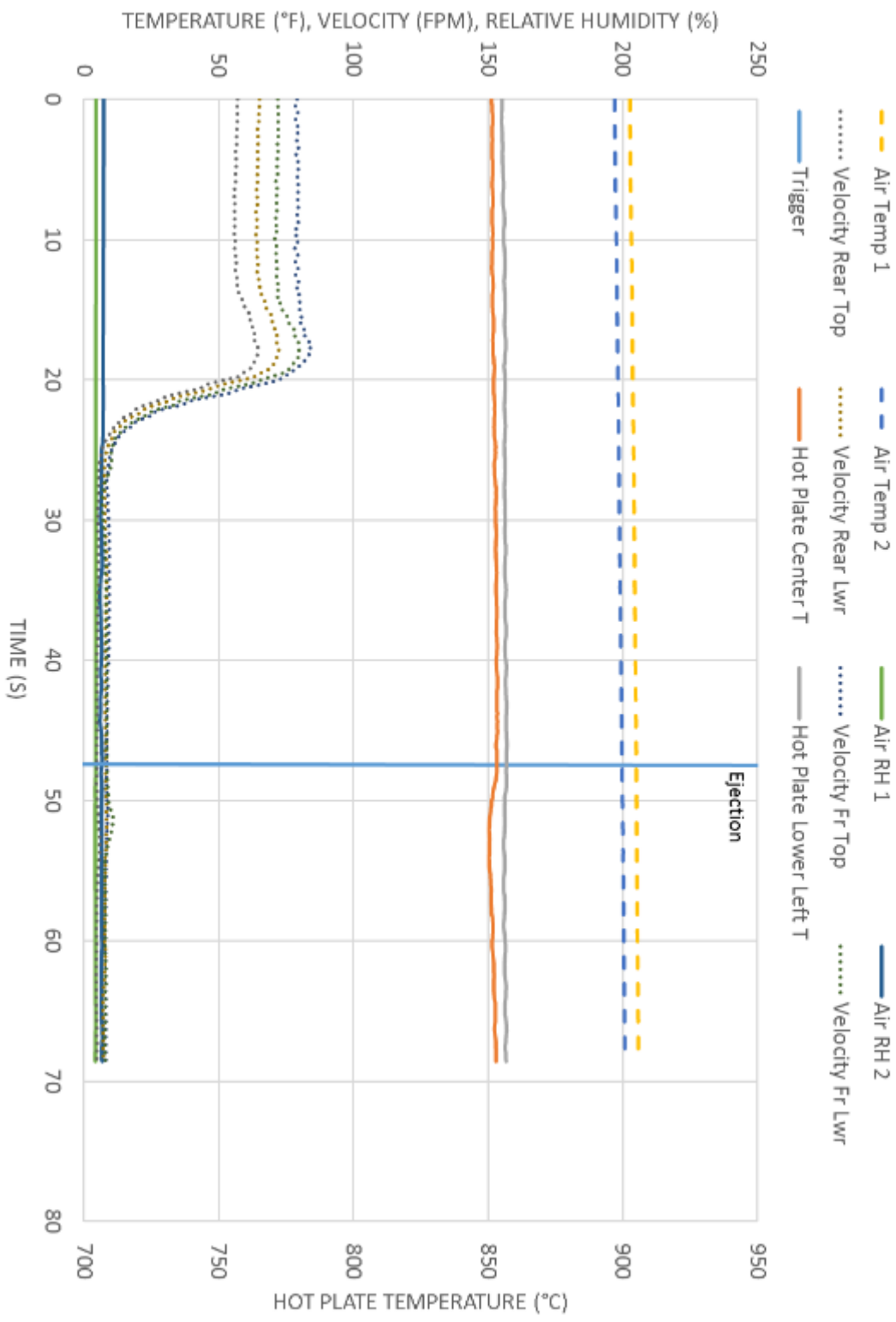
TEST 11 - R452B, 850°C HOT PLATE



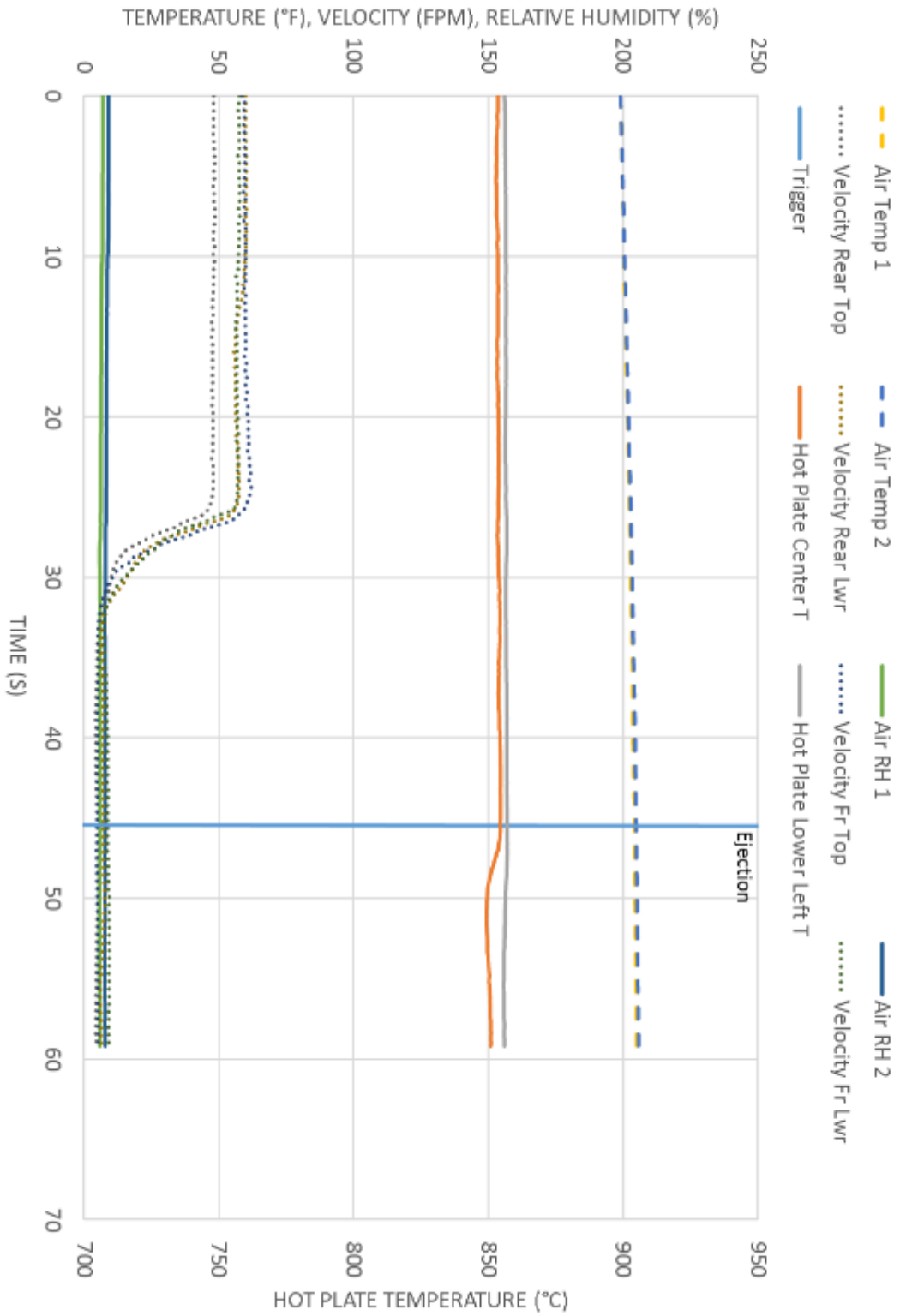
TEST 12 - R452B, 850°C HOT PLATE



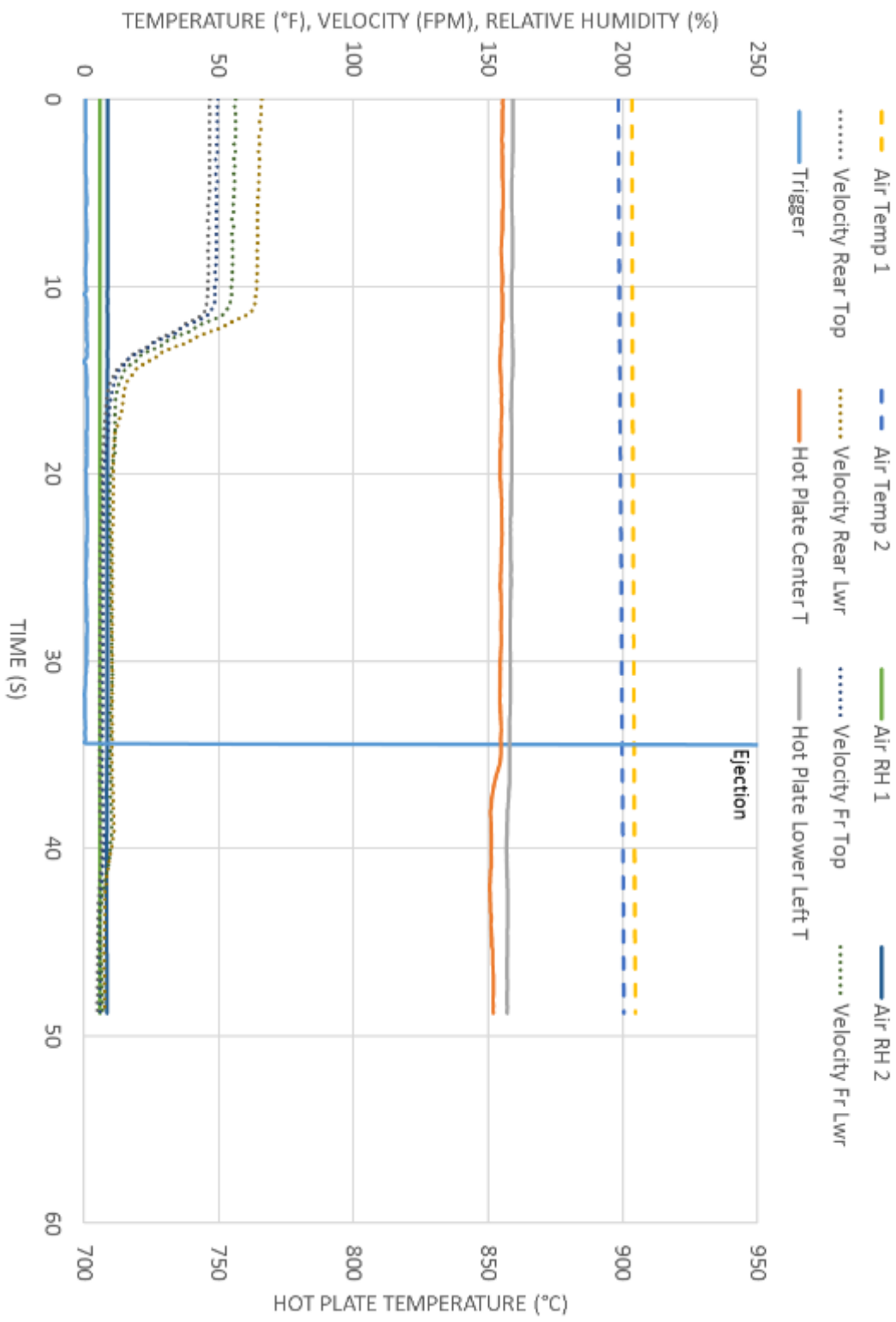
TEST 13 - R452B, 850°C HOT PLATE



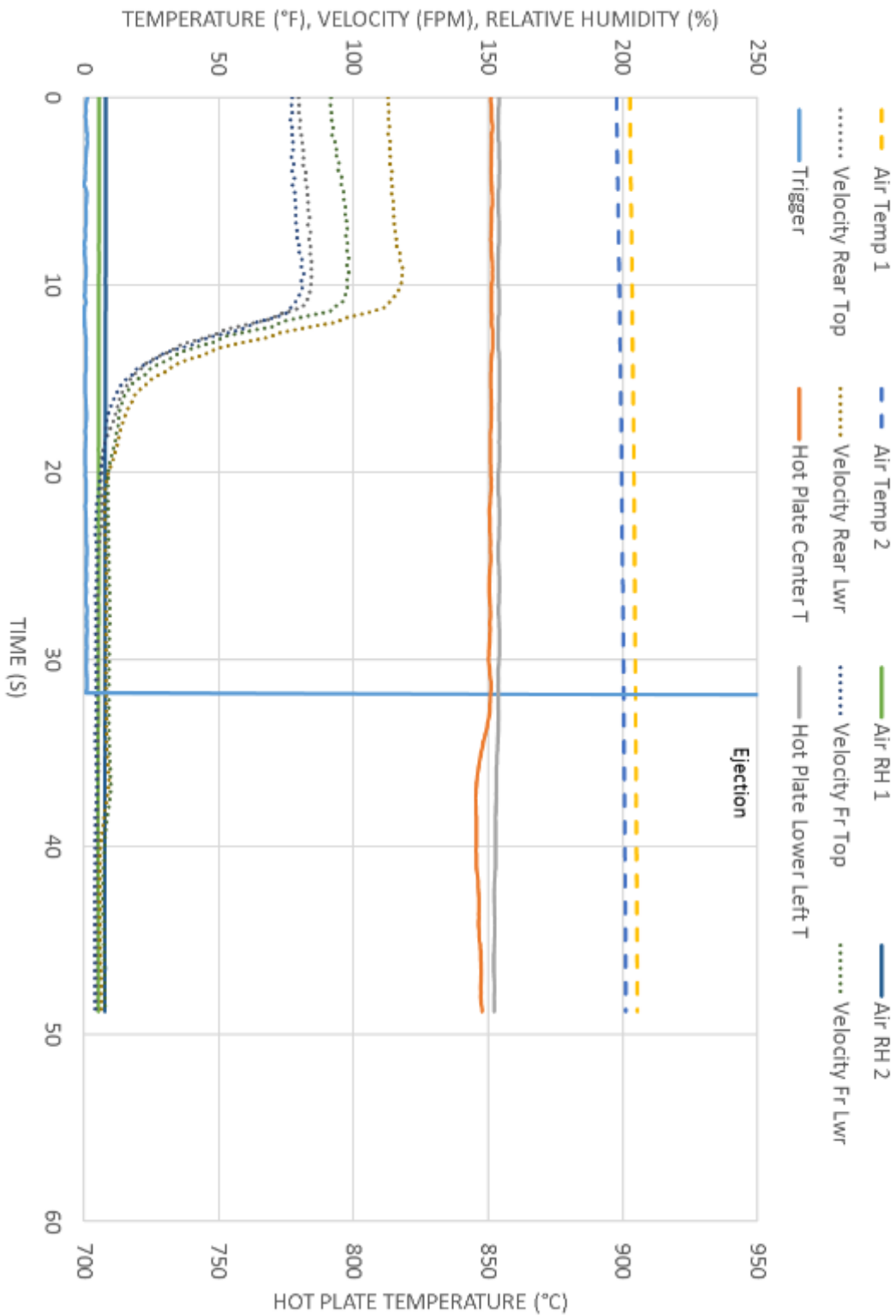
TEST 14 - R1234ZE, 850°C HOT PLATE



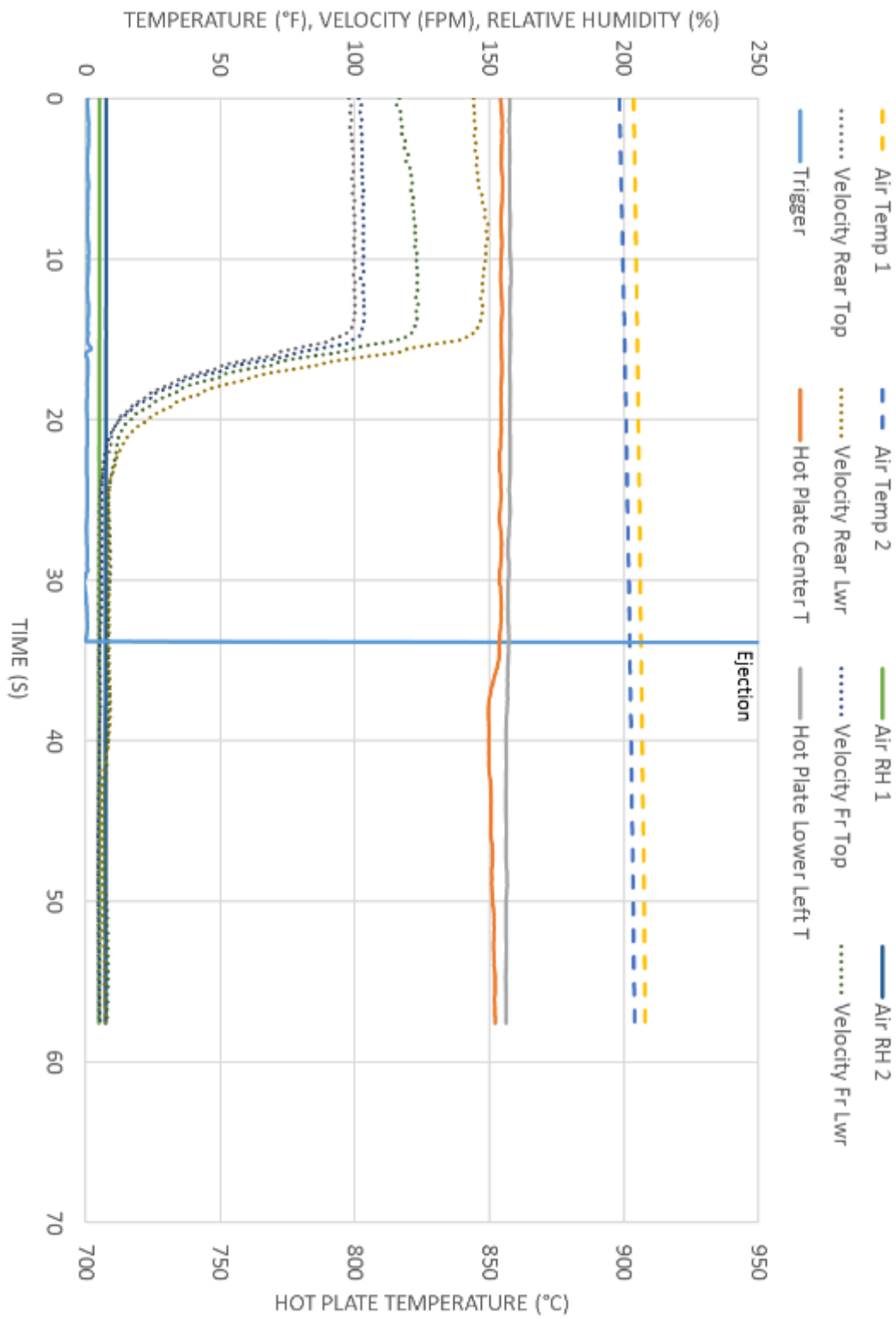
TEST 15 - R1234ZE, 850°C HOT PLATE



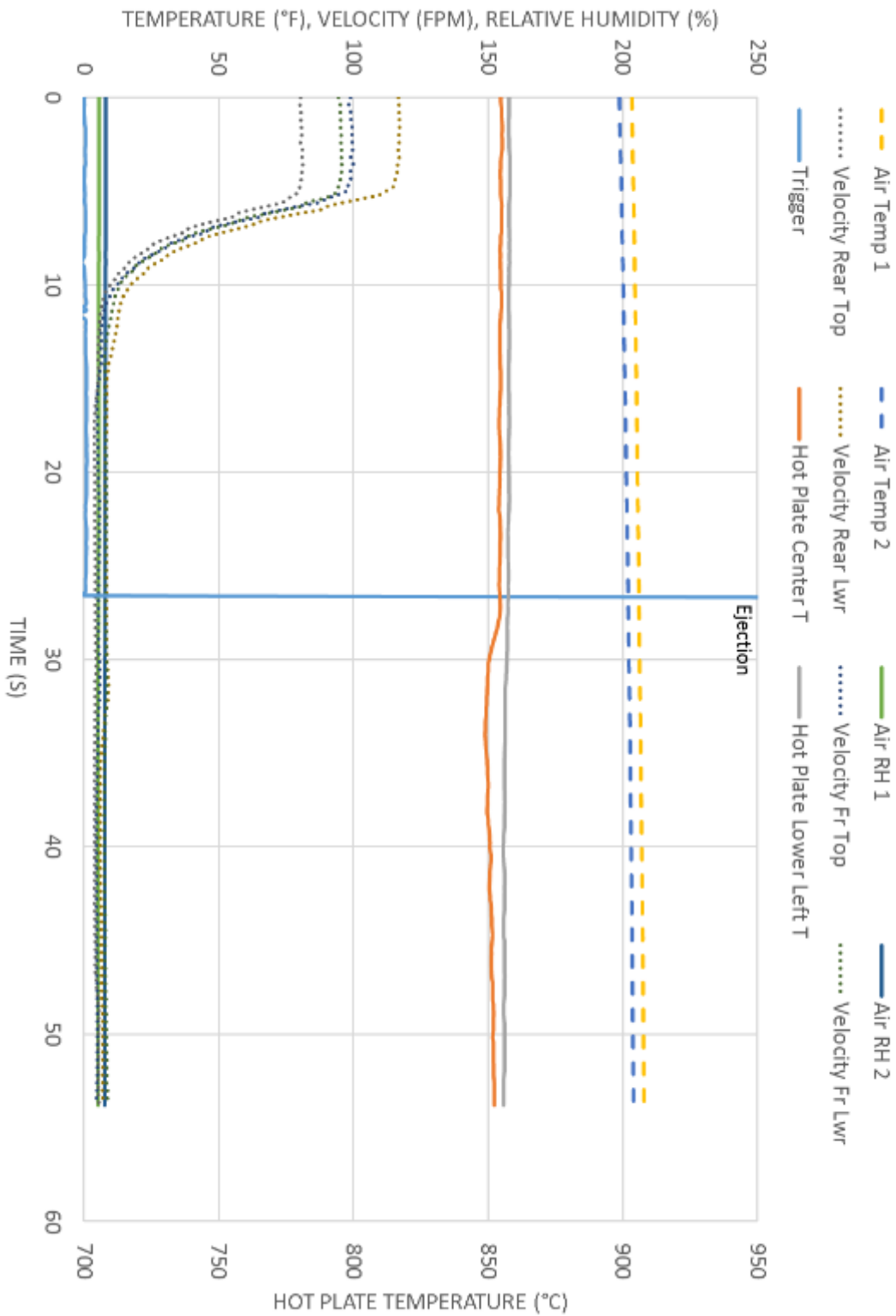
TEST 16 - R1234ZE, 850°C HOT PLATE



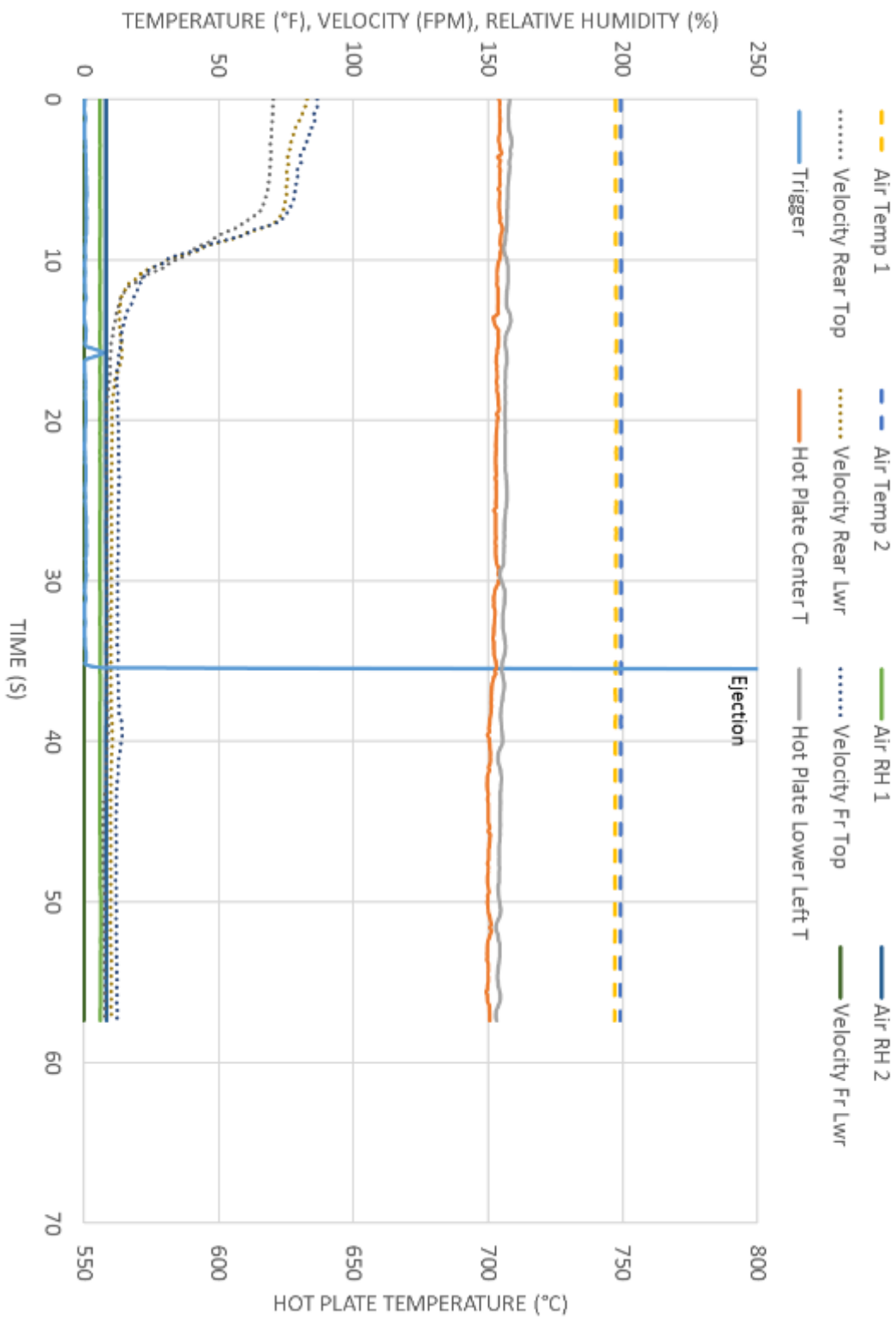
TEST 17 - R1234ZE, 850°C HOT PLATE



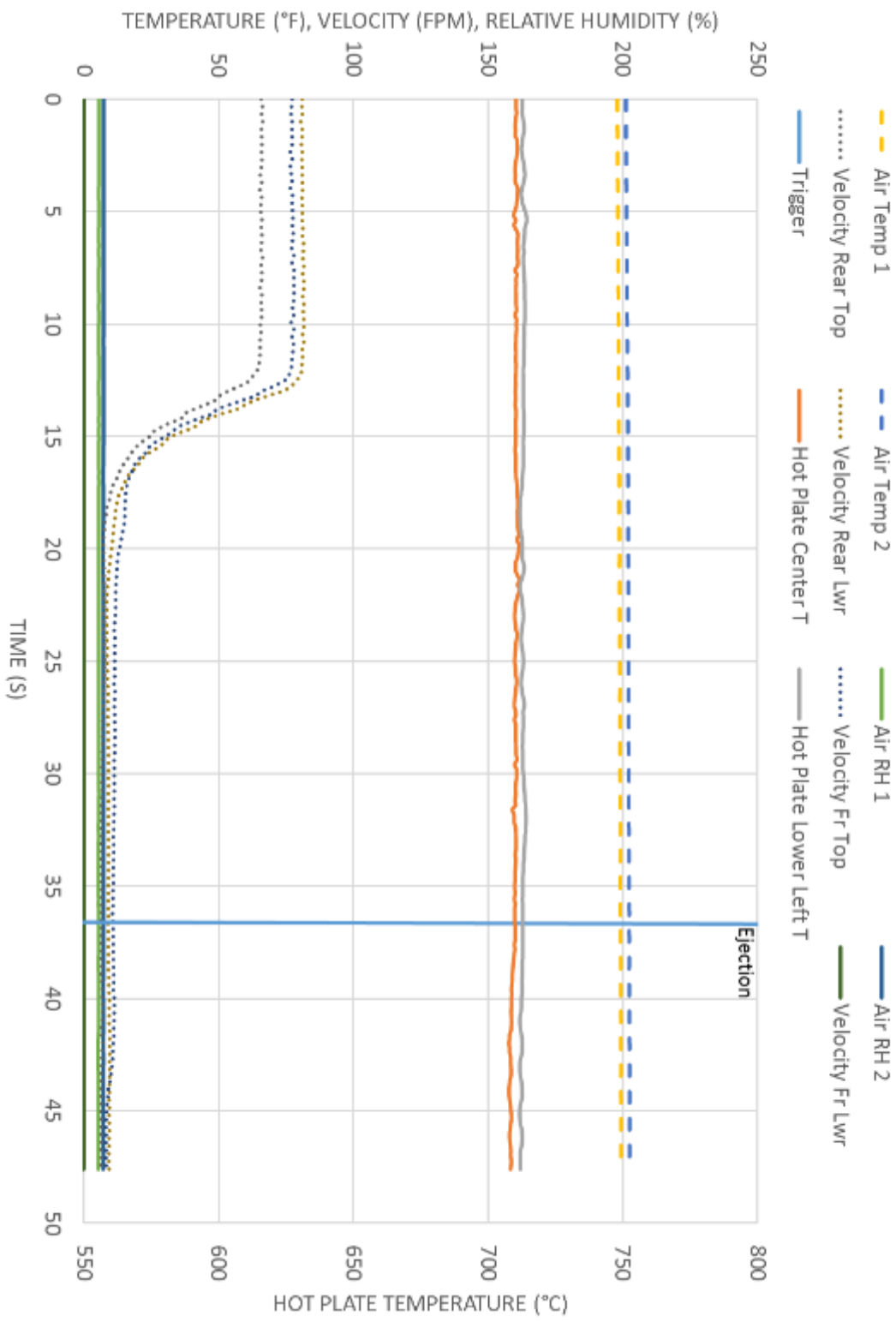
TEST 18 - R1234ZE, 850°C HOT PLATE



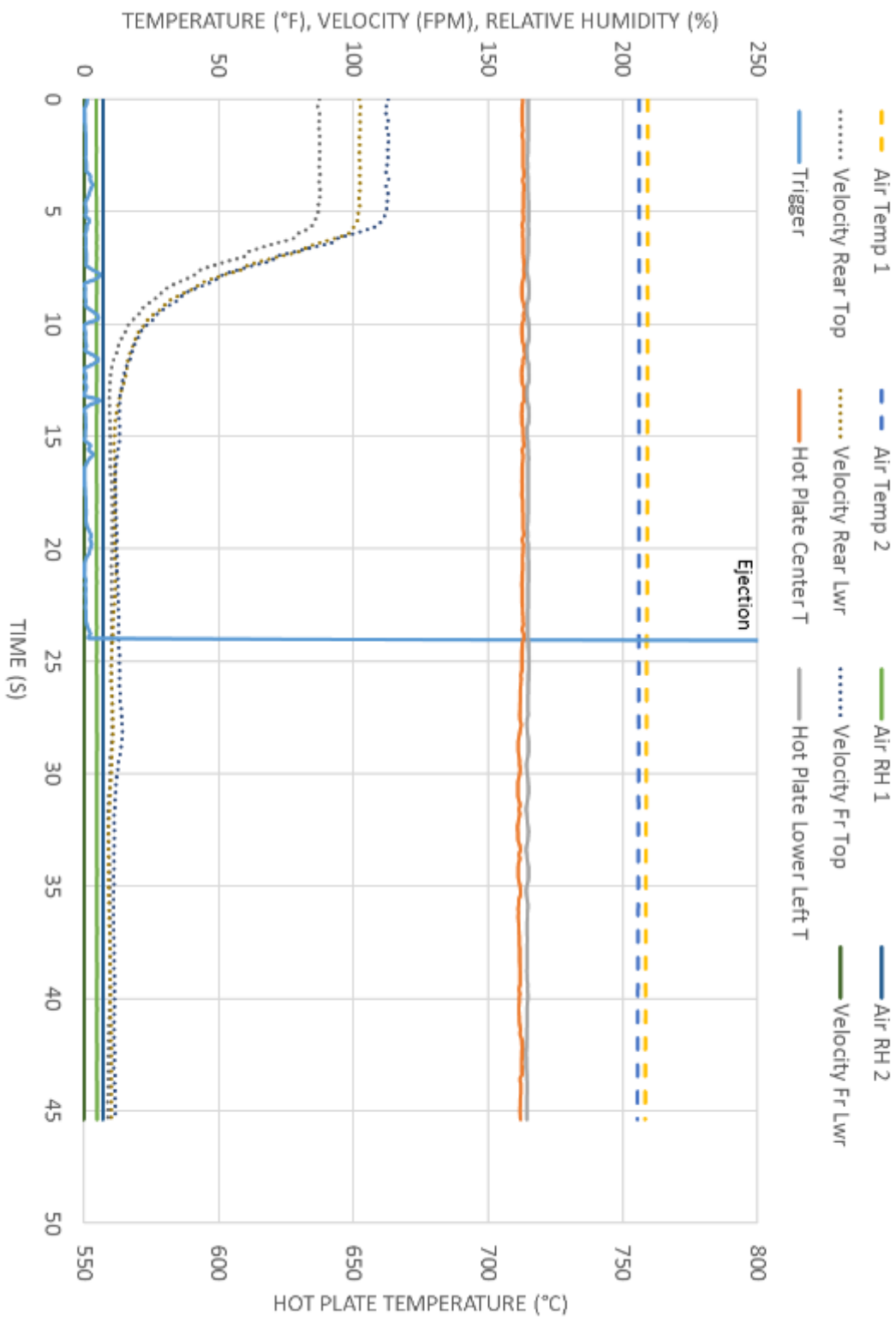
TEST 19 - R1234ZE, 3% OIL, 700°C HOT PLATE



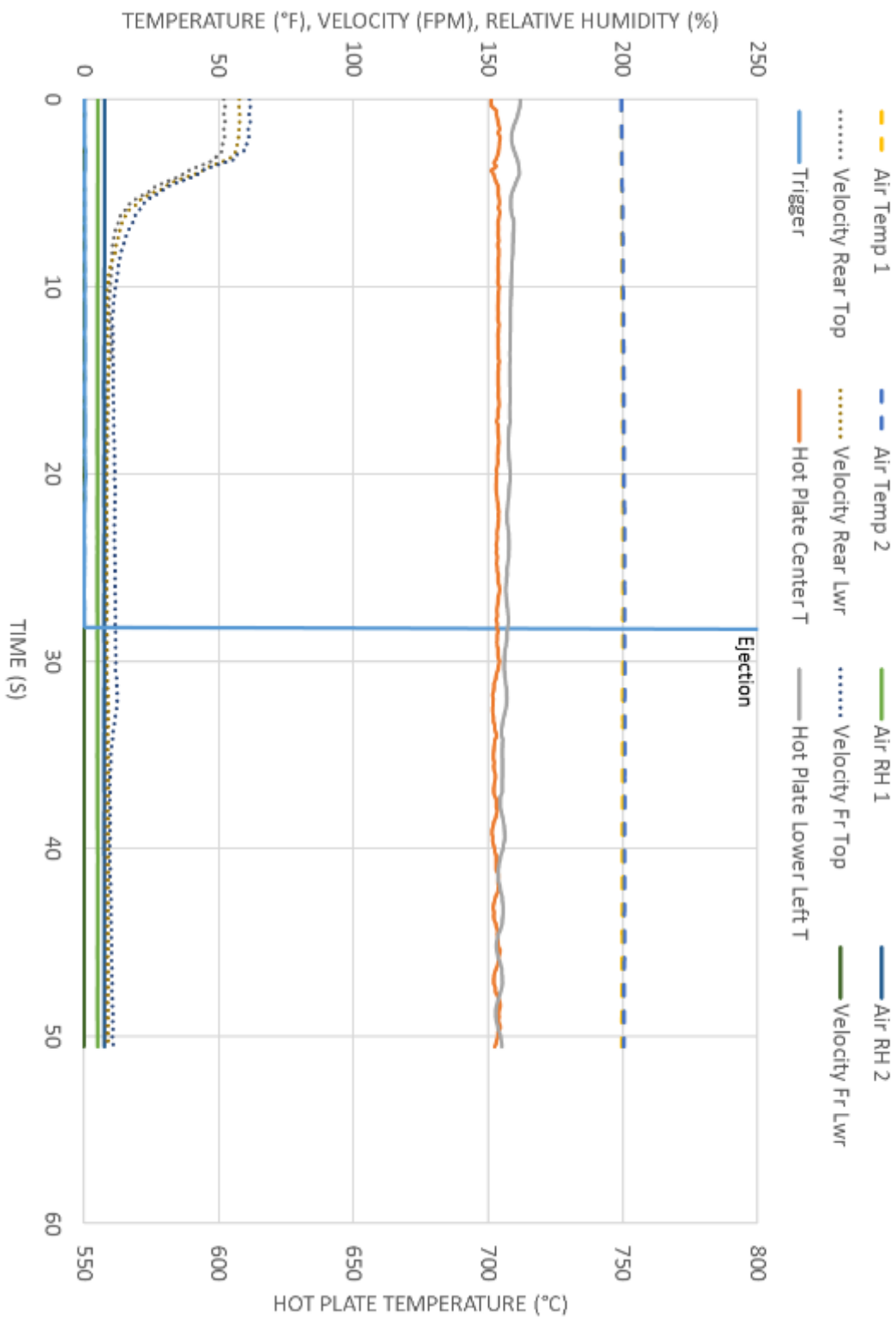
TEST 20 - R1234ZE, 3% OIL, 700°C HOT PLATE



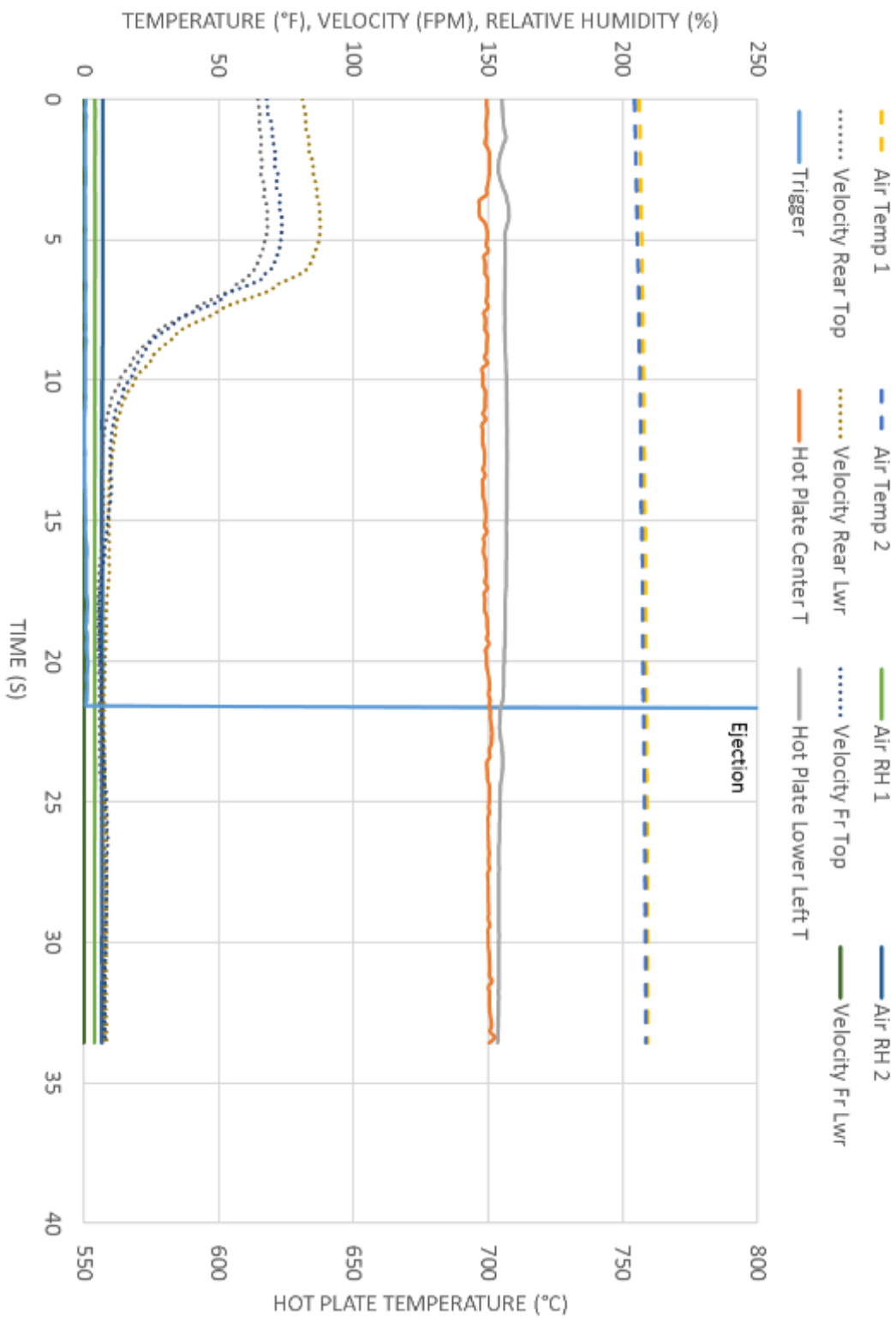
TEST 21 - R1234ZE, 3% OIL, 700°C HOT PLATE



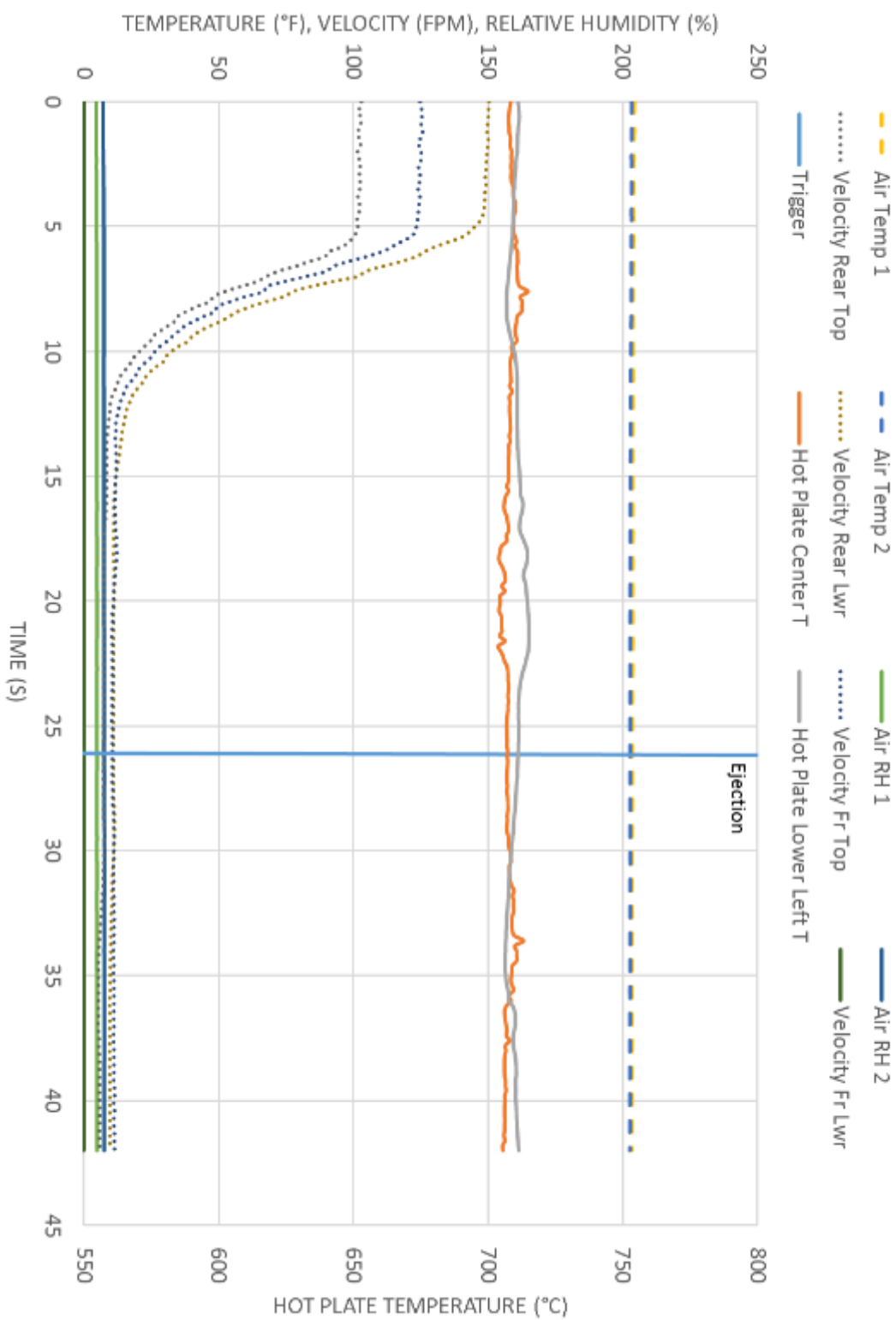
TEST 22 - R-1234ZE, 3% OIL, 700°C HOT PLATE



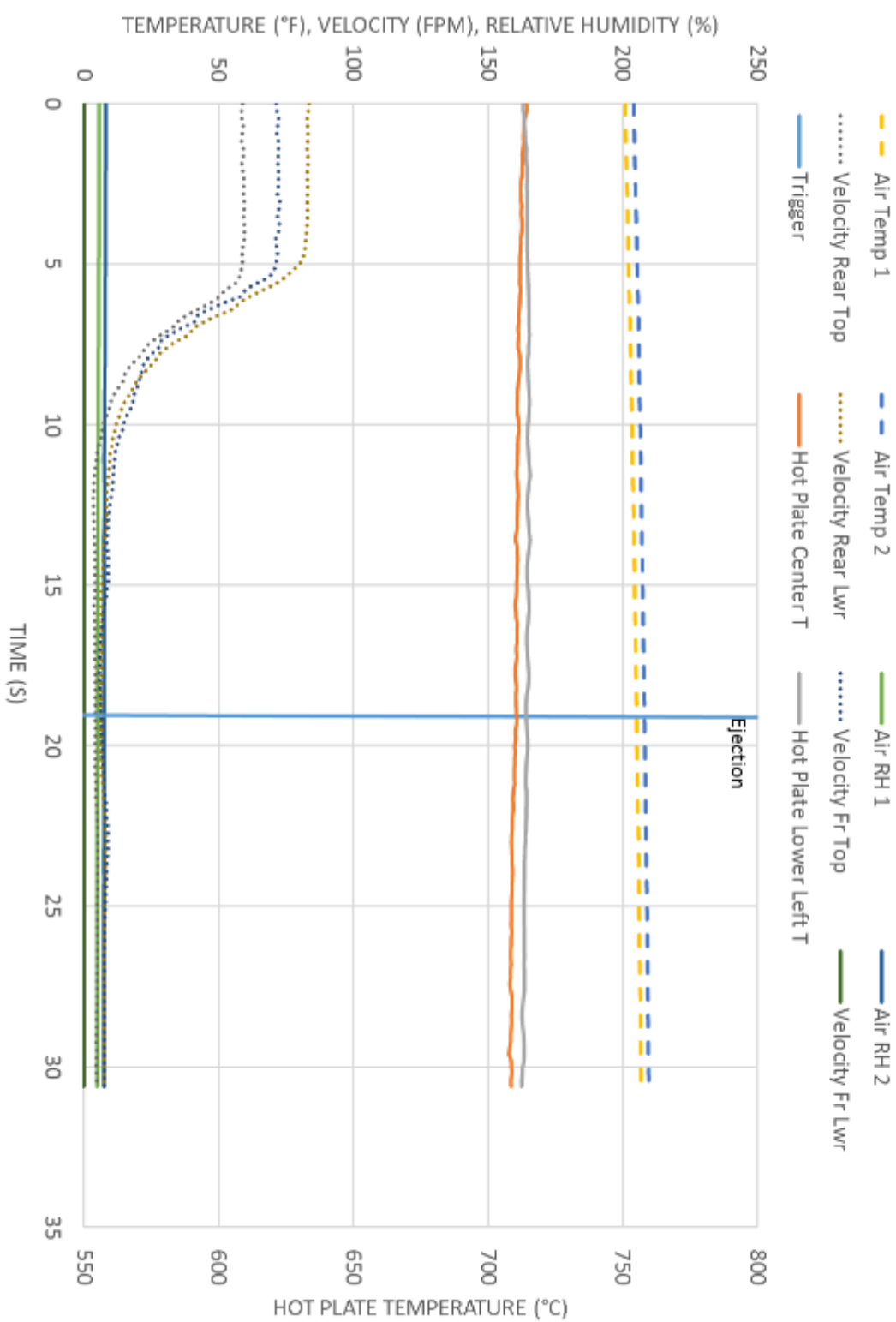
TEST 23, R-1234ZE, 3% OIL, 700°C HOT PLATE



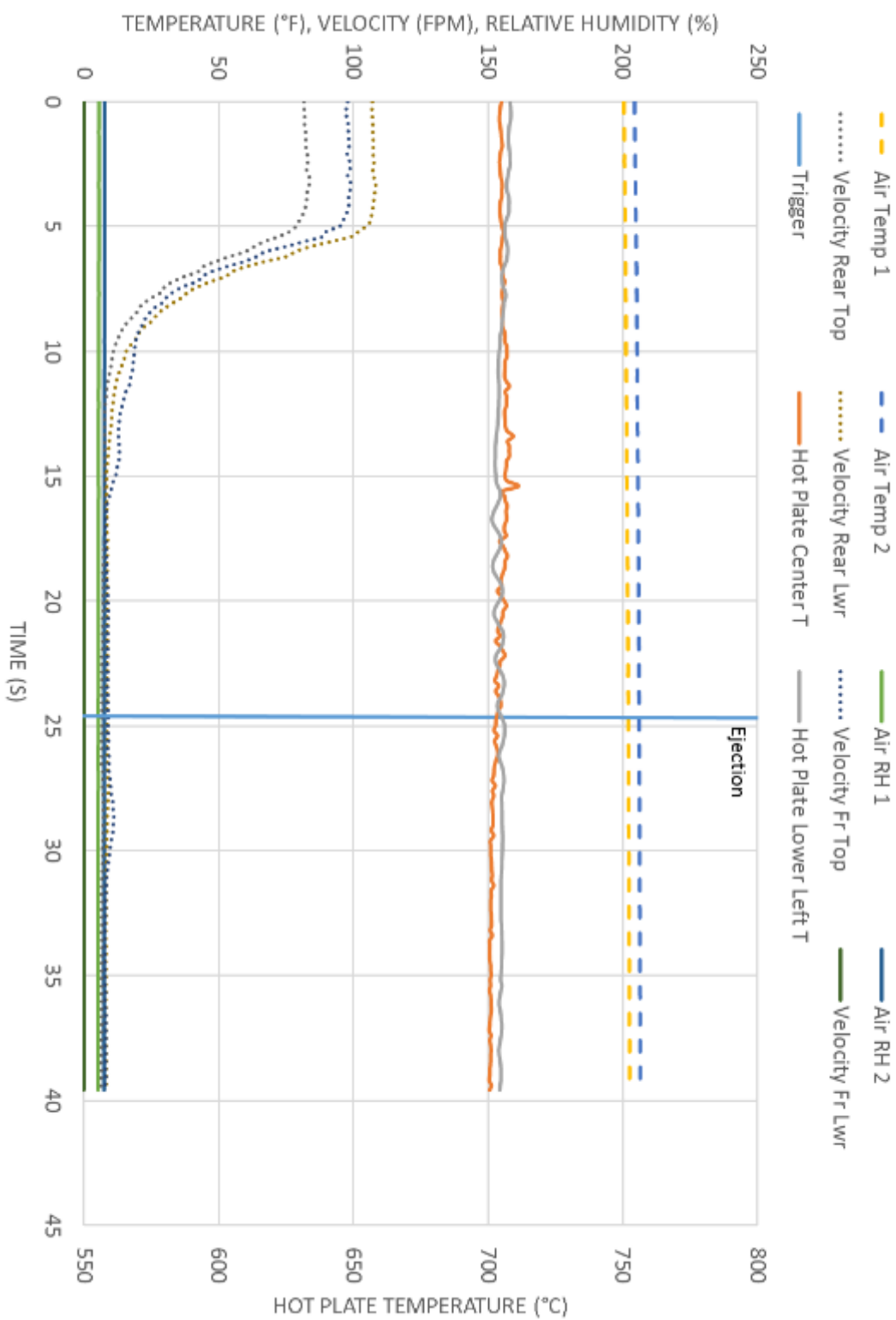
TEST 24 - R32, 3% OIL, 700°C HOT PLATE



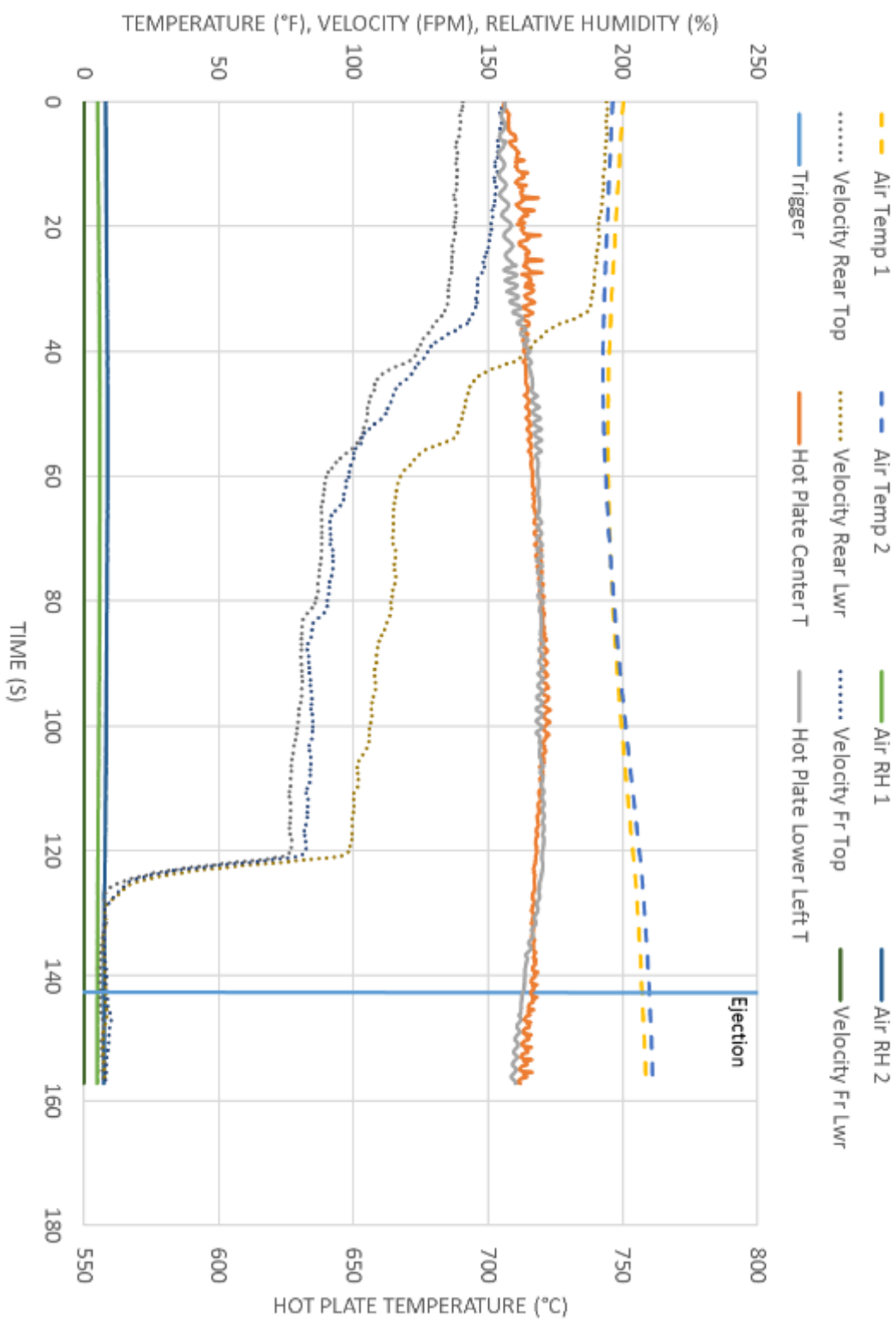
TEST 25 - R32, 3% OIL, 700°C HOT PLATE



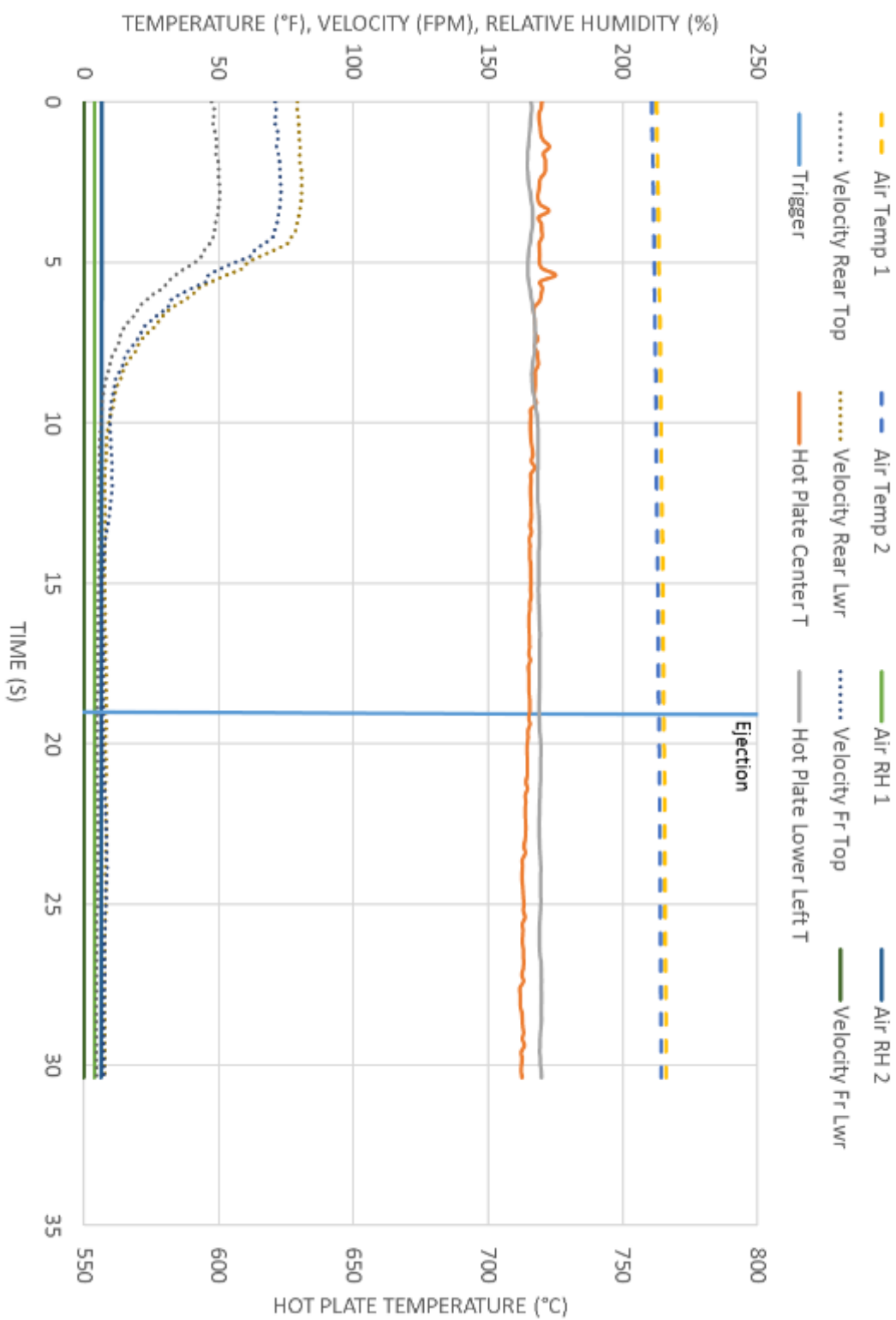
TEST 26 - R32, 3% OIL, 700°C HOT PLATE



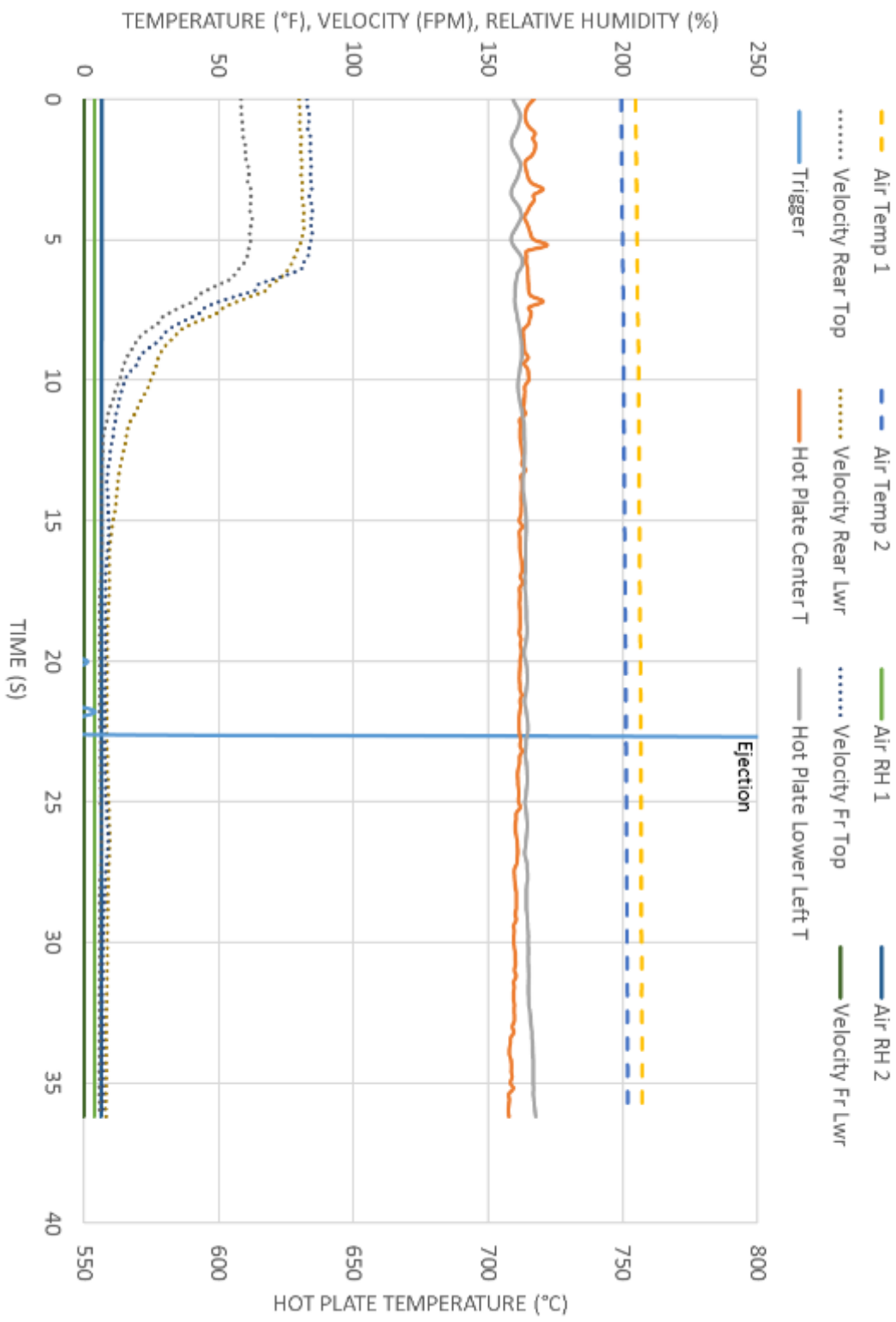
TEST 27 - R32, 3% OIL, 700°C HOT PLATE



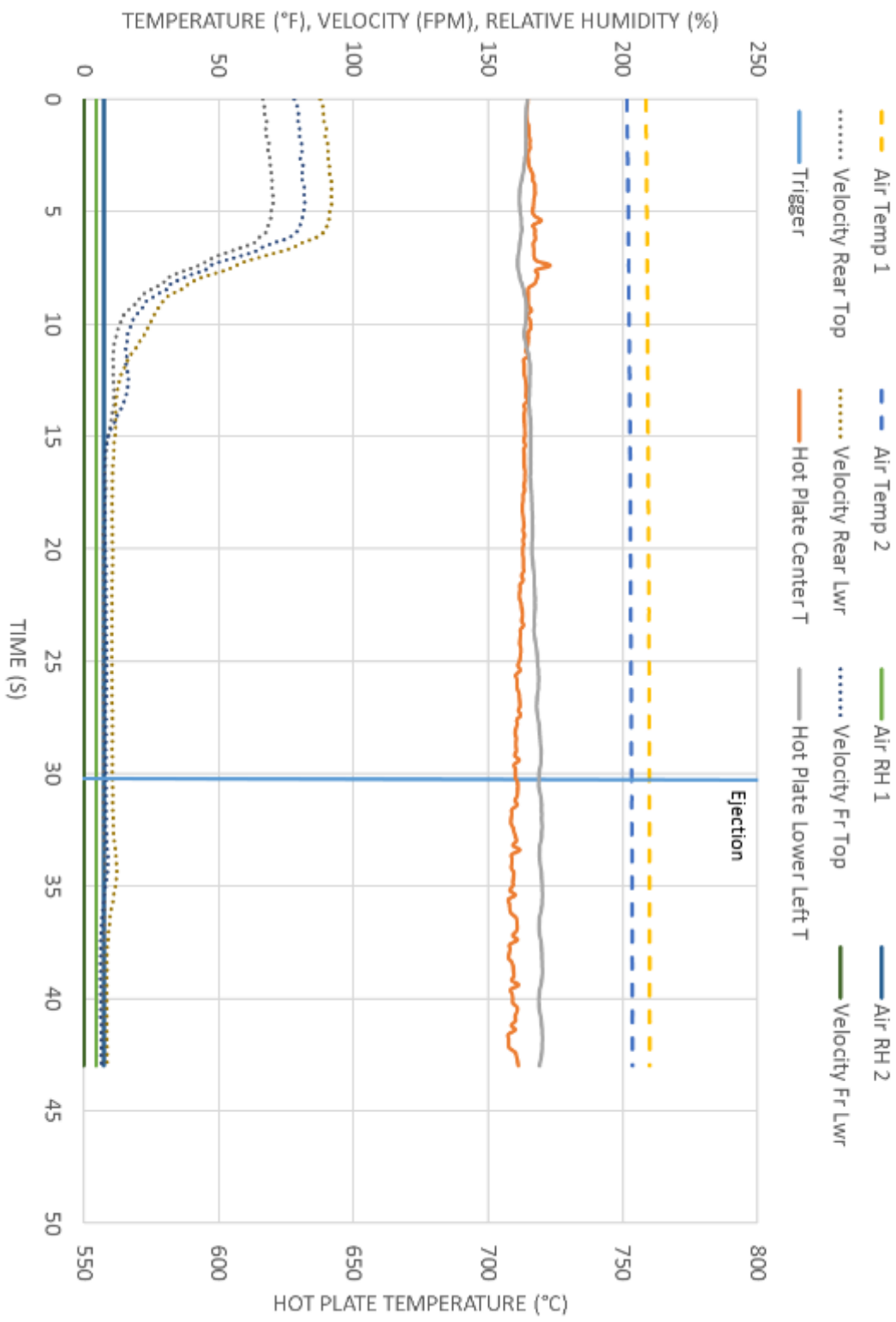
TEST 28 - R32, 3% OIL, 700°C HOT PLATE



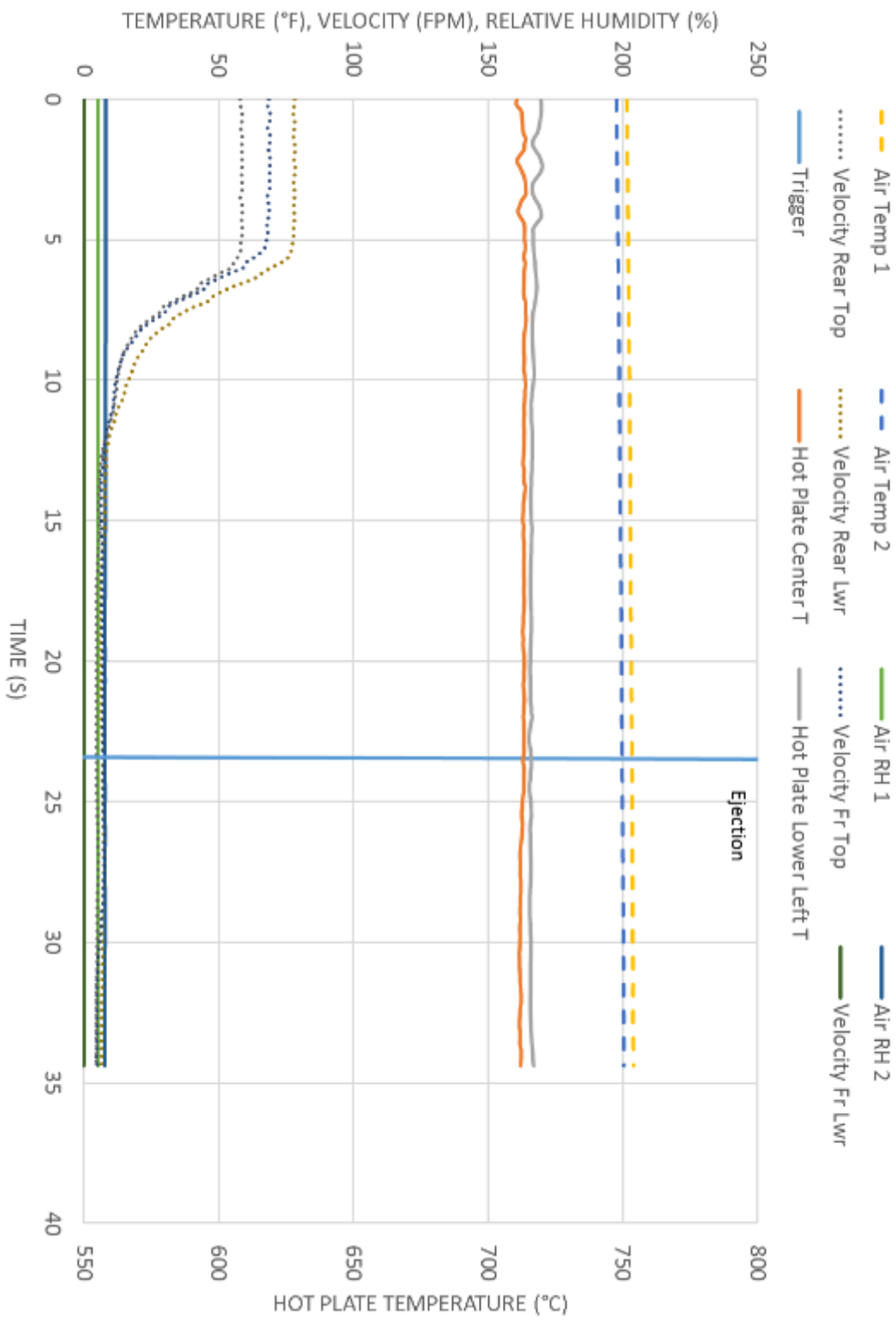
TEST 29 - R452B, 3% OIL, 700°C HOT PLATE



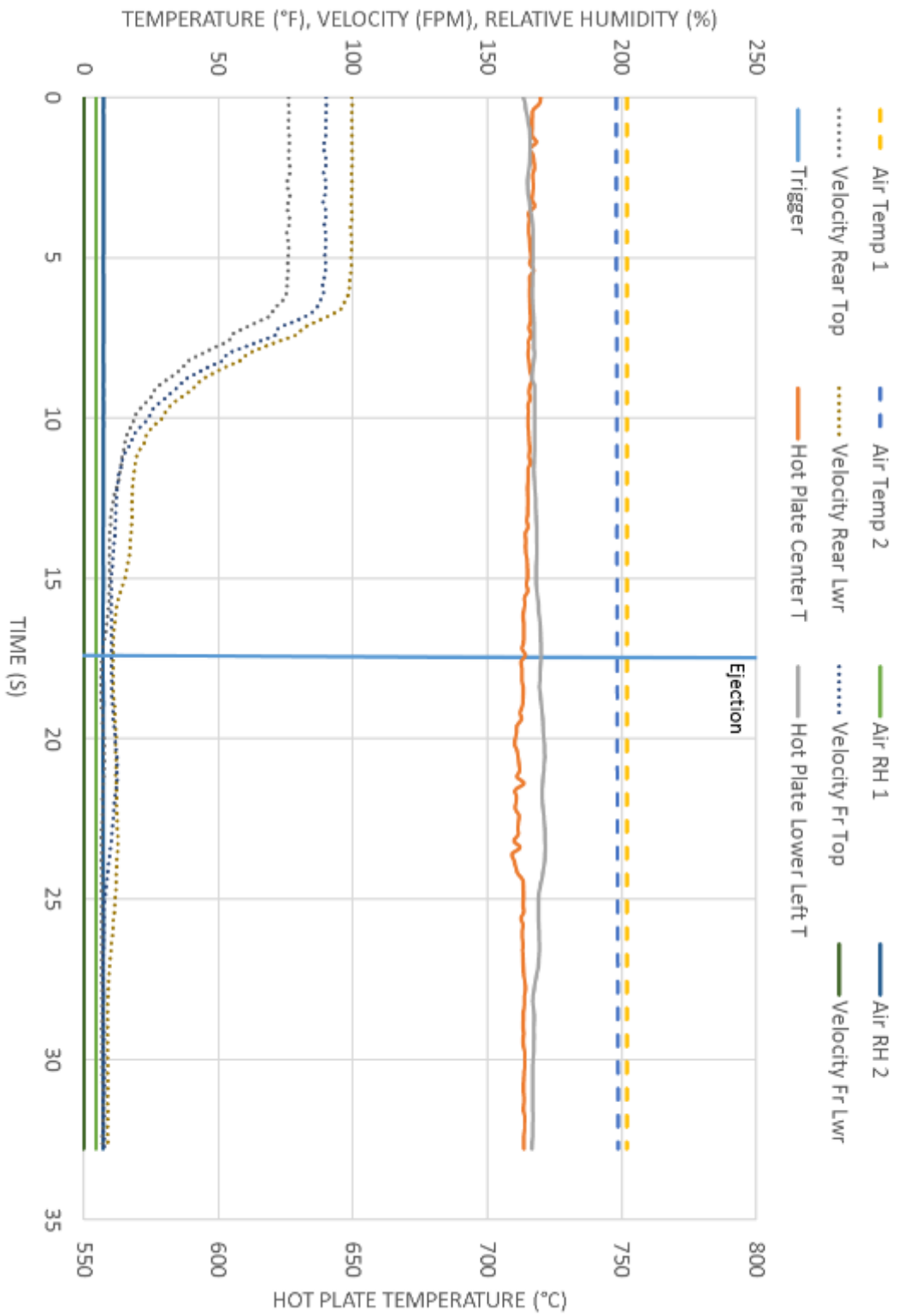
TEST 30 - R452B, 3% OIL, 700°C HOT PLATE



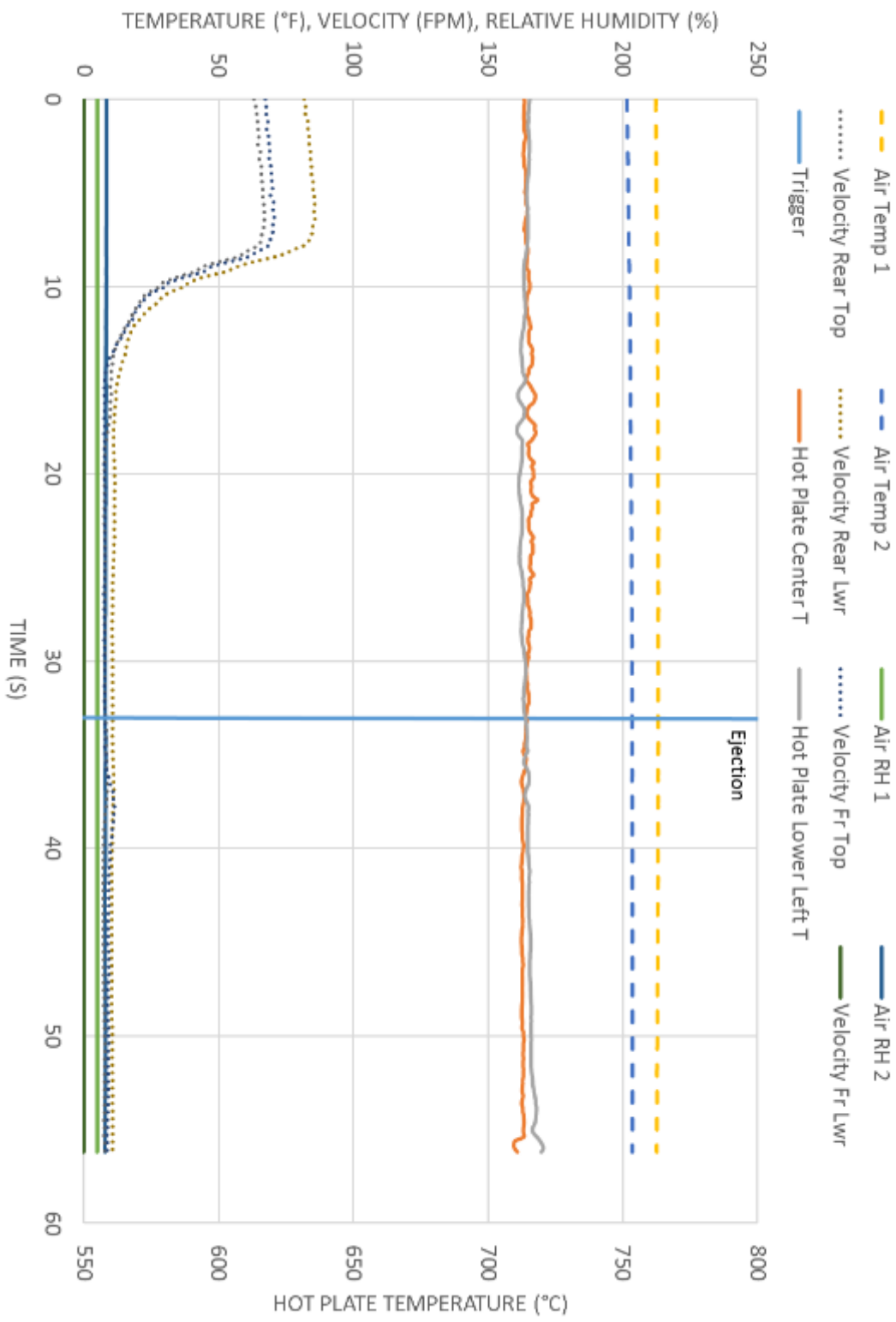
TEST 31 - R452B, 3% OIL, 700°C HOT PLATE



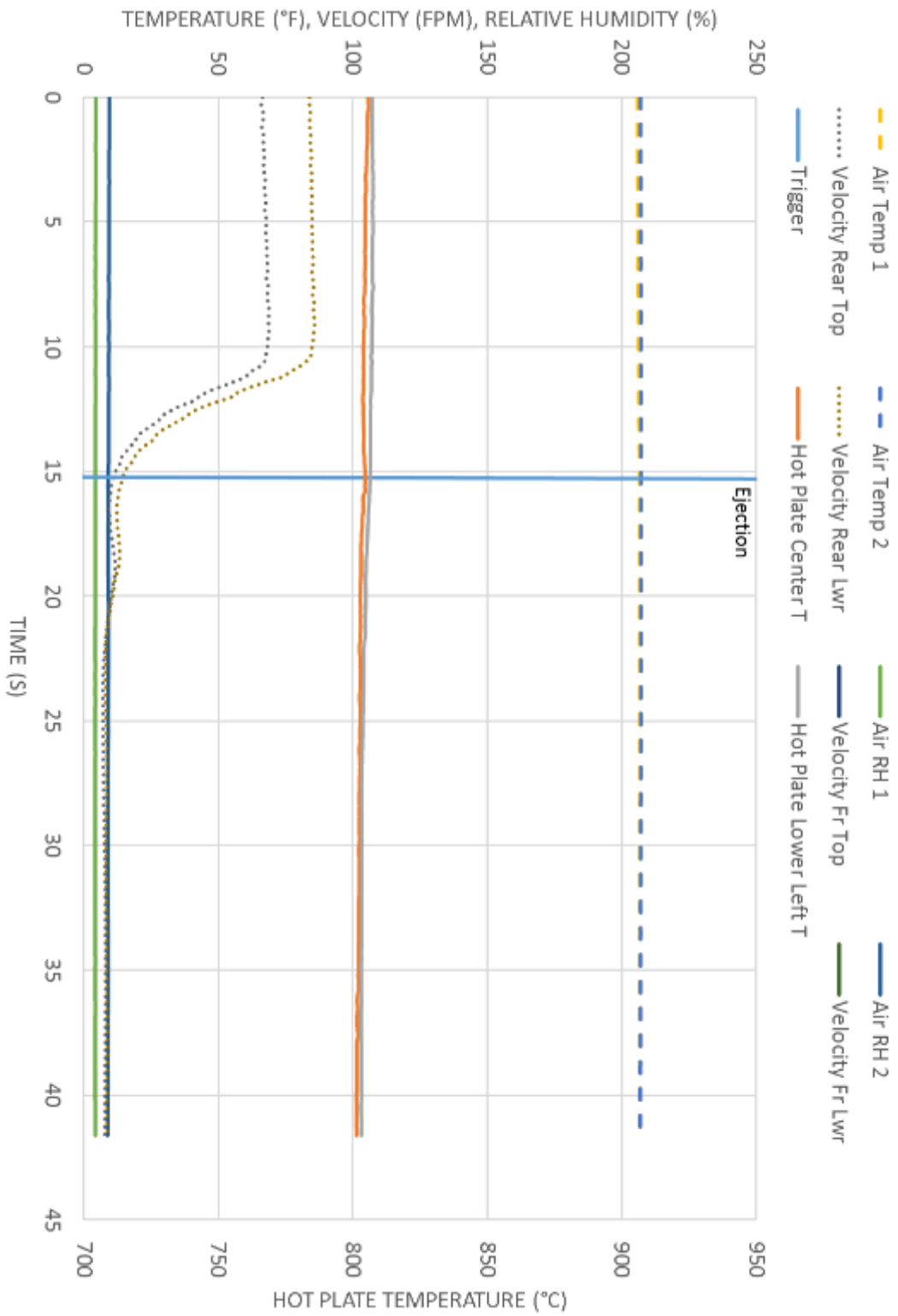
TEST 32 - R452B, 3% OIL, 700°C HOT PLATE



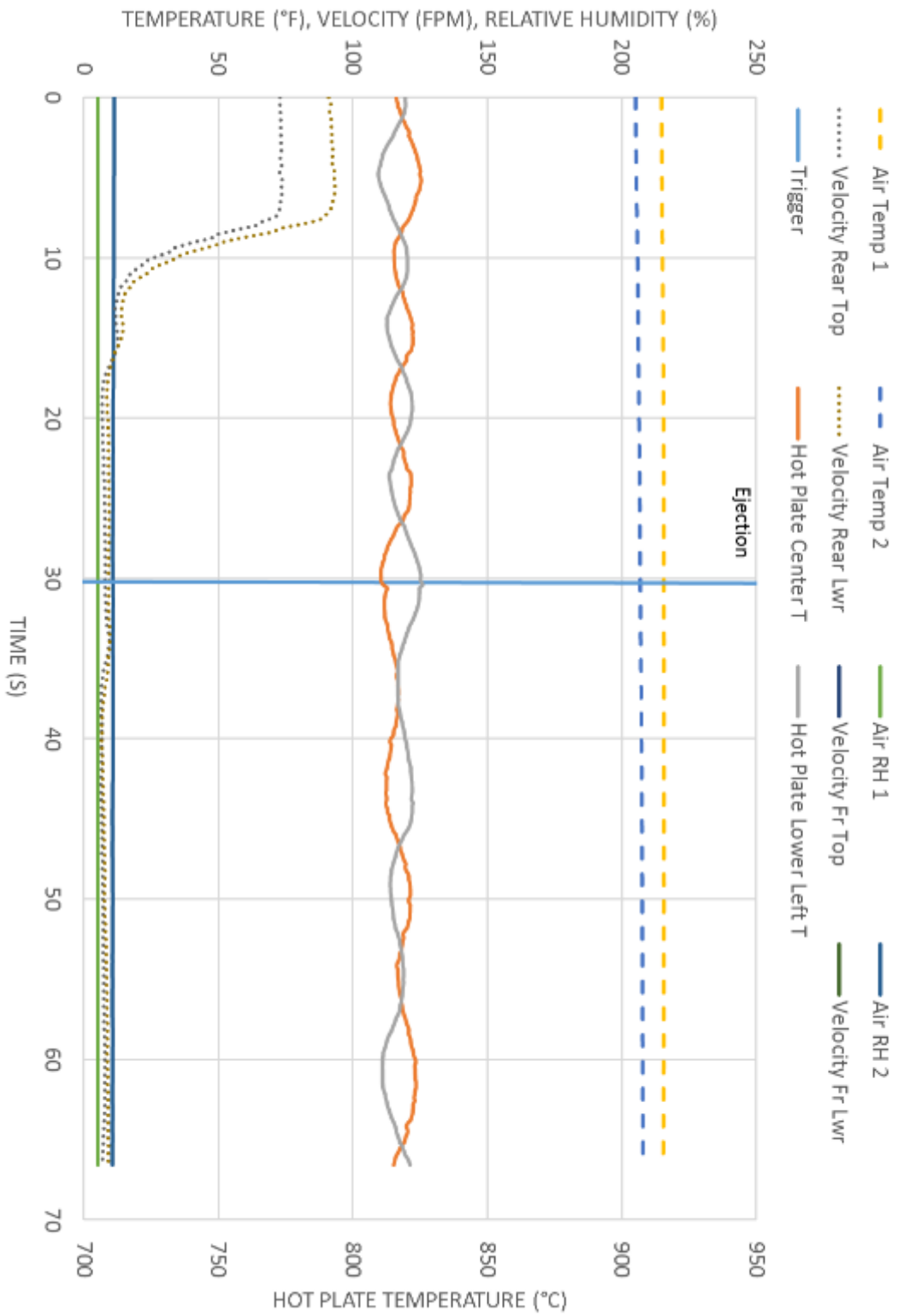
TEST 33 - R452B, 3% OIL, 700°C HOT PLATE



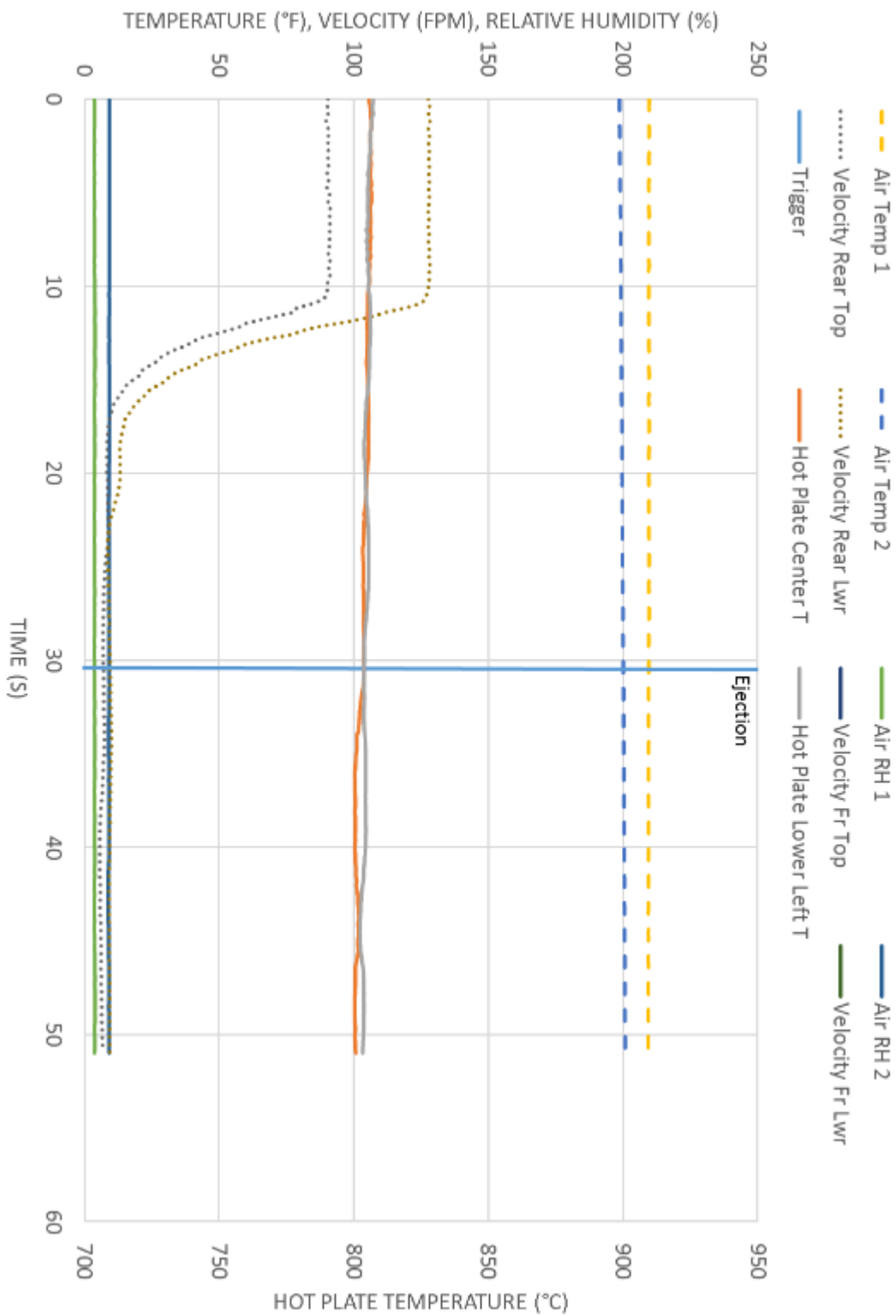
TEST 34 - R452B, 3% OIL, 800°C HOT PLATE



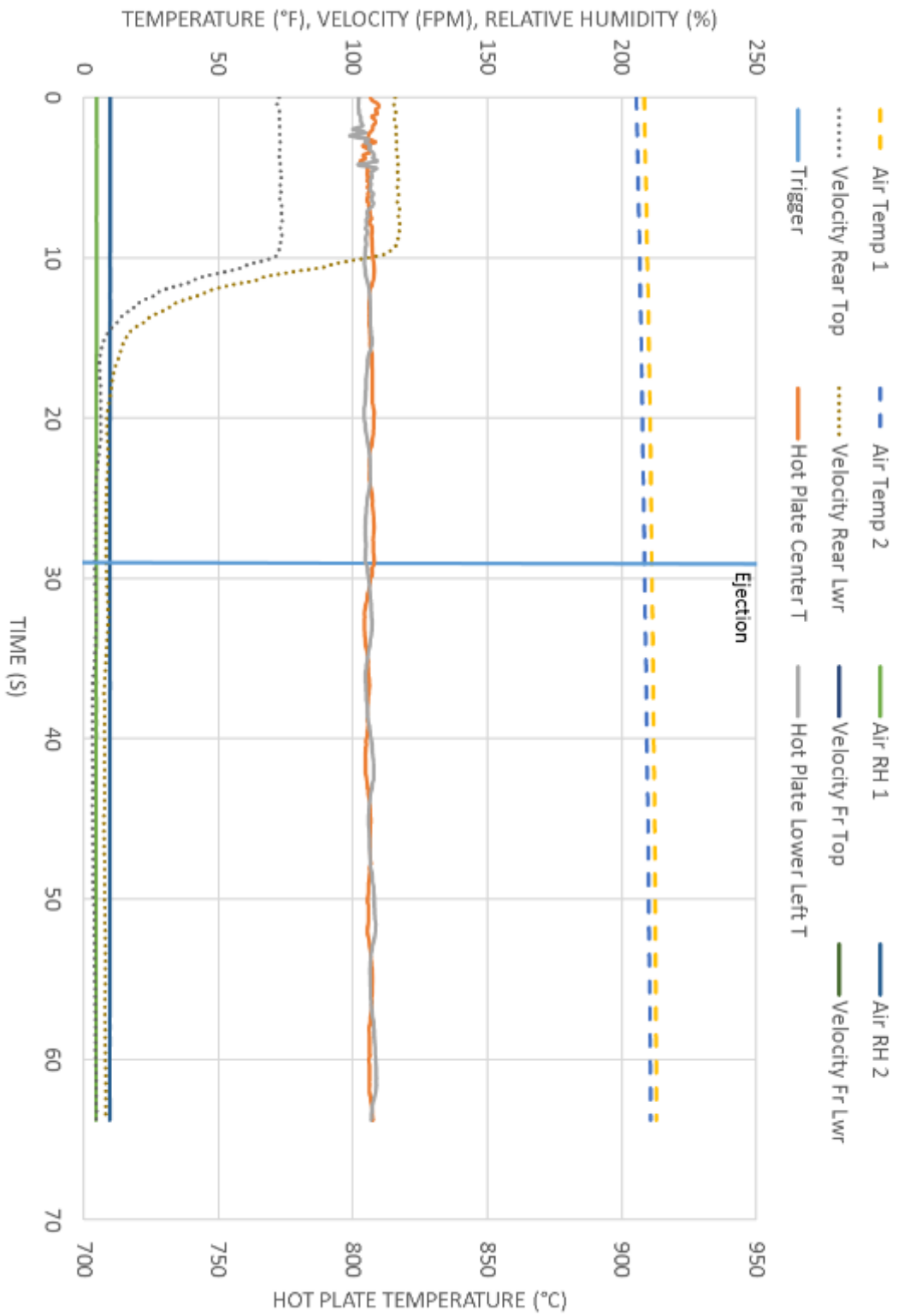
TEST 35 - R452B, 3% OIL, 800°C HOT PLATE



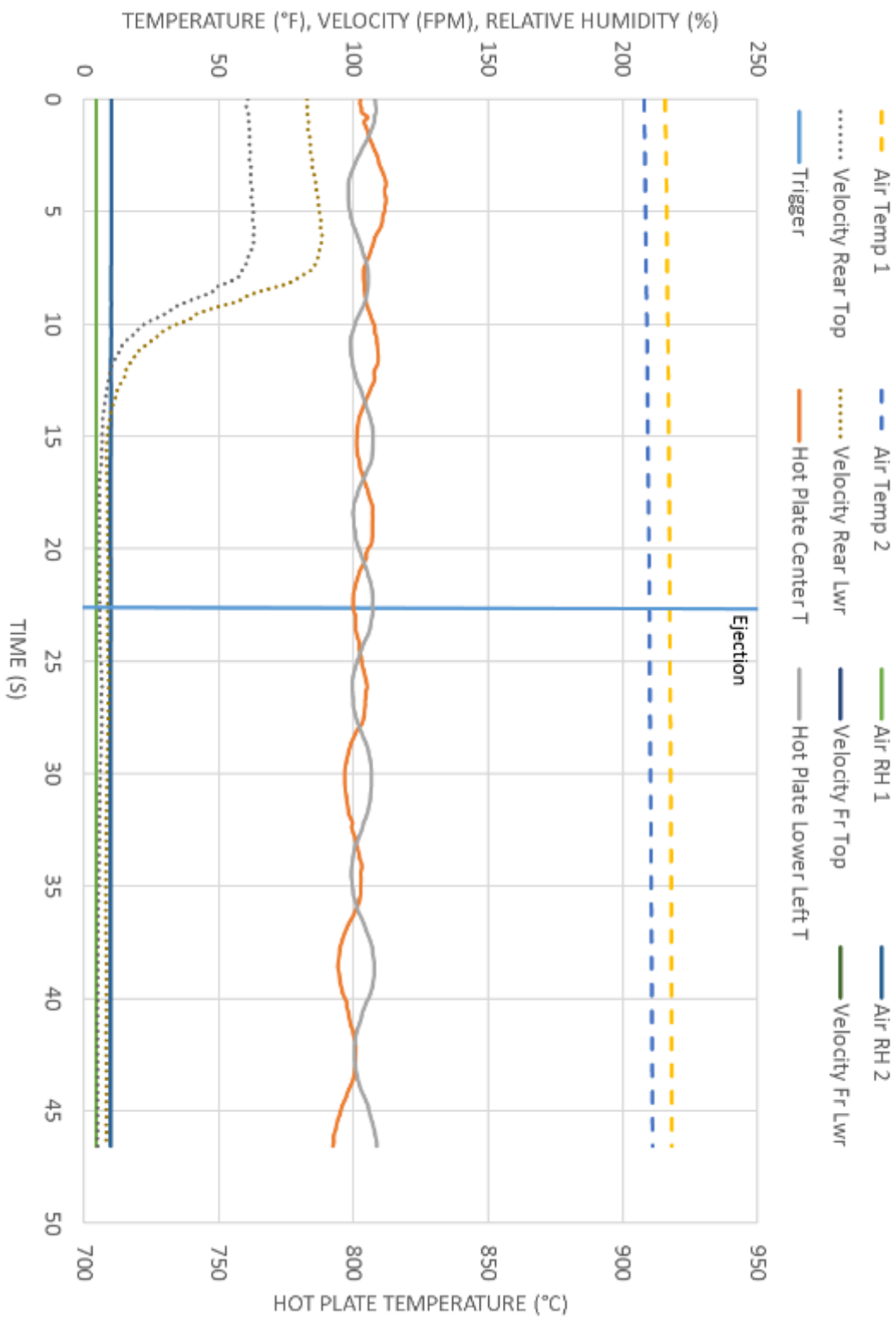
TEST 36 - R452B, 3% OIL, 800°C HOT PLATE



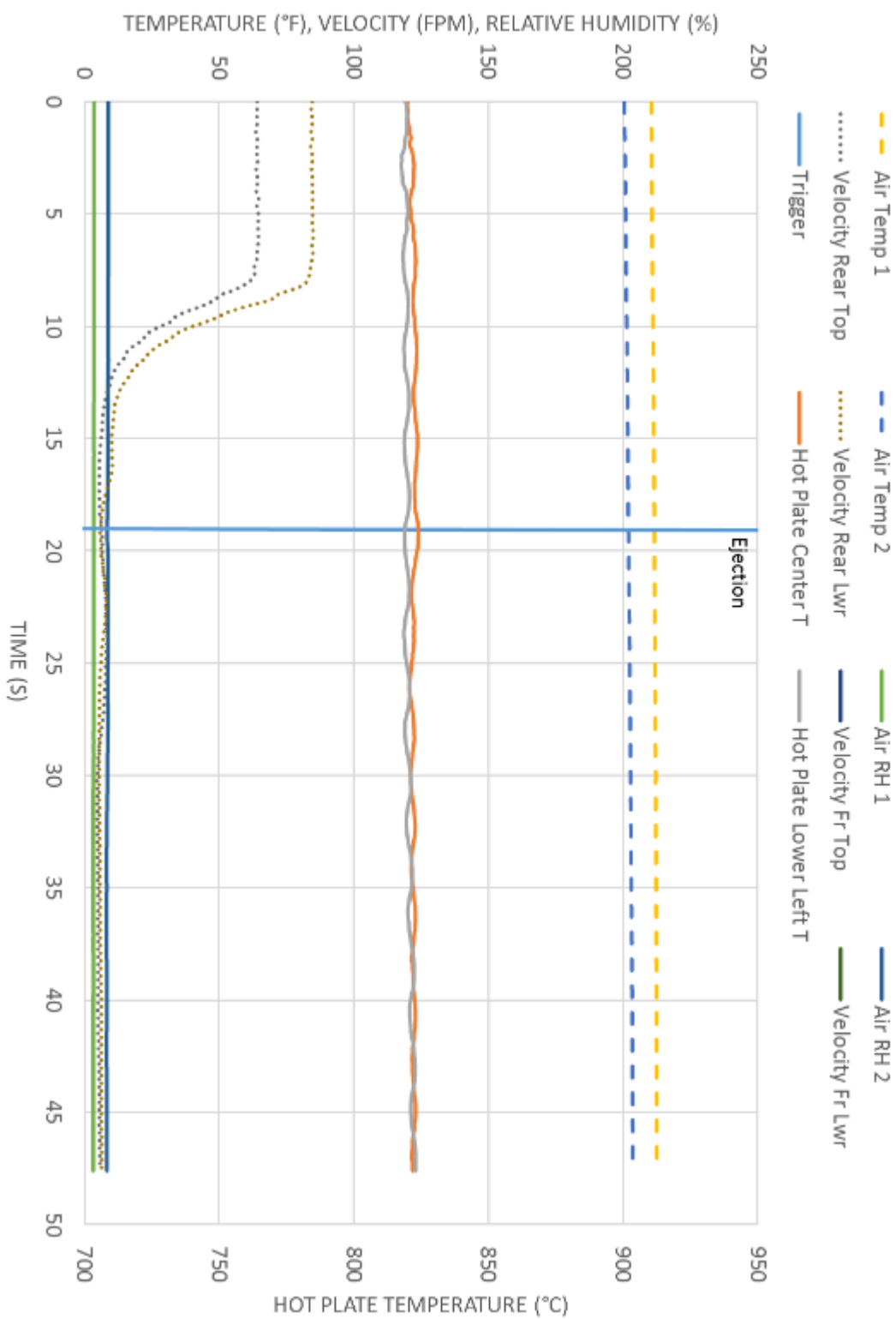
TEST 37 - R452B, 3% OIL, 800°C HOT PLATE



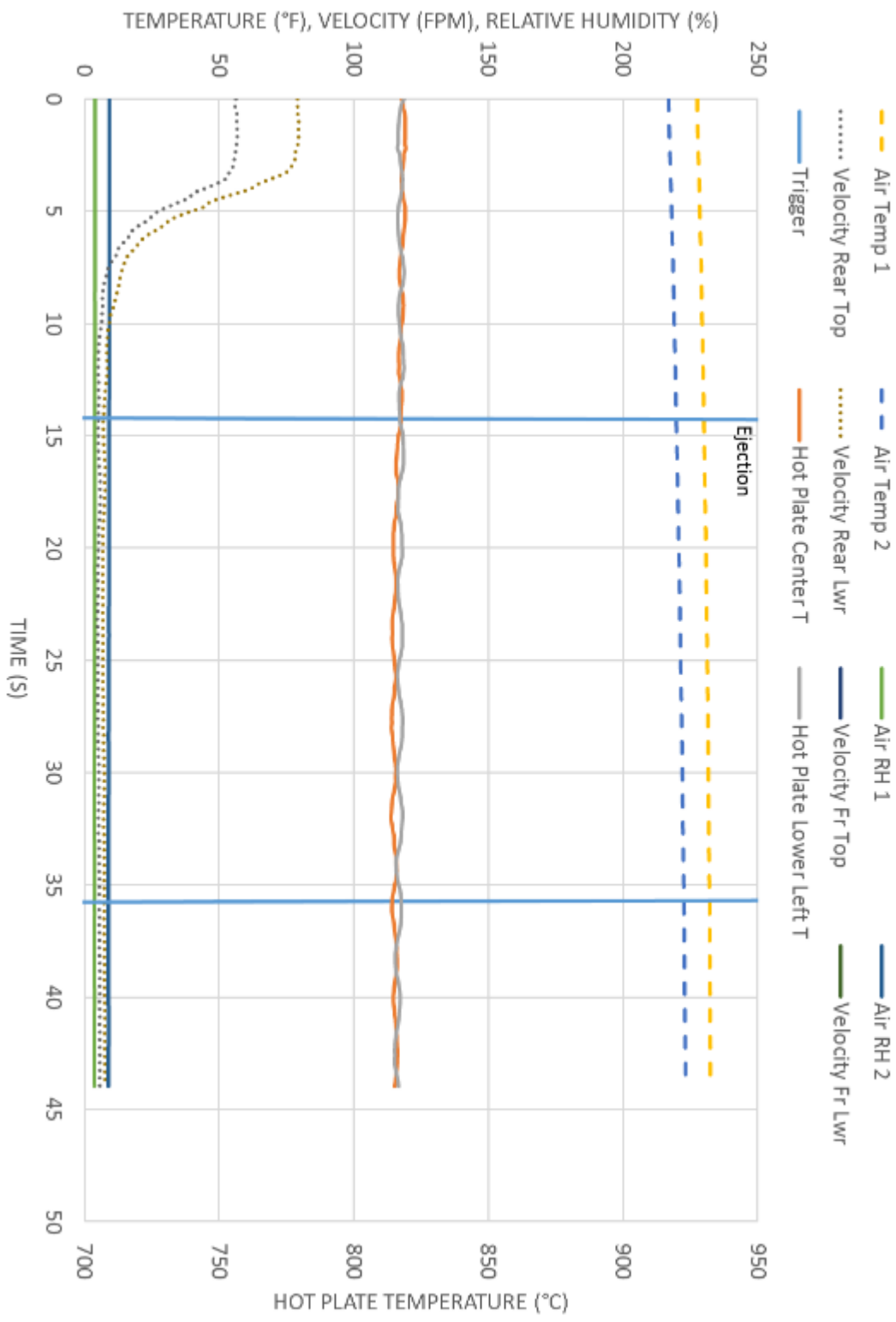
TEST 38 - R452B, 3% OIL, 800°C HOT PLATE



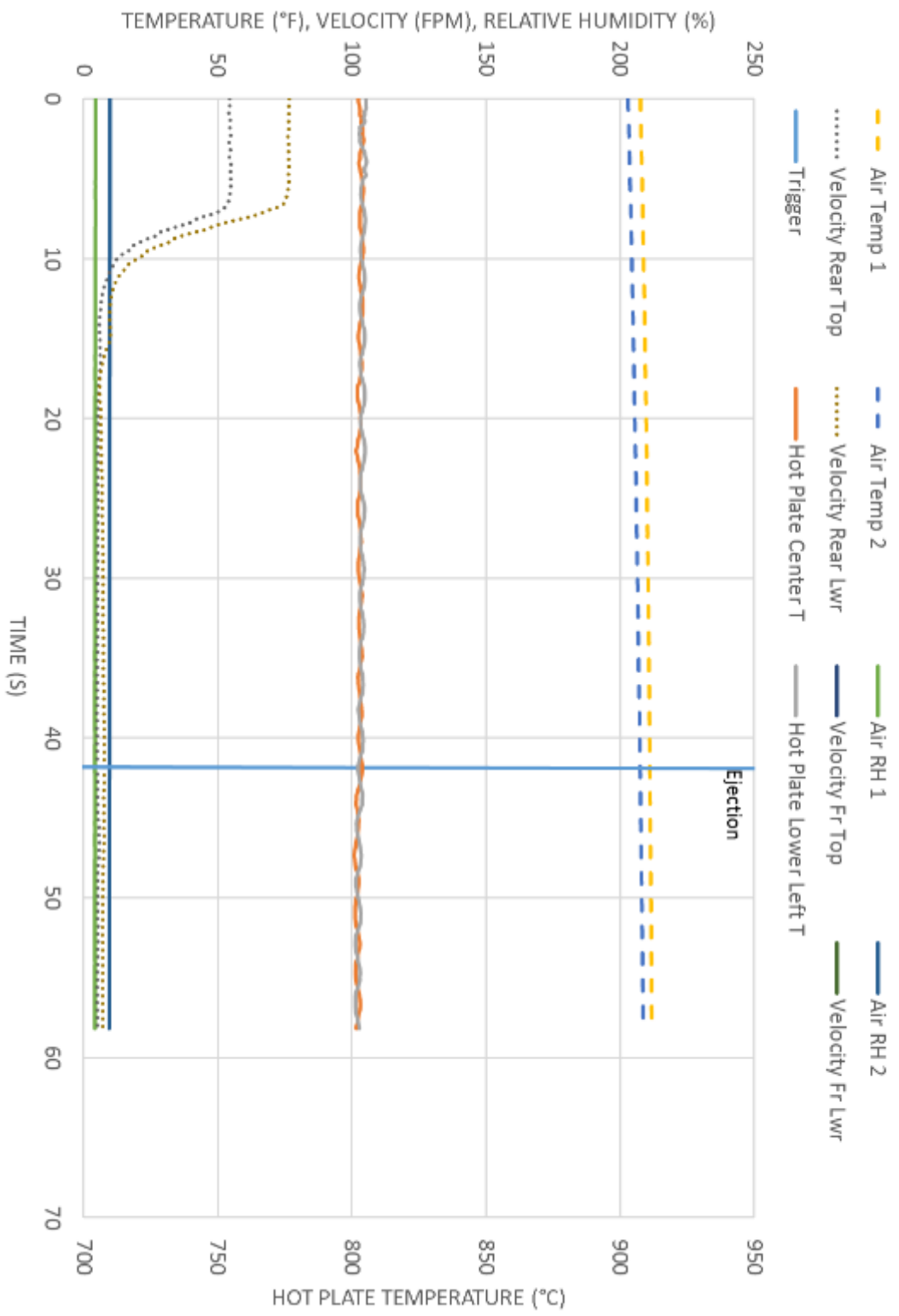
TEST 39 - R32, 3% OIL, 800°C HOT PLATE



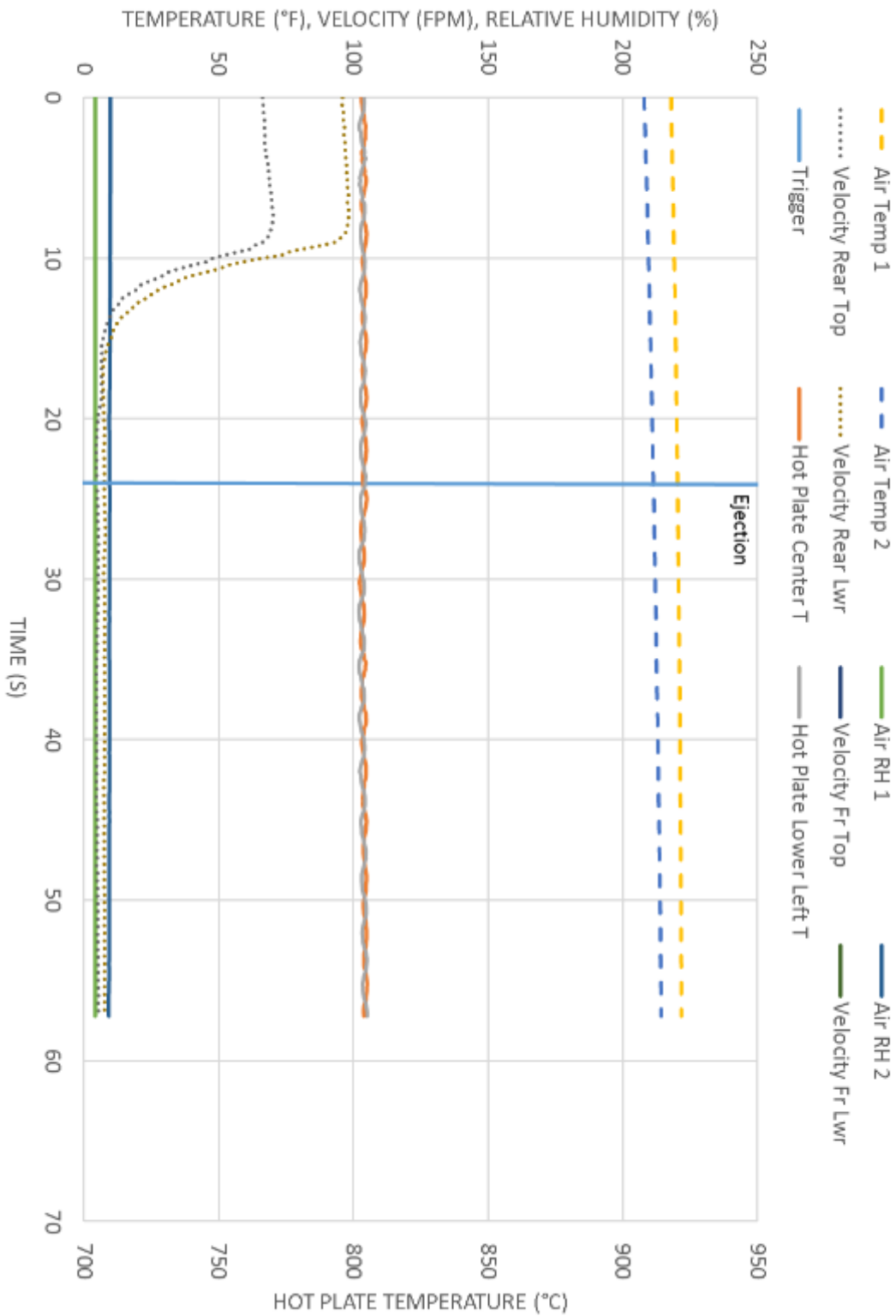
TEST 40 - R32, 3% OIL, 800°C HOT PLATE



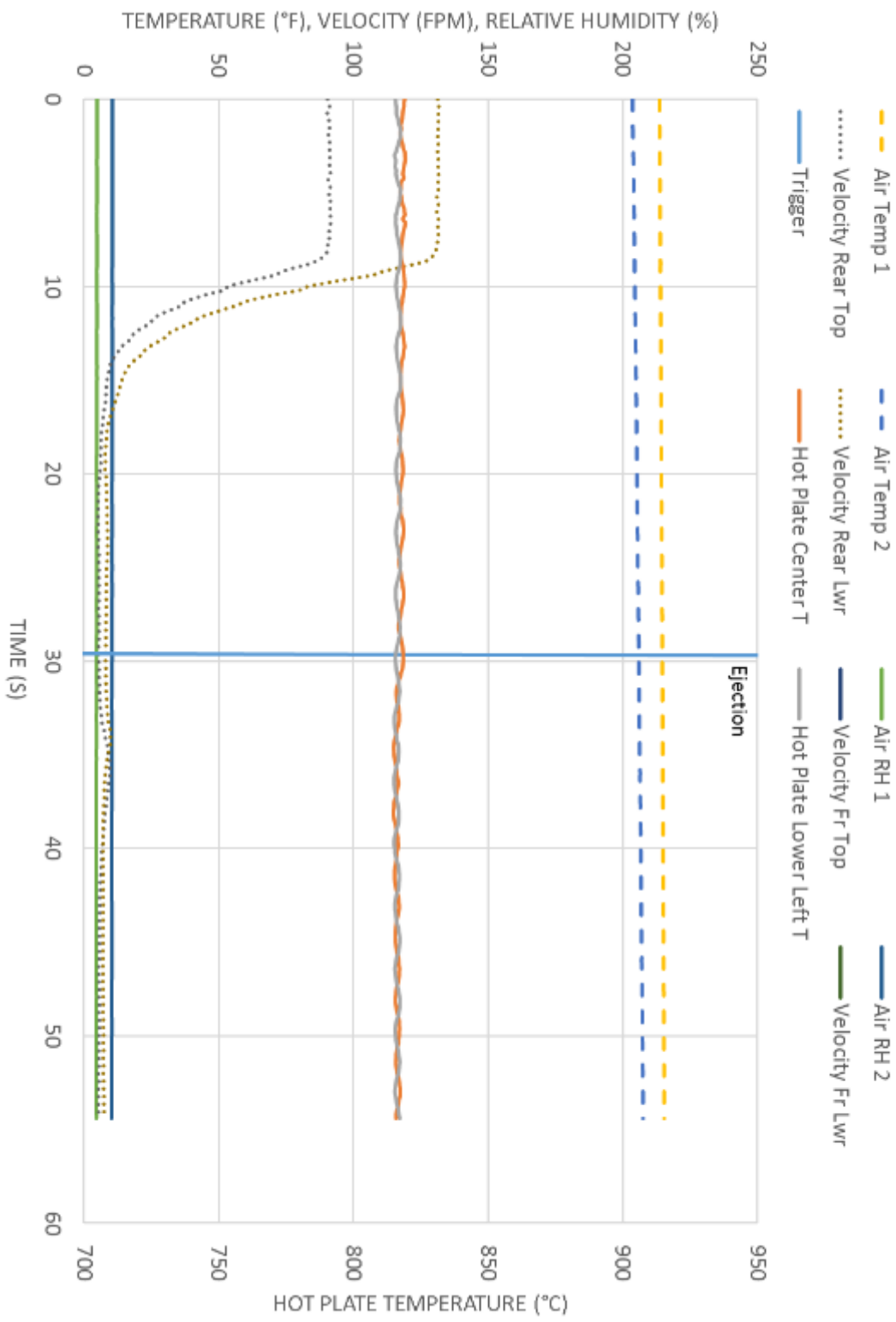
TEST 41 - R32, 3% OIL, 800°C HOT PLATE



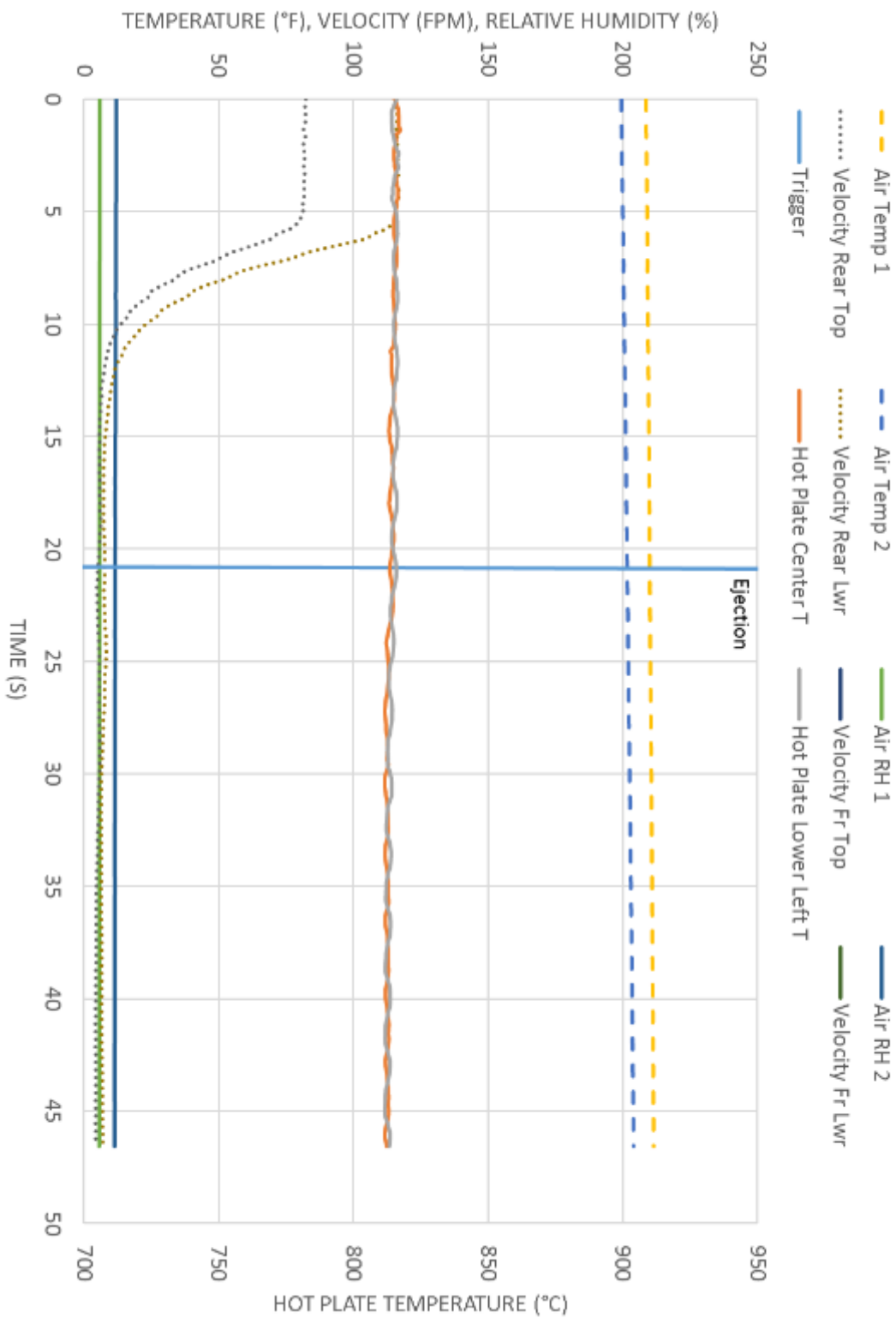
TEST 42 - R32, 3% OIL, 800°C HOT PLATE



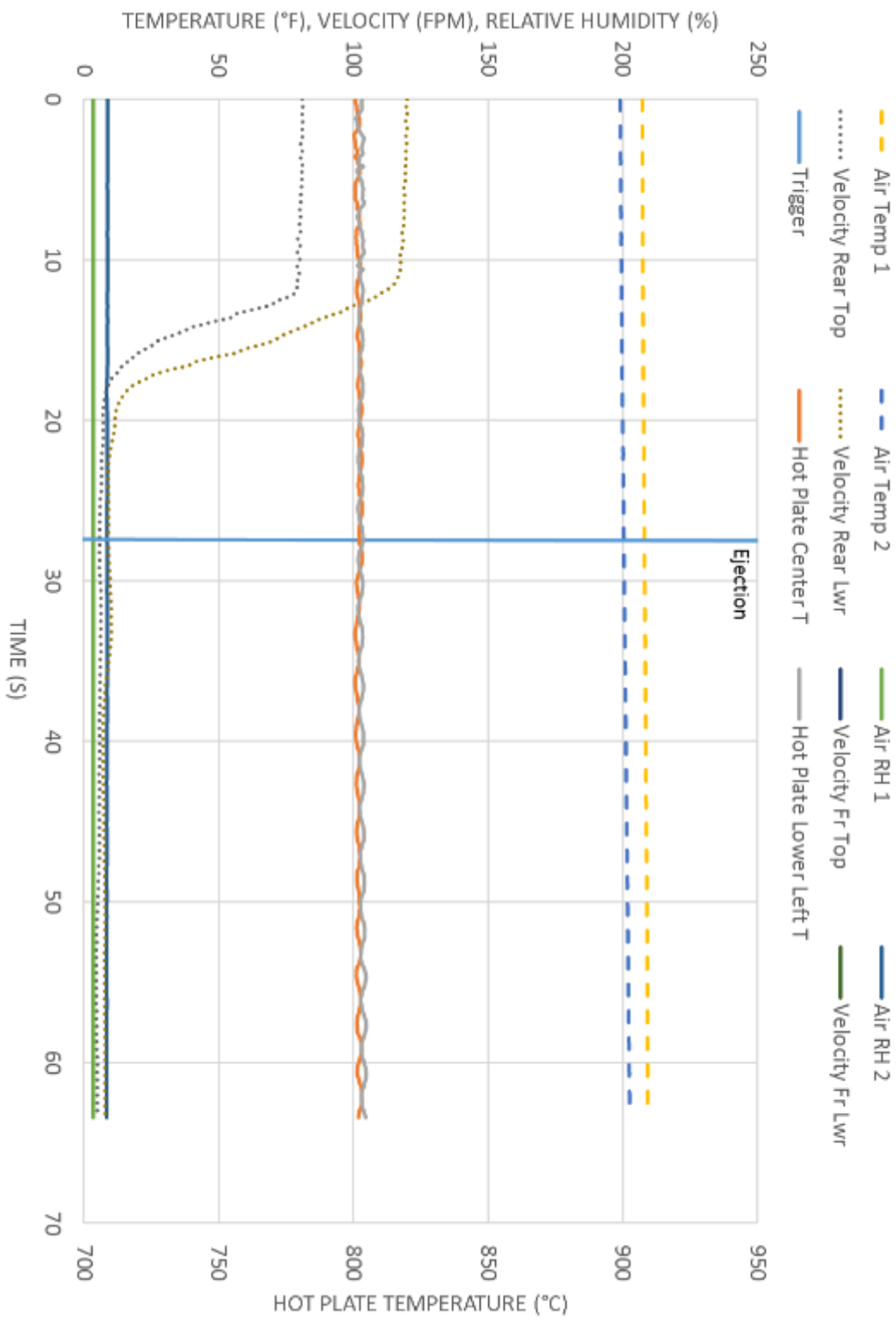
TEST 43 - R32, 3% OIL, 800°C HOT PLATE



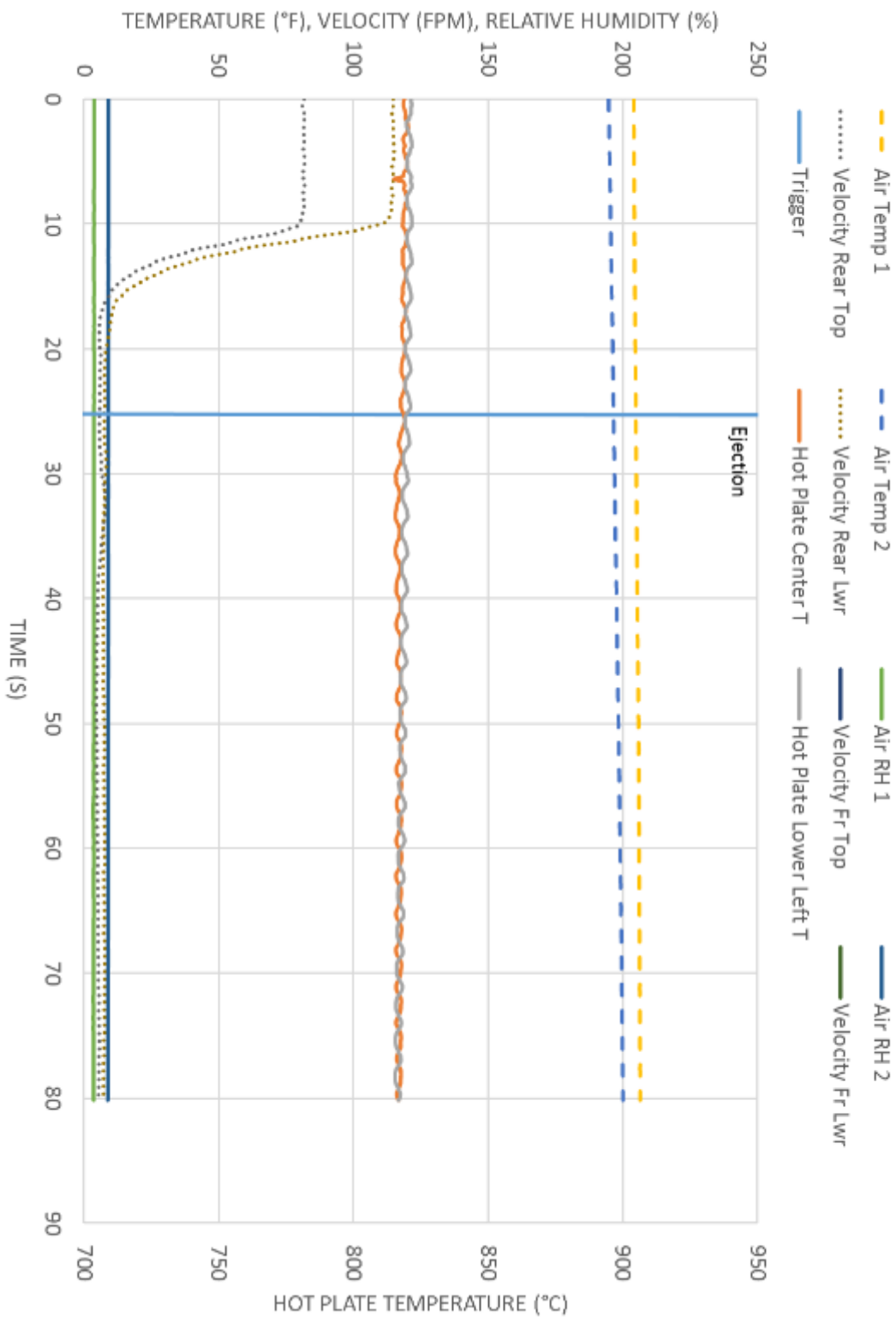
TEST 44 - R-1234ZE, 3% OIL, 800°C HOT PLATE



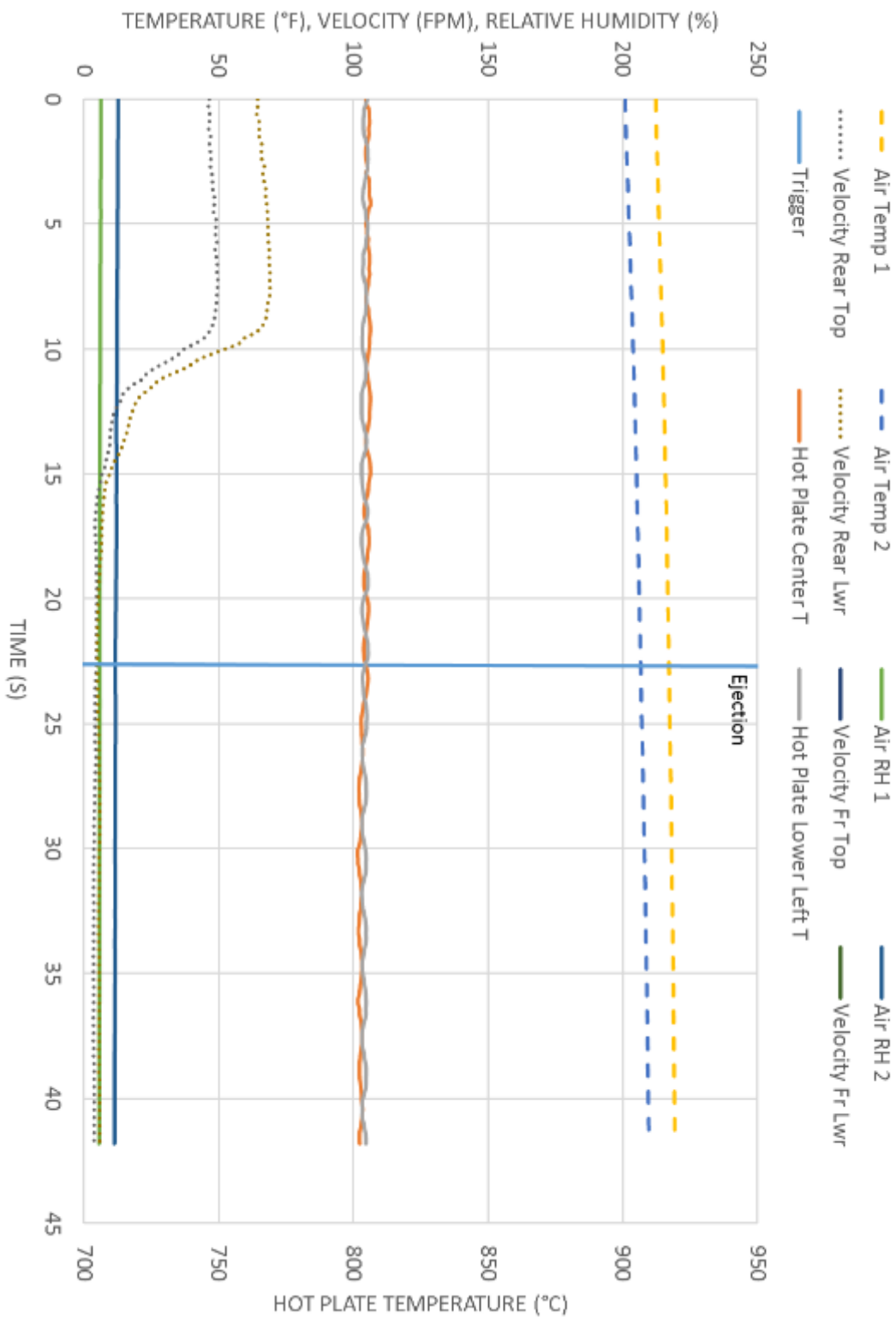
TEST 45 - R-1234ZE, 3% OIL, 800°C HOT PLATE



TEST 46 - R-1234ZE, 3% OIL, 800°C HOT PLATE



TEST 47 - R-1234ZE, 3% OIL, 800°C HOT PLATE



TEST 48 - R-1234ZE, 3% OIL, 800°C HOT PLATE

